INFLUENCE OF THE ACID-BASE PROPERTIES OF THE CoMo SUPPORTED CATALYSTS ON THE OLEFINS HYDROGENATION IN HDS ENVIRONMENTS

DAVID DE JESÚS PÉREZ MARTÍNEZ

UNIVERSIDAD INDUSTRIAL DE SANTANDER
FACULTAD DE INGENIERIAS FISICOQUIMICAS
ESCUELA DE INGENIERÍA QUÍMICA
DOCTORADO EN INGENIERÍA QUÍMICA
BUCARAMANGA
2010

INFLUENCE OF THE ACID-BASE PROPERTIES OF THE CoMo SUPPORTED CATALYSTS ON THE OLEFINS HYDROGENATION IN HDS ENVIRONMENTS

DAVID DE JESÚS PÉREZ MARTÍNEZ

Tesis presentada para optar al título de

DOCTOR EN INGENIERÍA QUÍMICA

Director: Prof. Aristóbulo Centeno Hurtado, Ph.D

Co-directora: Prof. Sonia A. Giraldo Duarte, Ph.D.

UNIVERSIDAD INDUSTRIAL DE SANTANDER
FACULTAD DE INGENIERIAS FISICOQUIMICAS
ESCUELA DE INGENIERÍA QUÍMICA
DOCTORADO EN INGENIERÍA QUÍMICA
BUCARAMANGA
2010

DEDICATORIA

A Dios a quien todo le debo.

A mi papá Gregorio Pérez González, a mi mamá Consuelo Martínez Ruiz y a mis hermanas María Consuelo, Ana María y Adrianita, quienes me apoyaron y alentaron en mi objetivo de llevar a feliz término esta tesis y que siempre tuvieron una palabra de aliento en los momentos de flaqueza.

A mis amigos que siempre estuvieron pendientes del desarrollo de mis estudios y que siempre me animaron a alcanzar este logro tan importante en mi vida.

David de Jesús Pérez Martínez

AGRADECIMIENTOS

- A mis directores de proyecto por ser mis guías, por sus valiosos consejos y por alentarme durante el desarrollo de esta tesis.

- A los evaluadores, el profesor Alexander Stumbo, la profesora Adriana Echavarría, la profesora Martha Niño y el profesor Álvaro Ramírez por sus comentarios y sugerencias y por el tiempo dedicado a la revisión detallada de esta tesis.

- Al profesor Eric Gaigneaux de la Universidad Católica de Lovaina en Bélgica y en general a los integrantes de la unidad CATA por recibirme en su laboratorio durante mi pasantía doctoral y por su colaboración con la caracterización de los catalizadores.

- A la profesora Elena Stachenko del CENIVAN-UIS por su colaboración con las pruebas de CG-MS.

- Al profesor Carlos A. Trujillo del laboratorio de Catálisis de la UNAL por su atención y colaboración durante una mini-pasantía en su laboratorio.

- A los hoy Ingenieros químicos: Giovanni, Vladimir, Albany, Carlos, Andrea, Ángela, Guillermo, Gustavo, Carlos, Jorge, Yuranis, María Elvira y Cindy, quienes desarrollaron su trabajo de grado dentro del marco de esta tesis doctoral y colaboraron con la realización de algunos experimentos.

- A los compañeros y profesores del CICAT-UIS.

- Al personal administrativo de la Escuela de Ingeniería Química quienes siempre me colaboraron en lo que estuvo a sus alcances.

TABLE OF CONTENTS

LIST OF FIGURES

LIST OF TABLES

LIST OF SCHEMES

RESUMEN

TITULO: **INFLUENCIA DE LAS PROPIEDADES ACIDO-BASE DE CATALIZADORES Co-Mo EN LA HIDROGENACION DE OLEFINAS EN AMBIENTES DE HDS.***

AUTOR: David de Jesús Pérez Martínez.**

PALABRAS CLAVES: nafta de FCC, octanaje, hidrodesulfuración, hidrogenación, cobalto, molibdeno, soporte, propiedades ácido-base.

El objetivo del hidrotratamiento de la nafta de FCC es eliminar al máximo los compuestos de azufre evitando la saturación de las olefinas. Se utilizaron varias familias de soportes para preparar catalizadores CoMo con el objetivo de analizar el efecto de las modificaciones del soporte en el hidrotratamiento de la nafta de FCC. Se usaron alúmino-silicatos amorfos (ASA), ASA modificados con sodio y alúmina modificada con boro, sodio o potasio. Los catalizadores preparados fueron caracterizados por DRX, XPS, Raman, isotermas de adsorción-desorción de nitrógeno, TPD de amoniaco, e infrarrojo de piridina y/o CO_2 adsorbidos. Aunque cada familia de soportes tiene diferentes propiedades superficiales se pueden encontrar algunos factores comunes a los catalizadores con mejores comportamientos. Se encontró que la modificación del soporte influencia el comportamiento catalítico debido a dos factores esencialmente. Por un lado, las propiedades ácido-base del soporte tienen una fuerte influencia en la distribución de las especies de Mo y Co en estado oxido. Por lo tanto, influencian también la actividad intrínseca en hidrodesulfuración e hidrogenación de los catalizadores. Por otro lado, el soporte mismo promueve reacciones de tipo ácido como la isomerización de doble enlace y esquelética, el craqueo y la alquilación. Estas reacciones compiten con la hidrogenación y la hidrodesulfuración y dependiendo de cuales son promovidas y de sus rendimientos, estas reacciones pueden ser beneficiosas o desfavorables para preservar el número de octano de la nafta de FCC. Los resultados mostraron que la presencia preferencial de sitios Brönsted débiles, los cuales promueven selectivamente la isomerización del doble enlace, al mismo tiempo que la promoción de un adecuado balance de la distribución de especies de Mo y Co; conduce a obtener catalizadores altamente activos hacia la HDS con poca incidencia en la reducción del octanaje de la nafta de FCC.

---

* Tesis para optar al título de Doctor en Ingeniería Química

** Facultad de Ingenierías Fisicoquímicas, Escuela de Ingeniería Química. Director: Prof. Aristóbulo Centeno, Ph. D. Co-directora: Prof. Sonia Giraldo, Ph. D.

ABSTRACT

TITLE: INFLUENCE OF THE ACID-BASE PROPERTIES OF THE CoMo SUPPORTED CATALYSTS ON THE OLEFINS HYDROGENATION IN HDS ENVIRONMENTS*

AUTHOR: David de Jesús Pérez Martínez**

KEYWORDS: FCC naphtha, octane number, hydrodesulfurization, hydrogenation, cobalt, molybdenum, support, acid-base properties.

The goal of the FCC naphtha hydrotreatment is to eliminate the maximum amount of sulfur impurities avoiding olefin saturation. Various sets of support families were used to prepare CoMo catalysts in order to analyze the effect of support modification on the FCC naphtha hydrotreatment. The support families used were amorphous aluminosilicates (ASA), sodium modified ASA, and alumina modified with boron, sodium or potassium. Prepared catalysts were characterized by XRD, XPS, Raman, nitrogen adsorption-desorption isotherms, ammonia TPD and infrared of adsorbed pyridine and/or CO_2. Although each support family has different surface properties, which influence in a different way the catalytic performance, some common factors were observed in the catalysts with better performances. It was found that support modification influences the catalytic performance by two essential factors. On one hand, the support acid-base properties and the different OH surface groups existing on its surface have a strong influence in the distribution of Mo and Co oxide species. By modifying the Mo and Co oxide species distribution the hydrodesulfurization and hydrogenation intrinsic activity of the catalysts are consequently affected. On the other hand, the support itself promotes side reactions, predominantly of acid-type nature, like double-bond or skeletal isomerization, cracking and alkylation. It was found that these reactions compete with the hydrodesulfurization and the hydrogenation. Additionally, it was found that depending on the acid-type reactions promoted and the yield of them, these could be helpful or detrimental to preserve the FCC naphtha octane number. Results shown that the preferential presence of weak Brönsted sites, which promotes selectively the double bond isomerization, at the same time that the promotion of an adequate balance of the Mo and Co species distribution conduct to obtain highly HDS active catalysts with low incidence in the reduction of FCC naphtha octane number.

---

* Thesis to obtain the degree of Doctor in Chemical Engineering.

** Faculty of Physical-chemical Engineering, Department of Chemical Engineering. Director: Prof. Aristóbulo Centeno, Ph. D. Co-director: Prof. Sonia Giraldo, Ph. D.

INTRODUCTION

Around the world a lot of efforts have been done to replace the petroleum derived combustibles for other alternative energy sources [1]. However, in the middle-term we will continue depending on petroleum derivatives as our main source of energy, especially as regard as our means of transportation [1]. Thus, the pre-treatment of the combustibles to remove the contaminant heteroatoms, in special sulfur, still have a great importance in the world ambit. Recently, the majority of the industrialized countries have strengthened their environmental legislations and the maximum content of sulfur in both gasoline and diesel has been lowered to concentrations as low as 10 ppm [2-5]. In this respect, although Colombian legislations are not so hard as that of the industrialized countries, in the resolution 1180 of 2006 the maximum permissible sulfur contents in gasoline and diesel to 300 and 500 ppm respectively were lowered [6].

The catalytic hydrotreatment (HDT) is at the time and it will be in the near future the most used technology to remove the sulfur out of the petroleum derivatives [2-5, 7, 8]. As its name indicates, it consists on a high temperature and pressure hydrogen treatment in the presence of a catalyst, which is conventionally Co(Ni)Mo(W)/Al_2O_3. However, in addition to heteroatoms (S, N, O, V, Ni…) removal, there are other reactions which are promoted under the hydrotreatment process like hydrogenation (HYD), hydrodearomatization (HDA), isomerization and cracking [2-5, 7, 8].

In the specific case of gasoline, this is a blend of different refinery streams like those coming from atmospheric distillation, reforming, isomerization or fluidized catalytic cracking (FCC) units, among others [2-4]. The gasoline coming from the first three units has its origin in the lighter petroleum fractions, which generally do not have an important sulfur content [3]. In addition, the feeds of the reforming and

isomerization units have been previously hydrotreated to protect the catalysts used in these processes [3]. On the contrary, the feeds of the FCC unit, like vacuum distillates and residues from the bottom of the atmospheric distillation unit, are quite heavy; consequently, they have high sulfur content [3, 4, 9-11]. This fact makes that the FCC naphtha which represents 30-40% of the gasoline pool contributes with 90% of the gasoline sulfur [3, 4, 9-11]. Thus, FCC naphtha is the most important stream as regards sulfur removal [3, 4, 9-11]. The sulfur compounds present in the FCC naphtha are mainly thiophene, its alkylderivatives and benzothiophene [2, 4, 9, 11]. These compounds are relatively easy to remove at the typical HDT conditions using the conventional catalysts [2, 4, 9, 11]. However, FCC naphtha has a considerable amount of olefins as well (20-40 %), which contributes enormously to improve the gasoline octane number [3, 4, 9-11] and they are saturated almost totally at typical HDT conditions using conventional catalysts. Therefore, the problem of the FCC naphtha HDT process is not the sulfur removal itself, but the significant reduction of the octane number caused by the olefin saturation. The development of catalysts with a high selectivity HDS/HYD of olefins (HydO) is one of the most viable options, with the advantage that it does not implicate extended reforms of the existing HDT units [2-4, 9-15].

The conventional HDT catalysts are composed by a group VI metal sulfide (Mo, W) promoted by a group VIII metal sulfide (Co, Ni) by a synergy effect between both sulfide phases that increases its HDT activity [7, 8]. Several theories have tried to explain this synergetic phenomenon, without an absolute acceptation of one of them [3, 7, 8, 16-19]. The promotion effect is not only on the HDS, but on all the reactions carried out in the sulfide phase, including HydO [3, 11-13, 20]. However, it has been observed that depending on the promoter used, some reactions are more promoted than others [3, 11-13, 20]. For instance, in the case of the conventional Co(Ni)Mo(W)/Al_2O_3, the Ni and Co addition promote similarly the HDS, however Ni promotes more the HydO than Co [2, 3, 9, 20, 21]. This explains

the better efficiency of the catalysts promoted by Co than the one of that promoted by Ni [20, 21].

In addition to the promoter effect it has been shown that the support of the catalyst has an important effect on its performance [2, 3, 10, 14, 15, 17, 18, 22-39]. It has been shown that support modification influence the dispersion, morphology, and coordination of the Mo species [24, 26, 29]. It has even been shown that by modifying the support it is possible to improve the transport of the so called spillover hydrogen [23, 27]. All these modifications, consequence of the sulfide phase – support interaction, conduct to variations in the activity and selectivity of the catalysts. This fact holds the essential idea of this Ph.D. thesis; the support modification is the way to obtain highly selective HDS catalysts.

In this sense, in the literature there is not a clear position about the influence of the support acid-base properties on the activity and selectivity of the catalysts to HDS. Some of the works, based in results using CoMo catalysts supported on basic materials, like MgO [31, 33], hydrotalcites [15] or alkaline metal modified aluminas [14], coincide that the HydO activity increased with the acidity of the catalysts. However, there are other reports where recognized acidic nature materials, like boron doped aluminas [34, 35, 38] and silica-alumina [24, 34], were used as supports of CoMo catalysts obtaining improvements in the selectivity HDS/HydO as well. Even, there is a work where the best selectivity to HDS was obtained by combining the introduction of K and P at the same time [40]. Thus, further investigations including systematic modifications of the acid-base properties of supports used for CoMo catalysts are needed. On the other hand, in another work, it is claimed that with support modifications the catalysts selectivity is more affected by the changes in the CoMo sulfided phase morphology as a consequence of support modification rather than by changes in catalysts acidity [41]. Thus, further investigations concerning support modifications must include also a

characterization of the Mo and Co phase in order to detect if the acid-base properties' changes are the main factor affecting the catalytic performance.

A fact which difficult the analysis of the preceding literature in order to elucidate the influence of supports on the catalytic performance in the HDT of FCC naphtha is the use of different feeds. These feeds sometimes are not so representative of the real reaction environment encountered in the FCC naphtha HDT process. For instance, some works used thiophene to evaluate the catalytic performance and they used the posterior hydrogenation of butene, the product of thiophene HDS, to calculate the selectivity HDS/HydO [24-26, 28, 29, 33-35, 38, 39]. However, in this case HDS and HydO are consecutive reactions, different to that found in the FCC naphtha HDT process, where parallel reactions exist. In other works, real refinery feeds were used. However their use makes very difficult the following of the different reaction schemes that the different compounds can undergo [11, 15, 22, 40, 41]. On the other hand, the works where model sulfur and olefin molecules were used are not so abundant [10, 12-14, 21, 42]. It must be also taken into account that FCC naphtha is composed by different kinds of olefins: linear, branched, with the double bond in internal or terminal positions [2-4, 9, 12, 13]. Thus, any attempt to understand the FCC naphtha HDT process must consider the use of these different kinds of olefins composing the model charge.

In this Ph.D. thesis it is intended to study the influence of support modifications on the catalytic performance in the HDT of synthetic FCC naphtha in order to develop a catalyst highly selective to the HDS which permits to minimize the octane number loss. The strategy followed was the systematic modification of the acid-base properties of the support by different ways in order to obtain a wide range of them. These supports were used to prepare CoMo catalysts and were evaluated in the HDT of synthetic FCC naphtha at typical industrial conditions. This synthetic FCC naphtha was composed by 2-MT, representative of the sulfur compounds, and olefins of different kinds, representative of the linear, branched terminal and

internal olefins present in the FCC naphtha. The acid-base properties of the catalysts were measured by different techniques (IR of pre-adsorbed pyridine and CO_2, TPD of NH_3 and CO_2) in order to determine the acid and basic sites density and strength, as well as the acid site nature (Brönsted or Lewis). The Mo and Co species in the oxide state was also determined using different techniques (XPS, Raman, and XRD). Thus, it was intended to qualitatively correlate the characterization results with the catalytic performance in order to infer some general conclusions about the influence of support modification on the catalysts activity and selectivity in the HDT of FCC naphtha.

In the first chapter, CoMo catalysts supported on aluminas modified with different contents of B, Na or K were used in order to essay modifications of a well known support as alumina in both senses: to make it more or less acidic. In the second chapter amorphous aluminosilicates (ASA) with different Si/(Si+Al) ratios were used as support in order to study a support with more flexible options to modify its acid properties. In the third chapter sodium modified ASA were used in order to obtain a fine control of the acid-properties. Finally, a fourth chapter was written in order to generalize some trends found using the different families of catalysts.

REFERENCES

[1] S. Ramesohl, F. Merten, Energy Policy. 34 (2006) 1251-1259.

[2] I.V. Babich, J.A. Moulijn, Fuel. 82 (2003) 607-631.

[3] S. Brunet, D. Mey, G. Pérot, C. Bouchy, F. Diehl, Appl. Catal., A. 278 (2005) 143-172.

[4] T.G. Kaufmann, A. Kaldor, G.F. Stuntz, M.C. Kerby, L.L. Ansell, Catal. Today. 62 (2000) 77-90.

[5] H. Topsøe, B.S. Clausen, F.E. Massoth, Hydrotreating Catalysis, Catalysis—Science and Technology, Springer-Verlag, Berlin, 1996.

[6] Ministerio de Ambiente, Vivienda y Desarrollo Territorial y Ministerio de Minas y Energía de la república de Colombia. Resolución 1180. 21 de Junio de 2006.

[7] P. Grange, X. Vanhaeren, Catal. Today. 36 (1997) 375-391.

[8] K.G. Knudsen, B.H. Cooper, H. Topsøe, Appl. Catal. A. 189 (1999) 205-215.

[9] C. Song, Catal. Today. 86 (2003) 211-263.

[10] J.-S. Choi, F. Maugé, C. Pichon, J. Olivier-Fourcade, J.-C. Jumas, C. Petit-Clair, D. Uzio, Appl. Catal. A. 267 (2004) 203-216.

[11] J.T. Miller, W.J. Reagan, J.A. Kaduk, C.L. Marshall, A.J. Kropf, J. Catal. 193 (2000) 123-131.

[12] S. Hatanaka, M. Yamada, O. Sadakane, Ind. Eng. Chem. Res. 36 (1997) 5110-5117.

[13] S. Hatanaka, M. Yamada, O. Sadakane, Ind. Eng. Chem. Res. 36 (1997) 1519-1523.

[14] D. Mey, S. Brunet, C. Canaff, F. Maugé, C. Bouchy, F. Diehl, J. Catal. 227 (2004) 436-447.

[15] R. Zhao, C. Yin, H. Zhao, C. Liu, Fuel Process. Technol. 81 (2003) 201-209.

[16] Y.W. Li, B. Delmon, J. Mol. Catal. A. 127 (1997) 163-190.

[17] M. Breysse, P. Afanasiev, C. Geantet, M. Vrinat, Catal. Today. 86 (2003) 5-16.

[18] M. Daage, R.R. Chianelli, J. Catal. 149 (1994) 414-427.

[19] H. Topsøe, B.S. Clausen, Catal. Rev. Sci. Eng. 26 (1984) 395 - 420.

[20] E. Krebs, B. Silvi, A. Daudin, P. Raybaud, J. Catal. 260 (2008) 276-287.

[21] M. Brémaud, L. Vivier, G. Pérot, V. Harlé, C. Bouchy, Appl. Catal. A. 289 (2005) 44-50.

[22] C. Yin, C. Liu, Appl. Catal. A. 273 (2004) 177-184.

[23] P. Baeza, M.S. Ureta-Zañartu, N. Escalona, J. Ojeda, F.J. Gil-Llambías, B. Delmon, Appl. Catal. A. 274 (2004) 303-309.

[24] V. La Parola, G. Deganello, A.M. Venezia, Appl. Catal. A. 260 (2004) 237-247.

[25] Y. Okamoto, K. Ochiai, M. Kawano, K. Kobayashi, T. Kubota, Appl. Catal. A. 226 (2002) 115-127.

[26] A.M. Venezia, F. Raimondi, V. La Parola, G. Deganello, J. Catal. 194 (2000) 393-400.

[27] P. Baeza, M. Villarroel, P. Ávila, A. López Agudo, B. Delmon, F.J. Gil-Llambías, Applied Catal. A. 304 (2006) 109-115.

[28] F. Dumeignil, K. Sato, M. Imamura, N. Matsubayashi, E. Payen, H. Shimada, Applied Catal. A. 287 (2005) 135-145.

[29] M.S. Rana, J. Ramírez, A. Gutiérrez-Alejandre, J. Ancheyta, L. Cedeño, S.K. Maity, J. Catal. 246 (2007) 100-108.

[30] F. Dumeignil, K. Sato, M. Imamura, N. Matsubayashi, E. Payen, H. Shimada, Appl. Catal. A. 241 (2003) 319-329.

[31] L. Kaluza, D. Gulková, Z. Vít, M. Zdrazil, Appl. Catal. A. 324 (2007) 30-35.

[32] T. Klicpera, M. Zdrazil, J. Catal. 206 (2002) 314-320.

[33] T. Klimova, D. Solís Casados, J. Ramírez, Catal. Today. 43 (1998) 135-146.

[34] C. Flego, V. Arrigoni, M. Ferrari, R. Riva, L. Zanibelli, Catal. Today. 65 (2001) 265-270.

[35] F. Dumeignil, K. Sato, M. Imamura, N. Matsubayashi, E. Payen, H. Shimada, Appl. Catal. A. 315 (2006) 18-28.

[36] G.M. Dhar, B.N. Srinivas, M.S. Rana, M. Kumar, S.K. Maity, Catal. Today. 86 (2003) 45-60.

[37] G. Muralidhar, F.E. Massoth, J. Shabtai, J. Catal. 85 (1984) 44-52.

[38] J. Ramírez, P. Castillo, L. Cedeno, R. Cuevas, M. Castillo, J. Palacios, A. López-Agudo, Appl. Catal. A. 132 (1995) 317-334.

[39] Usman, T. Kubota, Y. Araki, K. Ishida, Y. Okamoto, J. Catal. 227 (2004) 523-529.

[40] Y. Fan, J. Lu, G. Shi, H. Liu, X. Bao, Catal. Today. 125 (2007) 220-228.

[41] Y. Fan, G. Shi, H. Liu, X. Bao, Appl. Catal. B. 91 (2009) 73-82.

[42] N. Dos Santos, H. Dulot, N. Marchal, M. Vrinat, Appl. Catal. A. 352 (2009) 114-123.

1. CONTROL OF SELECTIVITY IN FCC NAPHTHA HYDROTREATING BY MODIFYING THE ACID-BASE BALANCE OF CoMo/γ-Al_2O_3 CATALYSTS

1.1. INTRODUCTION

It is well known that olefins present in the FCC naphtha are a major contribution to the octane number in gasoline [1]. Thus, it is imperative to eliminate the maximum amount of sulfur impurities impeding olefin saturation during the hydrotreating (HDT) of FCC naphtha [1]. The development of catalysts highly selective to the HDS reaction is the key to meet the environmental regulations regarding sulfur content in gasoline while preserving octane number [1]. Among the attempts to meet this purpose, support modification appears to be a good approach to obtain more selective catalysts [1-10]. In this sense, most works claim that an increment in the hydrodesulfurization/hydrogenation of olefin (HDS/HydO) selectivity can be observed using less acidic [1,2,9,10] carriers than classical γ-alumina. However, some successful works can be found using more acidic catalysts [3,8,9]. Thus, the particular influence of the acid-base properties of catalysts on selectivity is not yet clear. For instance, Mey et al. [2] found some selectivity improvements, using K doped CoMo/γ-Al_2O_3 catalysts, which were attributed to the modification of the catalysts acid-base properties. K introduction poisons the acid sites where the double-bond isomerization from internal to terminal positions is carried out [2]. Avoiding this reaction is a way to inhibit the hydrogenation because internal olefins are harder to hydrogenate than terminal ones [2,12]. On the other hand, in another work, it is claimed that with support modifications the catalysts selectivity is more affected by the changes in the CoMo sulfided phase morphology than by changes in catalysts acidity [7]. However, in this last work, a real feed was used and there is not information about the reaction schemes and the yields of the individual reactions involved in the reaction system [7]. Thus, with these contradictions in the literature, it is not clear whether the modification of the acid-base properties is the principal factor affecting the HDS/HydO selectivity in the HDT of FCC naphtha.

A fact that could account in some way for the contradictory results in the literature is the use of different kinds of feeds in the catalytic evaluation of the different works. On one hand, there are authors who used model feeds and based their explanations on proposing some kind of reaction schemes, but they used only one kind of olefin either linear or branched [2,3,6,8,11]. On the other hand, there are authors who used real feeds and try to follow the reactivity of the different kind of olefins, but due to the complexity of working with real feeds, it was difficult to propose reliable reaction schemes [4,7,9,10]. Thus, it is necessary a detailed study of the support effects on the HDT of FCC naphtha using model feeds with different kind of olefins. It is also necessary to include in this study the effect of support modification on the acid-base properties and the CoMo phase morphology.

In this chapter, the γ-alumina was modified with B, Na and K in order to obtain supports with a wide range of acid-base properties based on a relatively known support as the γ-alumina. These supports were used to prepare CoMo catalysts and their catalytic performance in the HDT of synthetic FCC gasoline (2-methylthiophene and different kind of olefins dissolved in n-heptane) was studied in detail. In order to elucidate which are the important factors for enhancing the HDS selectivity, the acid-base properties of the catalysts along with the distribution of the different Mo and Co species in the oxide state were determined.

1.2. Experimental

1.2.1. Preparation of catalysts

CoMo catalysts containing 10% MoO_3 and 2% CoO supported on a commercial γ-Al_2O_3 *Procatalyse* (BET surface area: 210 m^2/g, pore volume: 0.6 cm^3g^{-1}, pore diameter: 109 Å) modified with either B, Na or K were prepared. The dopant (B, Na or K), Mo and Co were deposited by successive incipient wetness impregnation. An initial impregnation step was performed either with a solution of H_3BO_3 in

methanol or an aqueous solution of either $NaNO_3$ or KNO_3. Subsequently, the solids were impregnated with an aqueous solution of $(NH_4)_6Mo_7O_{24}{\cdot}4H_2O$ (Merck), and finally the solids were impregnated with an aqueous solution of $Co(NO_3)_2{\cdot}6H_2O$. After each impregnation step, the solids were dried under air flow at 393 K for 12 h, and finally, air calcined at 773 K for 4 h. A CoMo catalysts supported on pure alumina *Procatalyse* was also prepared in the same way as a reference catalyst (named here CMA). The nominal content of B_2O_3 were 2, 3, 5 and 8 wt.%. In the case of Na and K nominal contents of 1, 3 and 5 wt.% were used. The CoMo catalysts modified with B, Na and K were named here CMAB(x), CMANa(x) and CMAK(x) respectively, where x represent the B_2O_3, Na or K contents respectively.

1.2.2. Characterization of Catalysts

1.2.2.1. Catalysts composition

An atomic absorption (AA) spectrophotometer Buck Scientific 210 VGP was used to verify the content of the impregnated metals (K or Na, Co and Mo). The wavelengths used were: 766.5 nm for K, 240.7 nm for Co and 313.3 nm for Mo.

The B content was analyzed by the inductively coupled plasma (ICP) technique. An ICP AES Thermo Jarrell Ash Iris apparatus was used.

1.2.2.2. Textural properties

Textural properties of both catalysts and supports were determined using N_2 adsorption-desorption isotherms obtained with a Quantachrome NOVA 1200 instrument. The catalysts were previously outgassed in vacuum all night at 343 K. The surface area (A_{BET}) was estimated by the BET method. The pore volume (PV) and average pore diameter (PD) were determined by the BJH method.

1.2.2.3. X-ray diffraction (XRD)

XRD was performed on a Siemens D5000 diffractometer using the Kα radiation of Cu (λ = 1.5418 Å). The 2θ range was scanned between 2 and 70º at a rate of 0.02 s^{-1}. Identification of the phases was achieved by using the ICDD-JCPDS database [13].

1.2.2.4. X-Ray photoelectron spectroscopy (XPS)

XPS analyses were performed on samples of the catalysts in the oxidized states with a Kratos Axis Ultra spectrometer (Kratos Analytical–Manchester–UK) equipped with a monochromatised Al X-ray source (powered at 10 mA and 15 kV). The sample powders were pressed into small stainless-steel troughs mounted on a multi-specimen holder. Prior to the XPS analysis the sample was evacuated overnight. The pressure in the analysis chamber was around 10^{-6} Pa. The angle between the normal to the sample surface and the lens axis was 0°. The hybrid lens magnification mode was used with the slot aperture resulting in an analyzed area of 700 µm × 300 µm. The pass energy was set at 40 eV. In these conditions, the energy resolution gives a full width at half maximum (FWHM) of the Ag 3d5/2 peak of about 1.0 eV. Charge stabilization was achieved by using the Kratos Axis device. The following sequence of spectra was recorded: survey spectrum, C 1s, O 1s, Al 2p, Mo 3d, Co 2p, dopant (B 1s, K 2p or Na 1s according to the support) and C 1s again to check the stability of charge compensation in function of time and the absence of degradation of the sample during the analyses. The binding energies (BE) were calculated with respect to the C-(C,H) component of the C 1s peak fixed at 284.8 eV. The spectra were decomposed with the CasaXPS program (Casa Software Ltd., UK) with a Gaussian/Lorentzian (70/30) product function after subtraction of a linear baseline. Molar fractions were calculated using peak areas normalized on the basis of acquisition parameters, sensitivity factors provided by the manufacturer and the transmission function. For the Mo 3d peak the energy

separation for the doublet was fixed at 3.15 eV. For the Co 2p in the case of oxidized state samples the separation of the doublet was not fixed.

1.2.2.5. Confocal laser Raman microscopy (Raman)

Raman was performed with a Labram spectrometer (Dilor) interfaced with an Olympus optical microscope. The excitation radiation was a He-Ne laser (780 nm) operated at a power of 10 mW. The 100x objective of the microscope was used, so that a spot of about 1 μm at the surface of the sample was measured at once. Spectra were obtained by averaging 25 scans of the Raman shift range between 1400 and 100 cm^{-1} recorded in 25 s with a spectral resolution of 1 cm^{-1}. The identity of the spectra obtained at different positions of each sample was systematically verified.

1.2.2.6. Acid-base properties

The acidic properties of catalysts in the oxide state were determined by NH_3 temperature programmed desorption (TPD) and Fourier transformed infrared (FT-IR) spectroscopy using pyridine as a probe molecule. On the other hand, the base properties of the alkaline metal modified catalysts were determined by FT-IR spectroscopy using CO_2 as probe molecule.

For NH_3 TPD experiments, the samples (100 mg) were placed in a quartz reactor and, then, covered by quartz beads. Outlet gases were analyzed with a mass spectrometer equipped with a quadruple mass filter (Balzers QMC 200). Samples were first dehydrated under pure He at 773 K until obtaining a flat water signal (m/z 17 and 18). Then, samples were cooled down under He flow to room temperature (RT). NH_3 adsorption was then performed by passing across the samples a flow of 5% NH_3 in He. Excess NH_3 was evacuated at RT by passing a flow of pure He until obtaining a flat NH_3 signal (m/z 15, 16 and 17). Desorption of the adsorbed NH_3 was performed by increasing the temperature until 873 K at 10 $K.min^{-1}$. The signal

corresponding to m/z of 16, assigned to NH_3, was used for the analysis of the NH_3 TPD curves.

FTIR spectra of pre-adsorbed pyridine or CO_2 were recorded with an IFS55 equinox spectrometer (Brücker) equipped with a DTGS detector using 100 scans and a resolution of 4 cm^{-1}. Catalyst and support powders were pressed (3 tons) into self-supported wafers (15 mg, 13 mm diameter) and placed in a homemade IR cell. Samples were first dehydrated under vacuum (<10^{-5} mbar) at 773 K for 2 h. After cooling down to RT, a first spectrum was taken as reference. Samples were then exposed to 10 mbar of pyridine for 30 min. FTIR spectra were recorded after outgassing the samples (<10^{-5} mbar) in four steps of 1 h: RT, 373, 473 and 573 K.

1.2.3. Catalytic evaluation

Catalytic tests were made in a continuous-flow stainless-steel fixed-bed reactor. The composition of the model charge was 2 wt.% 2-methylthiophene (2-MT) and 20 wt.% olefins dissolved in n-heptane. Dodecane (2 wt.%) was used as an internal standard for the chromatographic analysis. Two kinds of essays were performed. In the essays type A, a commercial mixture of 2,4,4-trimethyl-1-pentene (TM1P) and 2,4,4-trimethyl-2-pentene (TM2P) (3:1 approximately) was used. These are representative of terminal and internal branched olefins in FCC naphtha respectively. On the other hand, in the essays type B, 1-octene was used as a representative of linear olefins.

Before reaction, 0.35 g of catalyst (0.18–0.6 mm particle size) was dried in situ under N_2 flow (100 $ml.min^{-1}$) at 393 K for 1 h, and subsequently, activated with a H_2S/H_2 mixture (15/85, v/v) at 673 K (10 $K.min^{-1}$) for 3 h. Then, the following reaction conditions were fixed: 17 MPa, 523 K, liquid-flow rate of 20 $ml.h^{-1}$ and H_2/liquid feed ratio of 500. Under these conditions, the absence of any diffusion limitations was previously verified. Catalytic tests were conducted until reaching the

steady state. Condensable products were analyzed offline in a HP 6890 gas chromatograph equipped with a HP-1 column (100 m x 0.25 mm x 0.5 μm) and a FID detector. Product identification was performed by GC-MS analyses and by comparing the retention times of some reagent-grade pure compounds in the FID and FPD detectors in the same column.

1.2.4. Expression of results

Results of the catalytic test were expressed in terms of reactants conversion (% C.2-MT, C.TM1P, C.TM2P and C.1-octene) and products yield (%). The following equation was used to calculate the yield of the product P (Y.P), taking into account the conversion of reactant R:

$$Y.P = \frac{\text{mol } P_{output}}{\alpha_{RP} * (\text{mol } R_{input} - \text{mol } R_{output})} * 100 \qquad (1.1)$$

α_{RP} is the ratio between the stoichiometric coefficients of product P and reactant R.

In the case of essays type A, both kinds of olefins (TM1P and TM2P) give similar products; thus, the yield of the olefin products was calculated taking into account the addition of the amounts of both kinds of olefins (mol R = mol TM1P + mol TM2P).

1.3. Results and Discussion

1.3.1. Influence of the dopant (K, Na or B) on the acid-base properties of the catalysts

In Table 1.1, the total acidity and the acidity strength distribution measured by NH_3 TPD for the prepared catalyst are presented. The strength of the acid sites was arbitrarily classified as weak (<423 K), intermediate (423-573 K), and strong (>573)

according to the temperature of NH_3 desorption [15]. The arrows represent the increasing or decreasing tendency of the property with the actual increment in the dopant content. As expected for alkaline metal doped catalysts, the total acidity decreases with increasing alkaline metal content in comparison with the CMA catalyst. However, in catalysts with the same content of alkaline metal, different values of total acidity are observed depending whether K or Na was used. A high decrease of the total acidity of CMAK(1) is observed in comparison with CMA; with increasing the K content to 3 wt.% the decrease is low, but with the subsequent increment to 5 wt.% a high decrease is observed again. On the other hand, in CMANa(x) catalysts, with increasing the Na content up to 1 wt.% a relatively low decrease is observed in the total acidity, but with the subsequent increment to 3 wt.% the decrease is high. In general, for both CMANa(x) and CMAK(x) catalysts the population of weak sites increases with the alkaline metal content, whereas the population of intermediate and strong sites diminishes. However, the ratio of acid sites weak/(intermediate + strong) is higher for CMANa(x) than for CMAK(x) catalysts with the same alkaline metal content.

The total basicity was obtained from the integration of peaks in FT-IR spectra of adsorbed CO_2 after evacuation at 373 K, for the CMANa(x) and CMAK(x) catalysts. In the CMA spectrum, little peaks, which can be attributed to hydrogen carbonates, were observed at 1650 and 1460 cm^{-1} (not shown) [2]. With increasing the alkaline metals content, new peaks, which can be attributed to bidentate carbonates [2], appeared at 1580-1600 and 1340-1370 cm^{-1} (not shown). The total basicity increases with increasing the alkaline metal content, but again the nature of the alkaline metal influences the trend (Table 1). In the case of CMAK(x), only a low increment was observed when increasing the K content up to 3 wt.%, whereas the increment was higher when increasing it from 3 to 5 wt.%. On the other hand, for CMANa(x), the high increments were observed when increasing the Na content to more than 1 wt.%. The total basicity for the CMANa(x) catalysts was always higher than the one for CMAK(x) with the same alkaline metal content.

Table 1.1. Total acidity and acidity strength of the catalysts measured by NH_3 TPD.

Catalyst	Total acidity u.a.	Acidity distribution, %			Total basicity u.a.
		weak	medium	strong	
CMA	15	45	40	15	1.2
CMAK(1)	8 ↓↓	45 ↕	44 ↑	11 ↓	2 ↑
CMAK(3)	7 ↓	54 ↑↑	38 ↓	8 ↓	3 ↑
CMAK(5)	3 ↓↓	69 ↑↑	25 ↓	6 ↓	9 ↑↑
CMANa(1)	12 ↓	51 ↑	40 ↕	9 ↓	3 ↑
CMANa(3)	6 ↓↓	76 ↑↑	21 ↓	3 ↓	11 ↑↑
CMANa(5)	6 ↕	82 ↑↑	15 ↓	3 ↕	42 ↑↑
CMAB(2)	13 ↓	46 ↑	42 ↑	12 ↓	NA
CMAB(3)	17 ↑↑	45 ↓	43 ↑	12 ↕	NA
CMAB(5)	20 ↑↑	40 ↓	46 ↑	14 ↑	NA
CMAB(8)	34 ↑↑	42 ↑	45 ↑	13 ↓	NA

Weak: T<423 K; medium: 423<T<573 K; strong T>523 K
NA: not available

Similar results to the ones found in the present work have been shown by other authors [16,17]. This performance was attributed to the selective adsorption of K or Na on the Al^{+3} tetrahedrally-coordinated-Lewis sites of alumina, which gives rise to the formation of a $[\equiv Al{-}OH]^{-}K^{+}$ complex [16-18]. Thus, a double effect on the alumina surface is produced; stronger acid sites are poisoned and at the same time the complex formation increase the basicity of the site. This fact has been demonstrated by ^{27}Al-RMN studies where the disappearance of the band attributed to Al^{+3} was observed [18]. It was also demonstrated by FT-IR of the OH region [18] where it was observed that K introduction produces a diminution of the type Ia OH groups of the Knözinger and Ratnasamy [19] classification, which according to these authors are associated with the tetrahedral Al^{+3}. Besides the shifting of the IR band attributed to type Ia OH groups is an indication of the $[\equiv Al{-}OH]^{-}K^{+}$ complex presence after K introduction [18].

In the case of CMAB(x) catalysts, the total acidity decreases slightly for the catalysts with 2 wt.% B_2O_3 compared with CMA and, then, increases with increasing boria content (Table 1). Additionally, with increasing boria content, the weak acid sites slightly decrease whereas the intermediate ones slightly increase. Fig. 1.1 presents the Brönsted to Lewis ratio of the CMAB(x) catalysts obtained from the FT-IR of adsorbed pyridine after evacuation at RT, 373, 473 and 573 K. Peaks at 1620 and 1640 cm^{-1}, attributed in the literature [20,21] to ν_{8a} band of pyridine bonded to Lewis and Brönsted sites respectively, were mathematically decomposed using Gauss type curves and integrated. The values resulting from their integration were used for the estimation of the Brönsted/Lewis ratio. At RT and 373 K, the Brönsted/Lewis increased monotonously with increasing B_2O_3 content; however, the values for CMAB(2) and CMAB(3) were very close to each other. A similar trend was observed at 473 K, but in this case Brönsted acidity was only detected for catalyst with a content ≥ 5 wt.% B_2O_3, whereas at 573 K, Brönsted acidity was not detected for any of the catalysts. Thus, the acidity strength of Brönsted sites created with boron introduction, with the impregnation method and up to the B_2O_3 content used in the present work, seems to be rather weak.

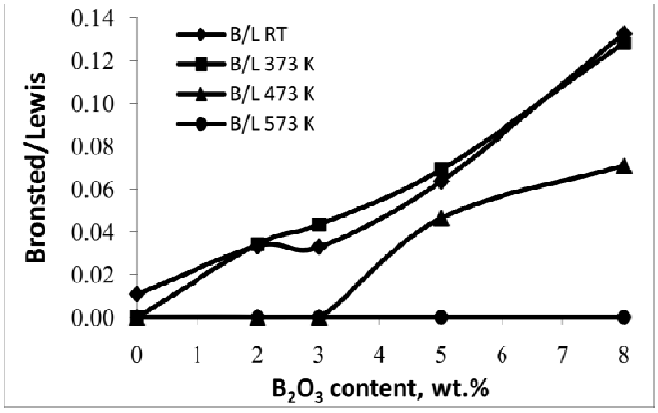

Fig. 1.1. Brönsted to Lewis ratio of CMAB(x) catalysts obtained by FT-IR of adsorbed pyridine after desorption at room temperature (RT), 373, 473 and 573 K.

The increase in the acidity strength, particularly in Brönsted acid sites, could be attributed to the boron deposition on the most basic OH groups on alumina surface [22], which origins the formation of a well dispersed layer of B species in trigonal (BO_3) and tetrahedral (BO_4) coordination [23,24-31]. According to Tanabe's [31] hypothesis about binary oxide systems, this borated species generate a charge excess in the alumina network giving rise to the increase in acidity. The increase in acid strength and Brönsted sites seems to be related to the relative content of tetrahedral B in the catalyst [23,24,26,30,32]. The increment in the acidity strength of boron doped catalysts will be expected because B (2.0) has a higher electronegativity than Al (1.5); thus, B-OH groups would have a higher acidity strength than Al-OH ones in the catalyst surface [28]. It is also reported that the extra oxygen in tetrahedral borated species would play a decisive role in its abilities to remove electron or donate protons [30].

1.3.2. Influence of the dopant on the Co and Mo coordination and speciation

Table 1.2 lists the textural properties of prepared catalysts. It can be observed that the A_{BET} of boria modified catalysts is almost not affected by boria introduction up to 5 wt.% boria content; but the catalyst with 8 wt.% boria content present a drastic diminution of the A_{BET}. In the case of the alkaline metals modified catalysts the A_{BET} diminishes with increasing alkaline metal content. Particularly high reductions in the A_{BET} compared with that of the CMA catalysts were observed for the catalysts with the highest content of alkaline metal.

Table 1.2. Textural properties of the prepared catalysts

Material	A_{BET} ($m^2\ g^{-1}$)	PV ($cm^3\ g^{-1}$)	PD (Å)
CMA	194	0.49	100
CMAB(2)	205	0.51	100
CMAB(3)	204	0.49	95
CMAB(5)	202	0.49	97
CMAB(8)	136	0.43	126
CMAK(1)	190	0.5	106
CMAK(3)	179	0.48	108
CMAK (5)	162	0.45	104
CMANa(1)	194	0.51	106
CMANa(3)	183	0.48	106
CMANa(5)	164	0.45	113

Fig. 1.2 shows the difractograms of CMA and CMANa(5) catalysts. All catalyst samples, but CMANa(5), exhibit similar spectra to the one of CMA, with only the broad bands typical of γ-Al_2O_3 with poor cristallinity [13]. The CMANa(5) catalyst presents in addition little sharp bands typical of $Na_2MoO_4.2H_2O$ [13].

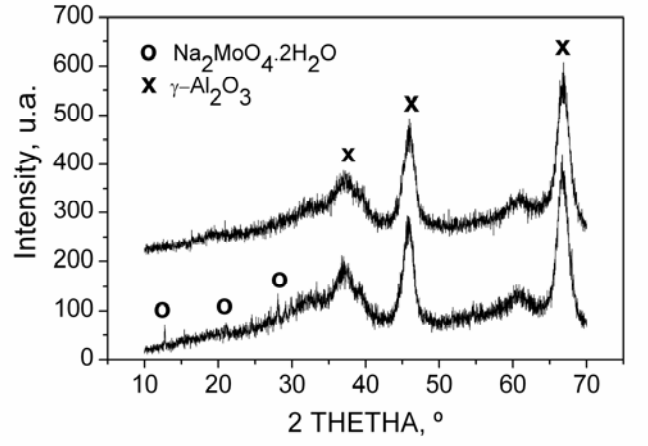

Fig. 1.2. XRD diffractograms of the catalysts CMA and CMNa(5).

Table 1.3 lists BE and FWHM extracted from the analysis of XPS spectra of Mo $3d_{5/2}$ and Co $2p_{3/2}$ of some selected catalysts samples in the oxide state. In addition, atomic ratios of Co 2p and Mo 3d relative to Al 2p are also given. The broadness of the Mo $3d_{5/2}$ and Co $2p_{3/2}$ peaks observed is an indication of several Mo(VI) and Co oxo-species [20]. Boron has not effect on the Mo $3d_{5/2}$ BE, but a slight broadening of the Mo $3d_{5/2}$ FWHM is observed in comparison to the CMA catalyst, which suggest the presence of other Mo moieties. On the contrary, with the introduction and increment in the content of alkaline metals, a slight shifting of the Mo $3d_{5/2}$ BE to lower values, as well as a narrowing of the FWHM are induced. The effect of the Na on the narrowing of the Mo peaks is higher than that of K. The narrowing of the peaks could be interpreted as a result of the transformation of the polymeric Mo species ($Mo_7O_{24}^-$) into monomeric species (MoO_4^-) as reported by other authors [33,34]. This fact is in accordance with the observed in XRD measurements, where the compound Na_2MoO_4 was found for the catalysts CMANa(5) and it will be addressed again in the Raman results.

Table 1.3. XPS analysis of some selected catalysts in the oxidized state.

Catalysts	Co $2p_{3/2}$		Co 2p relationships			Mo $3d_{5/2}$		Atomic ratios	
	BE	FWHM	ΔE_1*	ΔE_2†	Ip/Is‡	BE	FWHM	Co/Al	Mo/Al
CMA	781.43	2.96	15.71	5.28	0.62	232.7	2.06	0.032	0.053
CMAK(1)	781.53 ↕	2.90	15.65	5.47 ↑	0.62 ↕	232.7 ↕	1.91 ↓	0.031	0.049
CMAK(3)	781.3 ↓	2.84	15.61	5.51 ↑	0.79 ↑	232.5 ↓	1.79 ↓	0.029	0.043
CMAK(5)	780.51 ↓	3.11	15.55	5.98 ↑	0.85 ↑	232.4 ↓	1.75 ↓	0.042	0.050
CMANa(3)	781.04 ↓	2.72	15.61	5.47	0.75 ↑	232.5 ↓	1.63 ↓	0.028	0.043
CMAB(3)	781.71 ↑	3.10	15.67	5.24 ↕	0.62 ↕	232.7	2.19 ↑	0.030	0.049
CMAB(8)	781.75 ↑	2.86	15.63	4.86 ↓	0.46 ↓	232.7	2.19 ↑	0.032	0.046

*ΔE_1: energy difference between Co $2p_{3/2}$ and Co $2p_{1/2}$. †ΔE_2: energy difference between the principal photopeak and the satellite.‡Ip/Is: ratio between the intensity of the principal photopeak and its satellite.

In the case of the Co 2p spectra, patterns characteristic of oxidic cobalt are revealed, with two spin-orbit components (Co $2p_{3/2}$ and Co $2p_{1/2}$), the presence of

strong shake up satellites, and Co $2p_{3/2}$ BE of the principal photopeak of 781.1-782 eV. In order to determine the possible Co oxide species present in catalysts the spin-orbit splitting (ΔE_1), the energy difference between the principal photopeak and the satellite peak (ΔE_2), as well as the relative intensity of the principal to the satellite peak were taken into account [35]. These values are also reported in Table 1.3. It is known that ΔE_1 values of diamagnetic cobaltous compounds (Co^{3+}), cobalt metal and cobalt sulfide are ca. 15 eV; whereas ΔE_1 values of paramagnetic cobaltous compounds (Co^{2+}) are ca. 16 [33-37]. ΔE_2 values are affected by the coordination of Co^{2+} atoms with oxygen compounds: ca. 5 eV for tetrahedral coordination and ca. 6 eV for octahedral one [33-37]. The satellite peak of Co^{2+} compounds ($CoMoO_4$ and $CoAl_2O_4$) is much higher in intensity than that of Co^{3+}, Co^o or Co sulfide. Thus, compounds like Co_3O_4, which contains two distinct cobalt ions Co^{2+} and Co^{3+} in the ratio of 1:2, present a value of Ip/Is higher than that of Co^{+2} compounds [33-37].

According to these criteria, the values reported in Table 1.3 for the Co 2p XPS spectrum of CMA (Co $2p_{3/2}$ BE: 781.4 eV, ΔE_1: 15.71, ΔE_2: 5.28 and Ip/Is: 0.6) suggest the presence of a mixture of Co_3O_4, $CoMoO_4$ and $CoAl_2O_4$. The concentration of α-$CoMoO_4$, if any, should be low because the characteristic splitting of the O 1s signal of this compound [38] does not appear in the catalyst. When the concentration of alkaline metals increases further than 1 wt.%, the Co $2p_{3/2}$ BE is shifted to lower values at the same time that ΔE_2 and Ip/Is increase. This trend suggests that the concentration of Co_3O_4 increases at expenses of the concentration of either $CoMoO_4$ or $CoAl_2O_4$ [33-36]. On the other hand, when boria concentration increases, the Co $2p_{3/2}$ BE is shifted to higher values at the same time that ΔE_2 and Ip/Is decrease. This trend suggests that when boria concentration increases the concentration of Co_3O_4 diminishes and Co^{+2} compounds are formed. These Co^{2+} compounds are formed at expense of the free Co_3O_4 oxide; thus, we presumed these compounds should be associated to the support in the form of a cobalt aluminate or cobalt borate. Indeed, some authors

have claimed, in the particular case of Co/Al_2O_3, that boron suppresses the formation of Co_3O_4 due to an increase in the interaction between Co and the carrier [37].

As the catalysts studied contain d^o transition metal oxide species (MoO_3) and d^5 (CoO), the Raman spectroscopy technique was used to obtain information about the types of metal oxides species formed in the calcined catalysts [33,39]. Several factors such as metal loading, pH, precursor, impregnation method, and impurities are known to influence the exact position of the Raman bands. However, a preliminary assignment can be done based on the preceding literature [33,34,39-43].

Fig. 1.3, 1.4 and 1.5 show the Raman spectra of CMANa(x), CMAK(x) and CMAB(x) catalysts respectively. The CMA catalyst Raman spectrum has been included in all figures for comparison purposes. The CMA catalyst Raman spectrum shows a broad band at ca. 920-950 cm^{-1}, with shoulders at both sides (at ca. 900 and 960). There are also other broad bands at ca. 320-350, 225 and a little peak at ca. 820 cm^{-1}. First of all, it can be noticed that both Co and Mo are well dispersed on the pure alumina (CMA), due to the lack of peaks characteristic of Co compounds (450-700 cm^{-1}) and free MoO_3 aggregates (990-1000 cm^{-1}) [23,33,34,42-44]. Additionally, the presence of $Al_2(MoO_4)_3$ (1000-1010 cm^{-1}) can be ruled out [42]. The region 750–1000 cm^{-1} is where the bands for stretching of Mo–O bonds are typically observed [33,42]. Inside the broad band at ca. 920-950, a variety of Mo species could be placed; the more likely according to literature [33,34,39-43] are $Mo_7O_{24}^{6-}$ octahedral species (946-951 cm^{-1}, yellow lines in Fig. 3-5) and MoO_4^{2-} with distorted tetrahedral symmetry (at ca. 916 cm^{-1}, purple lines). Some contributions from Mo-O-Co stretching vibrations in $CoMoO_4$ species (930 and 870 cm^{-1}, blue lines) cannot be ruled out. However, because of the successive impregnation method used in the present work, the presence of this compound, if any, should be low [34], according to the one found in the XPS analysis. The

shoulder at ca. 900 cm^{-1} can be attributed to monomeric undistorted MoO_4^{2-} species (at ca. 892 and 807 cm^{-1}, red lines) and the other shoulder at ca. 960 cm^{-1} to larger polymeric species like $Mo_8O_{26}^{4-}$ (958-960 cm^{-1}).

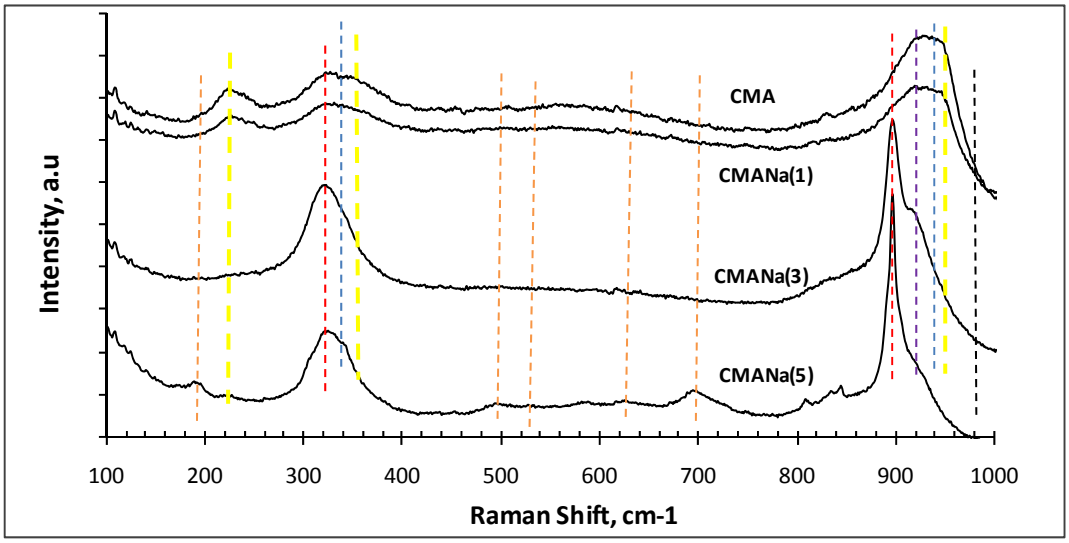

Fig. 1.3. Raman spectra of CMANa(x) catalysts.

The relative larger population of octahedral Mo species to tetrahedral species is in accordance with the displacement to the left of the equilibrium of heptamolybdate ions with the monomolybdate ones (equation 1.2) at the natural pH of the $(NH_4)_6Mo_7O_{24}{\cdot}4H_2O$ solution (pH 5-6) used for the impregnation in the present work [42]. It is known that at pH values higher than 6.5 the MoO_4^{2-} anion is stable [42]. According to equation 1.2, a decrease in pH to 4.5 leads to complete formation of $Mo_7O_{24}^{6-}$ and further decrease in pH to 1.5 leads to polymerization of $Mo_8O_{26}^{4-}$ [42] (equation 1.3).

$$Mo_7O_{24}^{6-} + 4H_2O \leftrightarrow 7MoO_4^{2-} + 8H^+ \qquad (1.2)$$

$$Mo_7O_{24}^{6-} + 7MoO_4^{2-} + 2H^+ \leftrightarrow [H_2Mo_8O_{26}]^{6-} \qquad (1.3)$$

In the case of CMANa(x) catalysts (Fig. 1.3), it is observed that in comparison with the CMA spectrum, with the introduction of only 1 wt.% Na, the intensity of the shoulder at ca. 900 cm^{-1} (undistorted MoO_4^{2-}) increased, whereas the shoulder at ca. 960 cm^{-1} ($Mo_8O_{26}^{4-}$) disappeared, and the intensity of the peak at ca. 950 cm^{-1} ($Mo_7O_{24}^{6-}$) diminished. In the CMANa(3) spectrum, the shoulder at ca. 900 cm^{-1} in CMA spectrum was transformed in a sharp peak, the peak at ca. 950 cm^{-1} almost disappeared, and the intensity of the peak at ca. 920 cm^{-1} diminished drastically. Finally, in the CMANa(5), it is only observed a sharp peak at ca. 900 cm^{-1} and a little shoulder at ca. 920 cm^{-1}. This is in accordance with the XRD analysis (Fig. 1.2) where the presence of crystalline Na_2MoO_4 was detected. Thus, this compound should be responsible of the peak at ca. 900 cm^{-1} [34,42,43]. The increasing narrowing of the Mo $3d_{5/2}$ band in the XPS spectra with the introduction of alkaline metals is also explained by the preference in the formation of tetrahedral Mo species [33,34]. Another noticeable fact in the CMANa(5) Raman spectrum is the appearance of bands at ca. 190, 490, 530, 630 and 690 cm^{-1}, which resembles F2g phonon modes (199, 621, 681 cm^{-1}), and Eg and A1g modes (477 and 525 cm^{-1}) present in Co_3O_4 Raman spectrum [34]. This is in accordance with the findings of the XPS analysis stated above. The formation of Co_3O_4 could be an explanation to the great reduction in the BET surface area observed in the CMANa(5) and CMAK(5) catalyst in comparison with CMA (around 30 m^2g^{-1}, Table 1.2). Some authors [41] have reported that when this compound is formed on the surface of the catalysts, it could conduct to the blocking of the pores and subsequently to a reduction in the BET surface area.

The trend shown in Fig. 1.4, with respect to the changes in the Raman spectra of CMAK(x) when increasing the K content, is similar to the one observed in the case of CMANa(x) spectra. However, in the case of K the transformation of the polymolybdates into monomolybdates is less drastic than in the case of Na, which suggests that the K_2MoO_4 formed are not crystalline in accordance with the XRD analysis where crystalline K_2MoO_4 was not found [43]. Another difference is the

fact that in the CMAK(5) spectrum the peaks corresponding to Co_3O_4 are more defined than in the CMANa(5) one.

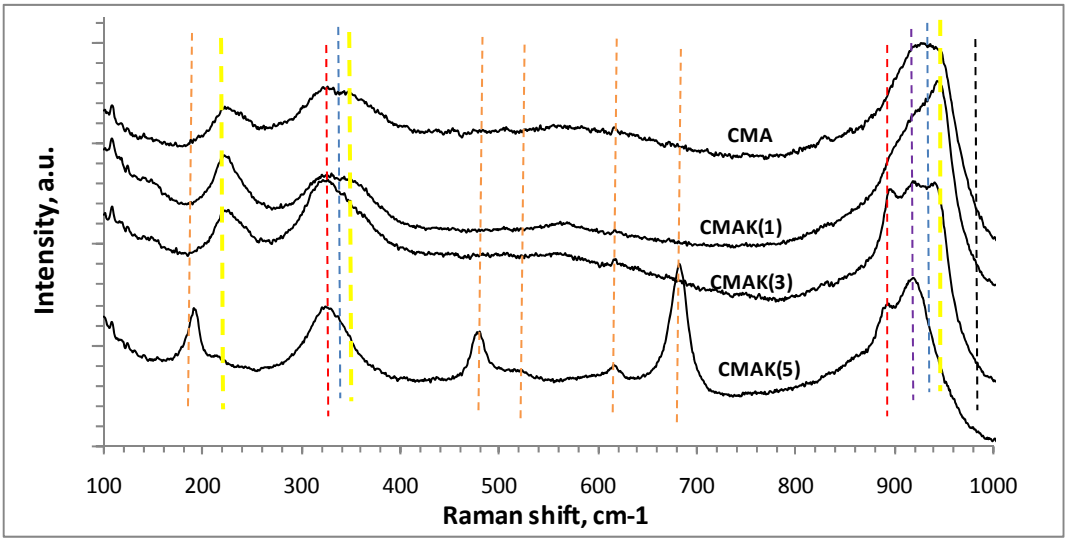

Fig. 1.4. Raman spectra of CMAK(x) catalysts.

On the other hand, in the case of CMAB(x) catalysts (Fig. 1.5) the evolution of molybdate species with increasing boria content was contrary to the one of the alkaline metals. When boria content was increased, there was a diminution of the peaks corresponding to monomolybdates and an increase in the relative intensity of the peaks corresponding to polymolybdates. Thus, in these catalysts the relative population of $Mo_7O_{24}^{6-}$ and $Mo_8O_{26}^{4-}$ to MoO_4^{2-} species is higher than in the case of the CMA. This is in agreement with XPS results, where a broadening of the Mo $3d_{5/2}$ band was observed.

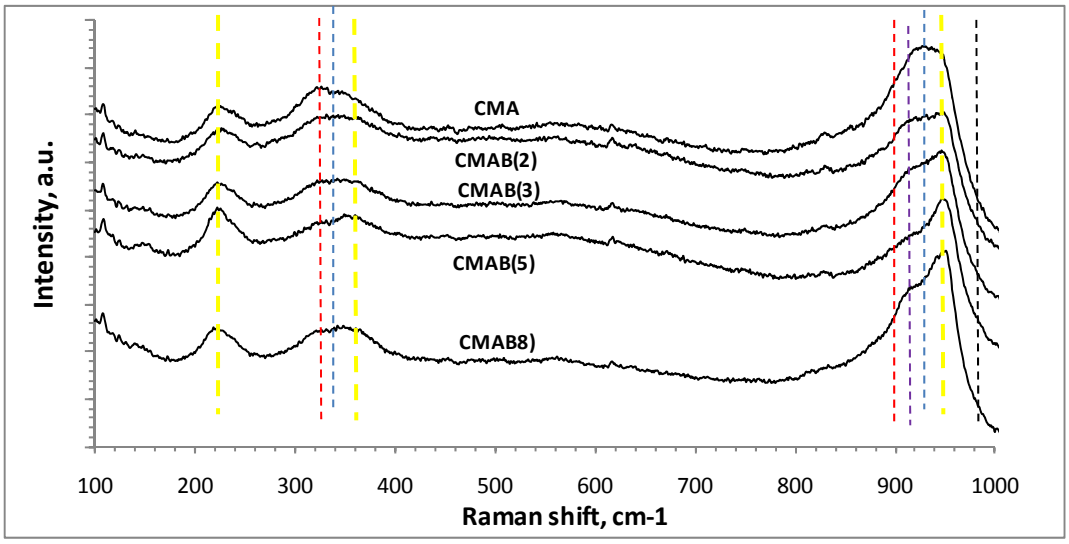

Fig. 1.5. Raman spectra of CMAB(x) catalysts.

Other authors have also found similar results using not only Raman, but also other techniques like UV-Vis DRIFT [23,33,34,44,45]. With increasing boria content on alumina, boria hydroxyls progressively replaced alumina ones beginning with the basic ones until formation of a cover layer [25,46]. The OH of some of the monomeric boria species would condense to form an oxygen bridge, which links one monomeric species with the one next to it to finally form a cover layer [25]. In a recent work of our group [46], we found that in borated aluminas with a boria content ≤ 5 wt.% there is a coexistence of boria and alumina hydroxyl groups. But, for a borated alumina with 8 wt.% boria content the surface is composed almost exclusively by boria hydroxyls. Consequently, if we need to support a metal on the surface of borated aluminas, according to the content of boria in the support, this metal would be attached either to a mixture of boria and alumina hydroxyls or to boria hydroxyls only. This fact could explain the formation of larger polymeric Mo species in detriment of monomeric ones because, on one hand, Mo is stronger bonded to Al than to B atoms [23,37,44,45], and on the other hand, the increase in boria content causes an increase in the local point of zero charge (PZC), which could cause a displacement of the equilibrium between monomeric and polymeric

Mo species (in equation 1.2 to the left and in the equation 1.3 to the right) [23,44,45].

1.3.3. Influence of the dopant on the catalytic performance

1.3.3.1. Reaction schemes

A lot of organic substances were found in the reactor outlet depending on the kind of olefin and on the catalysts used in the catalytic test. A complete identification of all reaction products was done. From this identification along with the comparison with other reactions schemes proposed in the literature [1-6,11], the following reactions schemes are proposed for 2-MT, branched (TM1P and TM2P) and linear (1-octene) olefins.

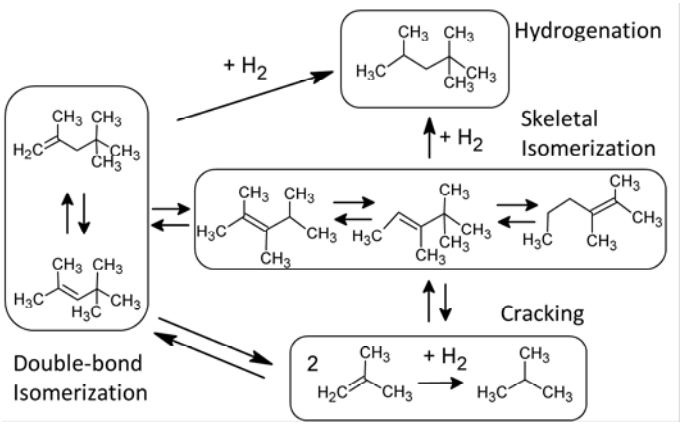

Scheme 1.1. Branched olefin reaction scheme.

In the scheme 1.1, it is observed that both kinds of branched olefins (TM1P and TM2P) are present in the feedstock; thus, there is an equilibrium between them related to the double-bond isomerization [2,4]. The HydO product is isooctane (iC8), the cracking ones are isobutene and isobutane (iC4s), and the skeletal isomerization ones (iC8-ske) are other trimethylpentenes different from 2,4,4-TMPs and dimethylhexenes in a lower proportion [2,4]. The yield of oligomerization

products was close to 1%; thus, they were not taken into account in the product distribution. Thiols were not observed, at least in quantifiable concentrations, maybe because their production is limited thermodynamically [2]. Thiol productions reported in other papers [2, 4, 11, 47] were always low. According to Hatanaka et al. [25] who studied the influence of various olefins in thiols production, 2,4,4-TMPs registered the lowest production in comparison with other olefins such as 1-octene, 1-hexene and cyclohexene. These authors [25] also report that thiols derived from 2,4,4-TMPs were only detected after H_2S extra-addition in the feed.

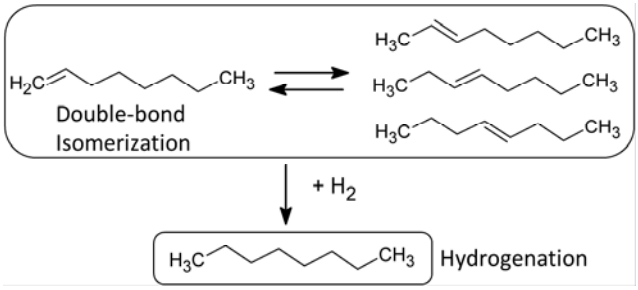

Scheme 1.2. Linear olefin reaction scheme.

In the scheme 1.2, it is observed that the main reactions that linear olefins undergo are the double-bond isomerization of 1-octene to internal olefins like 2-, 3- and 4-octenes (nC8s=) and the hydrogenation of both internal and terminal olefins to octane.

In the scheme 1.3, it is observed, on one hand, a typical HDS scheme with 2-methyltetrahydrothiophene (2-MTHT) as the main intermediate product from the hydrogenation pathway and C5 hydrocarbons (C5s) as the final HDS products [1,2,47,48]. On the other hand, alkylmethylthiophenes (AMT), product of the alkylation of 2-MT with the olefins present in the reaction environment, are also observed [49,50]. In the essays type A, the most abundant was

isobutylmethylthiophene (iC4MT), whereas in the essays type B, only octylmethylthiophenes (C8MT) were detected in minor amounts [1,49,50].

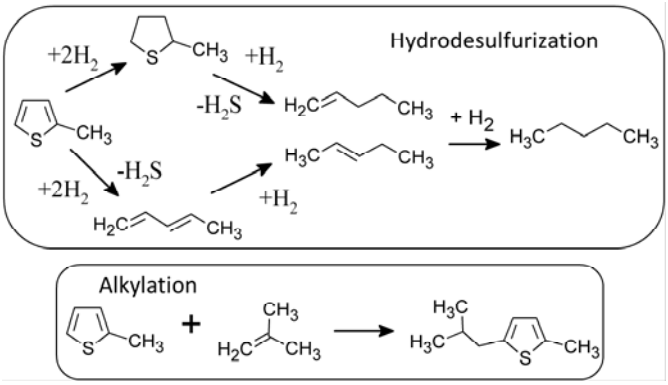

Scheme 1.3. 2-methylthyophene reaction scheme.

The yields of the products listed above, as well as reactants conversions in essays type A and B were plotted as a function of the dopant content (K, Na or B_2O_3) in Fig. 1.6, 1.9, 1.12 and 1.7, 1.10, 1.13 respectively. In these figures, product yields are represented in the form of stacked columns and conversions as points linked by lines. The zero value in the X axis represents the conventional CoMo catalyst supported on undoped γ-Al_2O_3.

Regarding selectivity, in essays type A two kinds of branched olefins were used: terminal (TM1P) and internal (TM2P). Thus, in order to take into account individually the reactivity of each olefin, two selectivities HDS/HydO were defined according to the olefin used to calculate it. The selectivity defined as the ratio between the HDS activity and the conversion of terminal branched olefins, named here as $S^{HDS/HydO-Bt}$ (equation 1.4) and the one defined as the ratio between the HDS activity and the conversion of internal branched olefins $S^{Hds/HydO-Bi}$ (equation 1.5). In this way cracking products are also taken into account as a detrimental reaction in the process. In essays type B, only 1-octene was used as

representative of linear olefins, thus the selectivity was defined as the ratio between the HDS products and the HydO products and named here as $S^{HDS/HydO-L}$ (equation 1.6).

$$S^{\mathrm{Hds/HydO-Bt}} = \frac{Y.C5s \times C.2MT}{C.TM1P} \quad (1.4)$$

$$S^{\mathrm{Hds/HydO-Bi}} = \frac{Y.C5s \times C.2MT}{C.TM2P} \quad (1.5)$$

$$S^{\mathrm{Hds/HydO-L}} = \frac{Y.C5s \times C_{2MT}}{Y.C8 \times C.1octene} \quad (1.6)$$

In the case of essays type B, in order to take into account the relative importance of the double bond isomerization with respect to the HYD, the ratio between the double-bond isomerization and the HYD of linear olefins (isom/HydOL) was also calculated. The selectivities calculated as well as the ratio isom/HydOL were plotted as a function of the dopant content (K, Na or B_2O_3) in Fig. 1.8, 1.11 and 1.14. The zero value in the X axis represents the conventional CoMo catalyst supported on undoped γ-Al_2O_3.

1.3.3.2. Catalytic performance of alkaline metals doped catalysts

In the Fig. 1.6, the conversion of reactants and the yield of products in essays type A for CMAK(x) catalysts are presented. The conversions of 2-MT, TM1P and TM2P diminished with increasing K content. In the case of CMAK(5) catalyst, the TM2P conversion was negative, i.e., TM2P was produced as a result of TM1P double-bond isomerization. Thus, the yield of products was calculated only taking into

account the TM1P conversion and a low yield of TM2P appears for this catalyst. Isooctane was the main product of olefins. A low yield of cracking and skeletal isomerization products, which disappeared progressively with increasing K content, is also observed. C5s were the main products of 2-MT, whereas a low yield of 2-MTHT, which increases when increasing the K content, is also observed. A very low yield of AMT is observed only for CMA and CMAK(1) catalysts. These changes in the product distribution in essays type A conduct to changes in the selectivity (Fig. 1.7.a). $S^{Hds/HydO-Bi}$ increased with increasing K content, and due to the negative conversion of TM2P mentioned already, the value for CMAK(5) was indefinite (∞). The low reactivity of internal olefins for CMAK(x) compared to the CMA catalyst was compensated with a high reactivity of the terminal ones. As a consequence $S^{HDS/HydO-Bt}$ diminished up to 3 wt.% K, and then it increased again.

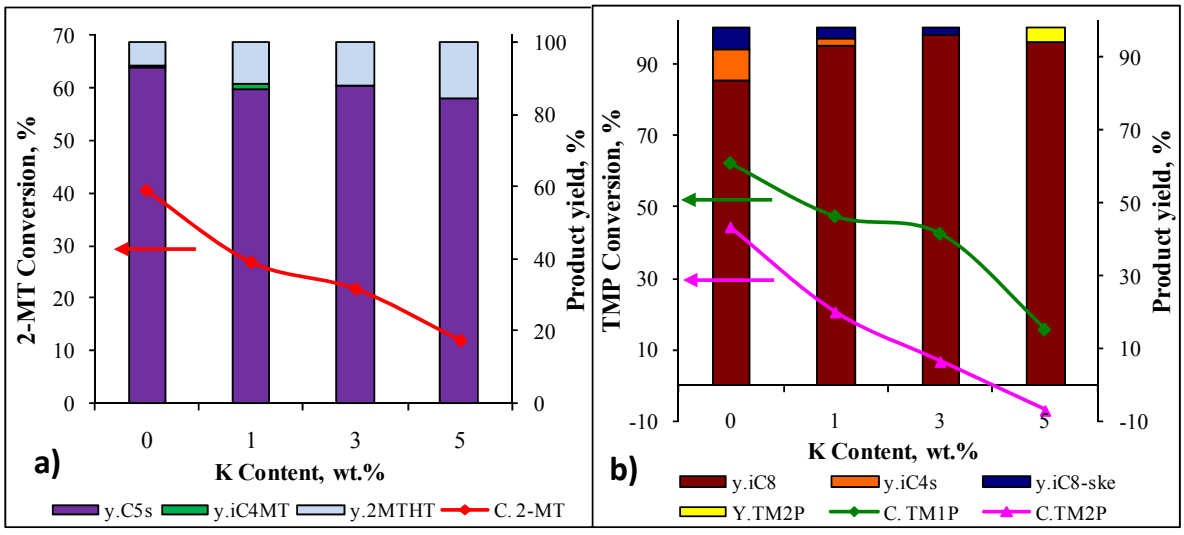

Fig. 1.6. Influence of the K content on the reactants conversion (lines) and product yields (stacked columns) of CMAK(x) catalysts in essays type A (branched olefins).

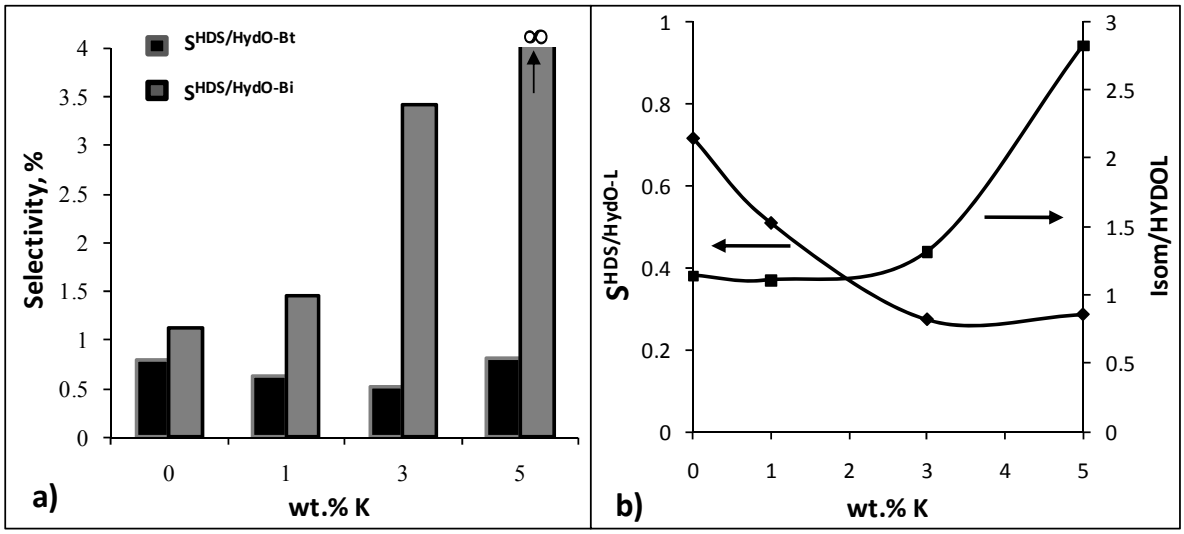

Fig. 1.7. Influence of the K content on the selectivities in napththa HDT of CMAK(x) catalysts in essays type A (a) and B (b).

In Fig. 1.8, the conversion of reactants and the yield of products in essays type B are observed. 2-MT conversion and the yield of its products have a similar performance than in essays type A. However, HDS activity was always lower than in essays type A, which indicates an inhibition effect of the linear olefins. The conversion of 1-octene was almost 100% for catalysts with up to 3 wt.% K and only diminished for CMAK(5). The main olefins product were nC8s= followed by octane. With increasing K content up to 1%, there are not significant changes in linear olefin products distribution, but subsequent increase in K content result first (1 to 3 wt.%) in a low increase of the yield of nC8s= at expense of the octane yield and after (3 to 5 wt.%) in a high one. As a consequence the ratio isom/HydOL also increases with increasing K content in the same way (Fig. 1.7.b). Increasing the nC8s= yield is important in the conservation of the gasoline octane number, because internal linear olefins have a much better octane number than external ones [51]. However, $S^{HDS/HydO-L}$ diminished drastically with increasing K content up to 3 wt.% K, and then it stayed approximately constant. Thus, it can be observed that with increasing the K content on alumina, the trends in olefins reactivity depends on the nature of the olefin (linear, branched internal or terminal).

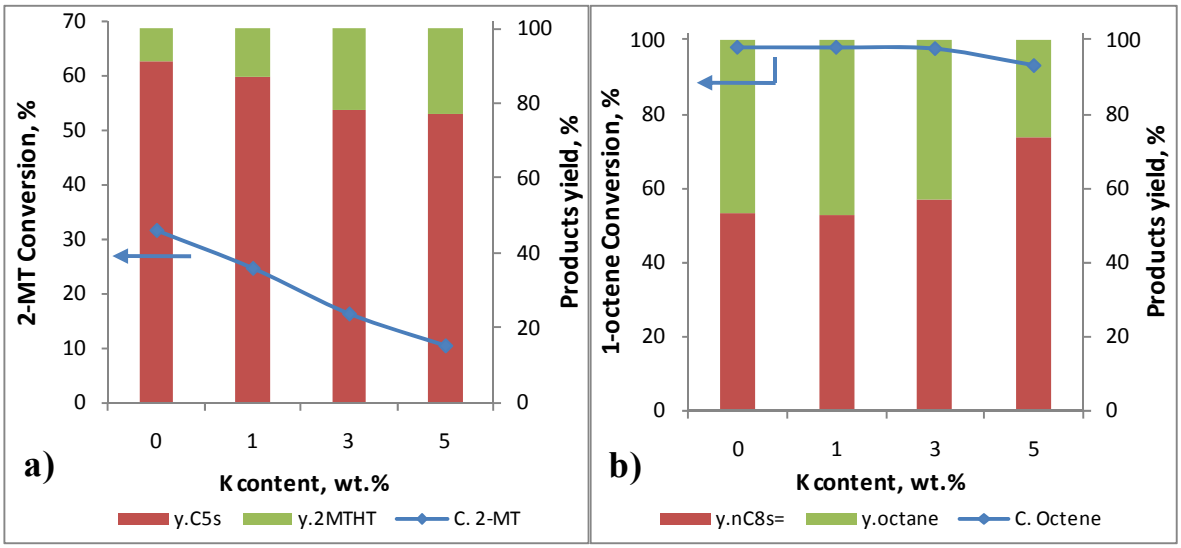

Fig. 1.8. Influence of the K content on the reactants conversion (lines) and product yields (stacked columns) of the CMAK(x) catalysts in essays type B (linear olefins).

In general, the trends in the catalytic performance of CMANa(x) catalysts with increasing alkaline metal content were similar to the ones of CMAK(x). However, it was observed that Na has less influence than K on the decreasing or increasing trend of the catalysts activity and selectivity at low contents (1 wt.%), but at higher contents (3 and 5 wt.%), the influence of Na was more important than that of K (Fig. 1.9 and 1.11). For instance, negative conversions of TM2P were registered for catalysts with Na contents since 3 wt.%. In consequence, the $S^{Hds/HydO-Bi}$ value (Fig. 1.10.a) for these catalysts was indefinite (∞). In addition, the ratio isom/HydOL (Fig. 1.10.b) passed through a minimum for the catalyst CMANa(1), but with subsequent increments in the Na content it was increased drastically and almost linearly.

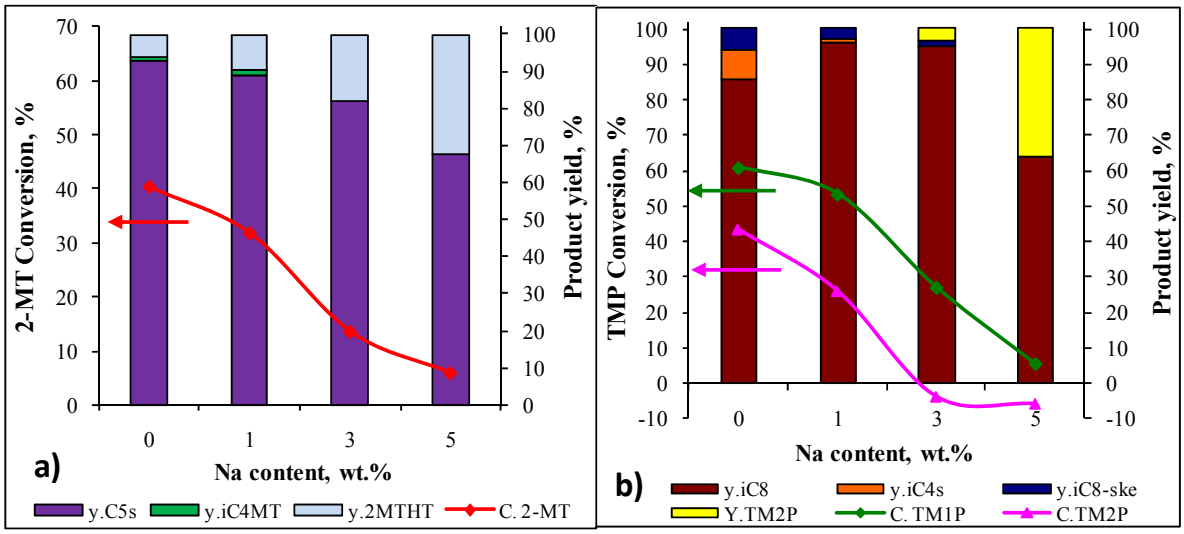

Fig. 1.9. Influence of the Na content on the reactants conversion (lines) and product yields (stacked columns) of CMANa(x) catalysts in essays type A (branched olefins).

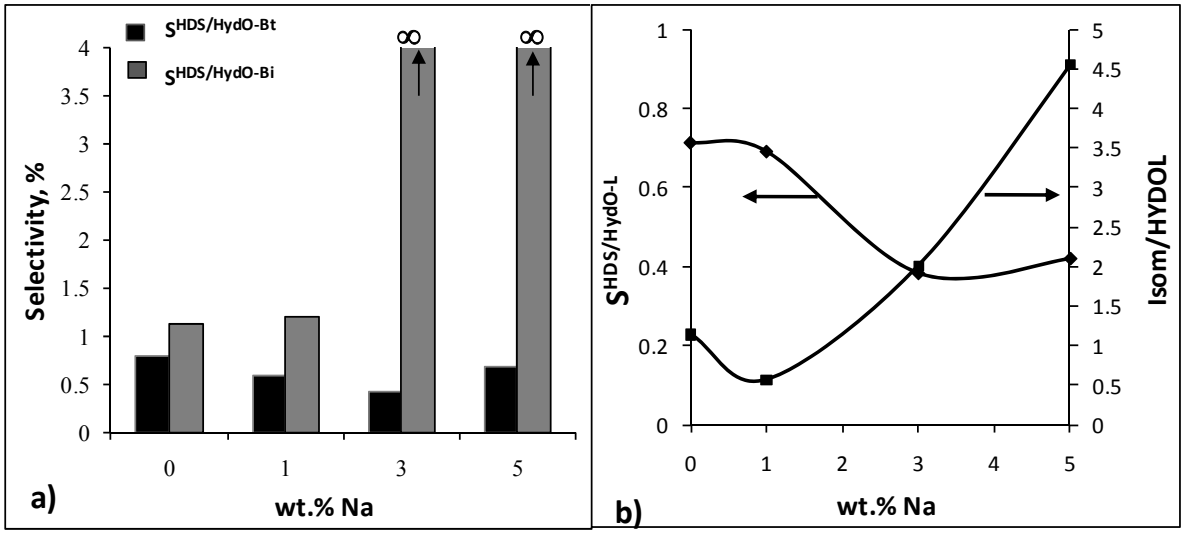

Fig. 1.10. Influence of the Na content on the selectivties of CMANa(x) catalysts in essaies type A (a) and B (b).

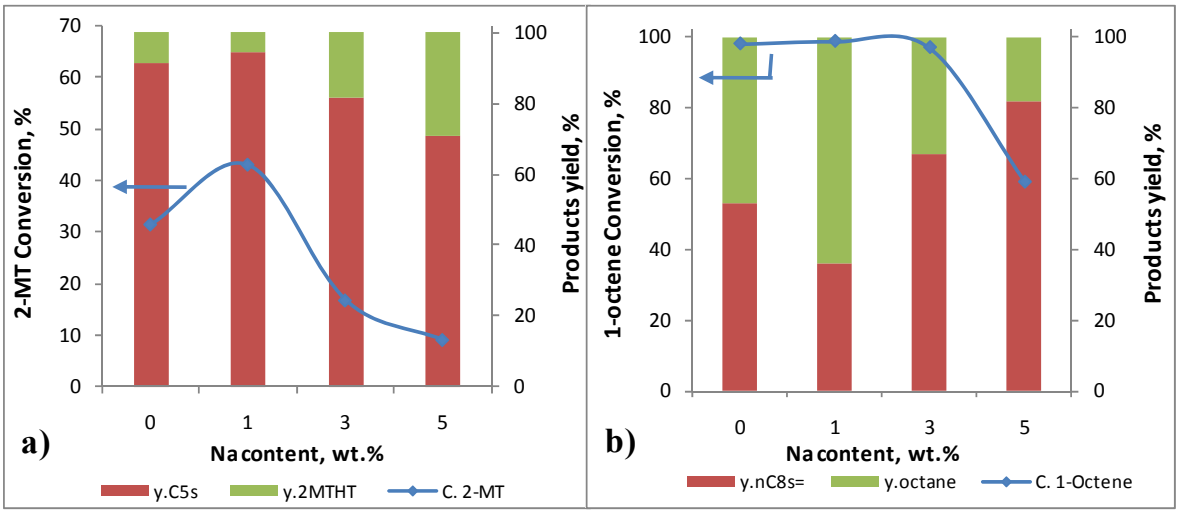

Fig. 1.11. Influence of the Na content on the reactives conversion (lines) and product yields (stacked columns) of CMANa(x) catalysts in the essays type B (linear olefins).

The reduction in the HDS and HydO activities with increasing alkaline metals content seems to be related to the changes observed in the distribution of Co and Mo oxide species observed by XRD, Raman and XPS (section 3.2). The introduction of alkaline metals conducted to a progressive replacing of Mo in octahedral polymeric environments by undistorted monomeric tetrahedral MoO_4^{2-} species like those found in K_2MoO_4 and Na_2MoO_4 compounds. These compounds are recognized for being difficult to reduce/sulphidate and, thus, its presence conduct to a less active sulphide phase [43,52]. On the other hand, the increase in the strength of the Mo-support interaction caused by the formation of alkaline metals molybdates gives rise to the segregation of the Co phase, detected by the formation of Co_3O_4 on the catalysts with 5 wt.% alkaline metal content. The formation of this compound has also been associated with a less active sulphide phase [34,48]. In addition, the formation of crystallites larger enough to be detected by the XRD like those of Na_2MoO_4 found in the CMANa(5), along with the formation of Co_3O_4 has been associated with pore blockage on the catalytic surface, reducing the A_{BET} of the catalyst and consequently the number of available active sites [33,34]. It was also observed that at low content (1 wt.%), the effect of

Na in the reduction of the HDS and HydO activities was lower than the one of K, but the opposite was found at higher contents of alkaline metal (3 and 5 wt.%). This is explained because at high alkaline metal contents the formation of compounds K_2MoO_4 and Na_2MoO_4 is favoured, but the Na_2MoO_4 formed is more crystalline [43] and the sizes of the crystallites were higher, as observed in the XRD and Raman results (section 3.2).

The important reduction in the acid sites density and strength observed with increasing the alkaline metal content account for the diminution and posterior disappearance of the yield of cracking, alkylation and skeletal isomerization, reactions known to proceed through the adsorption on acid sites [3,21,53]. However, it cannot explain the trend of the double-bond isomerization. In essays type B, it was barely affected by the introduction of 1 wt.%, and its yield increased with the subsequent increments in the alkaline metal content. Increases in the double-bond isomerization were also evidenced in essays type A by the negative conversions of TM2P in the case of CMAK(5), CMANa(3) and CMANa(5) catalysts. On the other hand, the trends in the increment of basicity for CMANa(x) and CMAK(x) catalysts match the one in the increment of the double-bond isomerization yield. Solid basic catalysts have been recognized early as efficient catalysts for the double-bond migration of alkanes with one advantage over solid acid ones, which is its lack of C-C bond cleavage ability [54,55].

To explain the changes in selectivity, two facts have to be taken into account. First, the changes in the distribution of the Co and Mo species, precursors of the sulphide phase, cause the reduction of the HDS and HydO activity. Thus, with the introduction of the alkaline metals the intrinsic HYD activity of the active sites decreased. The order of reactivity of the olefins found in literature is linear terminal > linear internal > branched terminal > branched internal [1,2,4,12, 47,56]. This is explained by the steric effect caused by the substitution of hydrogen atoms linked to carbon atoms making part of the double bond [12]. Therefore, it would be

expected that if the intrinsic HYD activity of the active site decreased, the HYD of the more reactive olefins would be less affected than the one of the harder to hydrogenate ones. This fact could account for the order observed in the values of the selectivities: $S^{Hds/HydO-Bi} > S^{HDS/HydO-Bt} > S^{HDS/HydO-L}$, as well as for the low increases of $S^{Hds/HydO-Bi}$ with increasing alkaline metal content up to 1 wt.%, and for the increase in $S^{HDS/HydO-Bt}$ with increasing alkaline metal content from 3 to 5 wt.%. However, it does not explain the prominent increments in $S^{Hds/HydO-Bi}$ with increasing the alkaline metal content to more than 1 wt.%, especially the indefinite values observed in the catalysts with negative C.TM2P, which indicates that another fact has to be taken into account for these catalysts.

It has been shown in literature [2,4] that the isomerization of the double bond, from terminal to internal positions, could play an important role in avoiding HYD of the branched olefins because it helps to produce less active olefins. In this work, it was observed that the catalysts with higher selectivity $S^{Hds/HydO-Bi}$ (CMAK(5), CMANa(3) and CMANa(5)) are the same with larger increments in the double-bond isomerization from external to internal positions in both type A and B essays. Therefore, in these catalysts the increments in the double-bond isomerization could explain why the conversion of internal olefins diminished much more than the HDS activity. In the case of the reactions with linear olefins, double-bond isomerization was also important because internal linear olefins have an octane number much higher than the one of terminal ones [51].

1.3.3.3. Catalytic performance of CMAB(x) catalysts

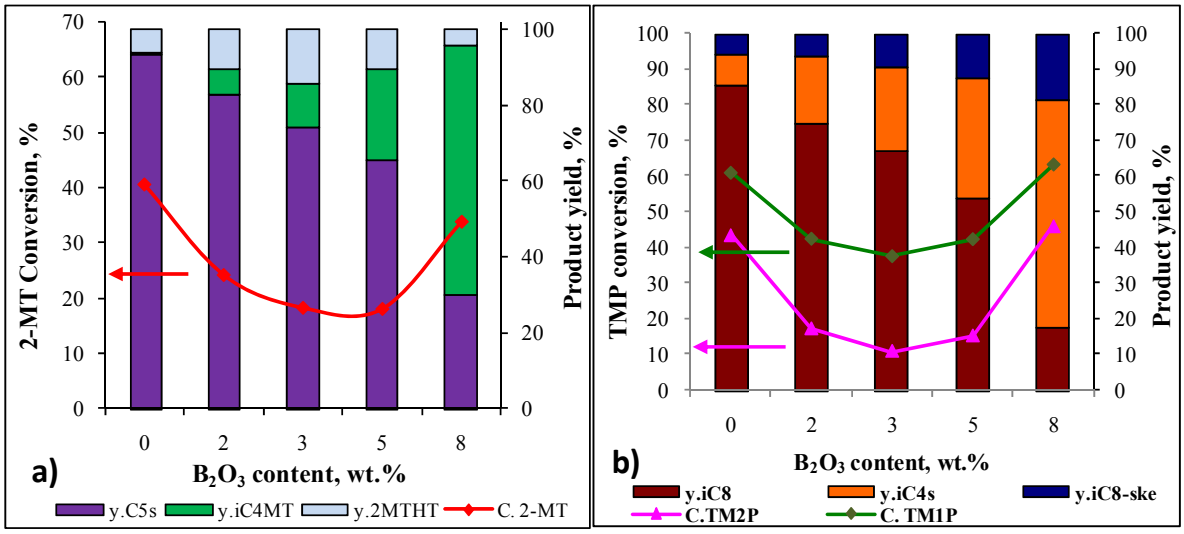

Fig. 1.12. Influence of the B content on the reactants conversion (lines) and product yields (stacked columns) of CMAB(x) catalysts in essays type A (branched olefins).

In essays type A, the conversion of all reactants passed through a minimum for the catalysts with 2, 3 and 5 wt.% B_2O_3 and increased again for CMAB(8) (Fig. 1.12). Opposite to the observed in the catalysts supported on alumina doped with alkaline metals, the introduction of boron on the support promoted all acid type reactions and inhibited the HDS and the HydO. AMT products increased at expense of the yield of HDS products in essays type A and B (Fig. 1.12 and 1.14). At the same time, the yield of skeletal isomerization, as well as cracking products increased at expense of the yield of HydO ones in essays type A. In essays type B, the yield of double-bond isomerization products also increased at expense of the HydO ones. Regarding to the selectivity of CMAB(x) catalysts, the $S^{Hds/HydO-Bi}$ pass through a maximum for the catalysts with 2 and 3 wt.% B_2O_3 and then diminished with subsequent increments in the B content (Fig. 1.13). $S^{HDS/HydO-Bt}$ diminished with increasing B content as $S^{HDS/HydO-L}$ did, whereas the ratio isom/HydOL increased.

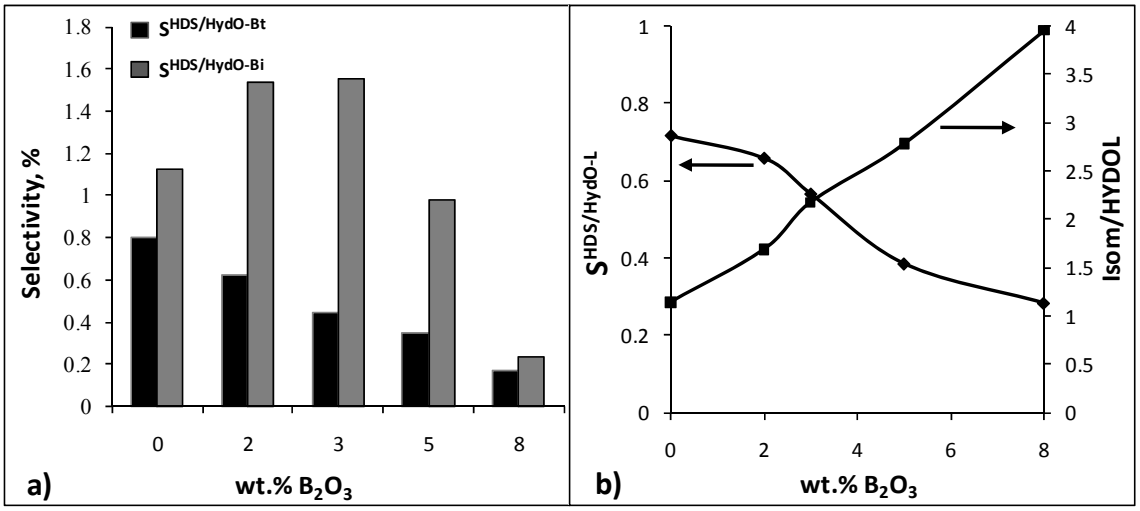

Fig. 1.13. Influence of the B content on the selectivties of CMAB(x) catalysts in essays type A (a) and B (b).

The effect of boron introduction on the catalysts was opposite to the one of alkaline metals, in both, the acid-base properties and the Co and Mo oxide state speciation. Boron introduction causes an increment in the acidity, specially the Brönsted acidity, which increases in density and strength (section 1.3.1). This increment in Brönsted acidity with increasing boria content correlates well with the increment in the yield of all of the acid-type reactions. Acid-type reactions such as skeletal isomerization and cracking of olefins, and alkylation of 2-MT with olefins are accepted to proceed via carbenium ion intermediates, which normally needs the presence of a Brönsted acid site to take place [3,21,53]. Thus, when both acid sites (especially Brönsted) and coordinatively unsaturated sites (CUS) of Mo promoted by Co are present on the catalysts surface, the comparatively low energy needed to perform the acid type reactions, in comparison with HDS and HydO [1,53], causes that when the acid sites density and strength increase, reactant molecules adsorb preferentially in this kind of sites, thus competing with the adsorption in CUS sites. As a consequence, the HDS and HydO reactions are inhibited, as described above.

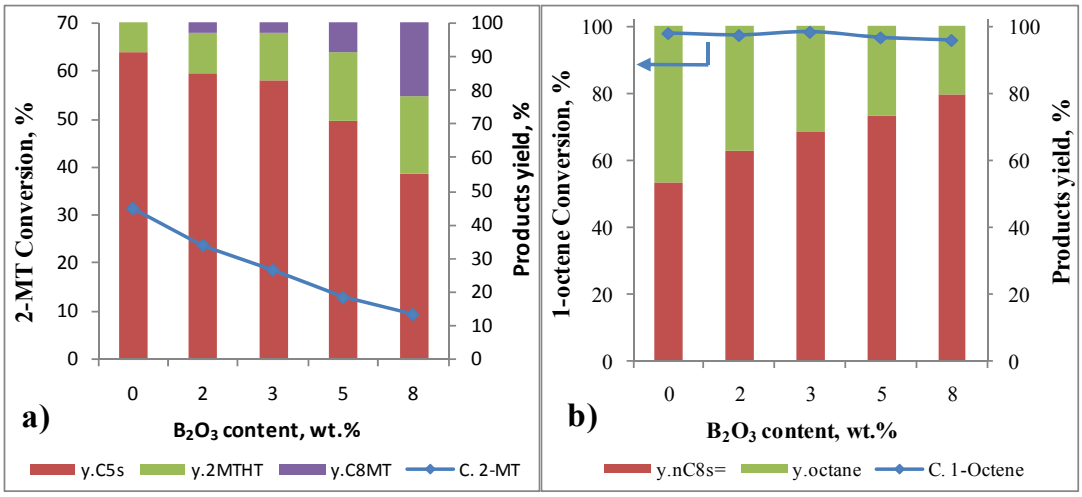

Fig. 1.14. Influence of the B content on the reactants conversion (lines) and product yields (stacked columns) of CMAB(x) catalysts in essays type B (linear olefins).

Additionally, it is important to take into account that according to literature, weaker Brönsted acid sites are able to perform isomerization reactions, whereas stronger Brönsted acid sites are needed for cracking and alkylation [53]. This could be observed in the present work in the case of CMAB(2) and CMAB(3), which only have very weak Brönsted acid sites (Fig. 1.1). In this catalysts, the yield of all of the acid-type reactions increase in comparison with CMA; however, the double-bond isomerization was more promoted than cracking and alkylation, as seen in Fig. 1.12 in the case of branched olefins and Fig. 1.13 in the case of linear olefins. In the case of essays type A, there is no direct evidence of the occurrence of the double-bond isomerization, but its existence can be inferred from the increase in the difference of TM2P and TM1P conversions in comparison with the CMA catalysts. On the other hand, in the catalysts with higher boria content (5 and 8 wt.%), cracking and alkylation are extensively promoted, even, in the case of CMAB(8), these reactions are more important than HDS and HydO. It is interesting that as in the case of alkaline metal doped catalysts, the catalysts where the double-bond isomerization was more promoted than cracking and alkylation were the same with the higher values of $S^{Hds/HydO-Bi}$.

As shown in Raman and XPS results, the boron introduction conducts to a progressive increment of the relative population of polymeric Mo species ($Mo_7O_{24}^{6-}$ and $Mo_8O_{26}^{4-}$) to the one of monomeric ones (MoO_4^{2-}). The formation of larger polymeric species with boron introduction suggests a detriment in the Mo dispersion as seen in Table 1.3. This fact along with the increase in Brönsted acid sites density and strength, which gives origin to a competition between acid sites and the CUS for the adsorption of the reactants, could account for the reduction in the HDS and HydO activities. However in the case of the catalysts with 2 and 3 wt.% boria content, only weak Brönsted sites were detected. These weak Brönsted sites promote more the double-bond isomerization reaction than cracking, giving as a result an increase in the selectivity $S^{Hds/HydO-Bi}$ and the ratio isom/HydOL. Another reaction that plays an essential role is the skeletal isomerization because it is also in competition with the HydO and its products have an octane number similar to the one of TM1P and TM2P.

1.4. CONCLUSION

In general, improvements in the selectivity HDS/HydO taking into account only internal olefins, as well as in the ratio double-bond isomerization to HydO of linear olefins were observed when the alumina was modified either to be more acidic (B) or more basic (K, Na). This fact was related for both modifications to the promotion of the double-bond isomerization reaction from external to internal positions. This reaction, on one hand, competes with the HydO and, on the other hand, produces olefins more difficult to hydrogenate. In addition, in the case of linear olefins, the ones with the double bond in internal positions have a much higher octane number than the terminal ones. In the case of alkaline doped catalysts it was found that double-bond isomerization was related to the existence of basic sites, which do not have the C-C bond cleavage ability. However, in the case of boron modified catalysts, the double-bond isomerization was related to the existence of Brönsted acid sites, which also promotes cracking and alkylation of olefin reactions. Thus, it

was observed that there is a range of boria contents, in which the catalysts have only weak Brönsted acid sites, where there is a higher promotion of the double-bond isomerization than cracking and alkylation reactions. Skeletal isomerization was also found to help avoiding the HydO reaction. However, the improvements in the selectivity HDS/HydO taking into account only internal olefins, as well as in the ratio double-bond isomerization to HydO of linear olefins encountered with dopants deposition on alumina surface were accompanied by a decrease in the HDS activity. This decrease was found to be related to changes in the distribution of Co and Mo species in the oxide state. In the case of boron where more side reactions with higher yields were observed, it was found that a competition factor between acid sites and CUS plays an important role as well.

1.5. REFERENCES

[1]. S. Brunet, D. Mey, G. Pérot, C. Bouchy, F. Diehl, Appl. Catal. A 278 (2005) 143-172.

[2]. D. Mey, S. Brunet, C. Canaff, F. Maugé, C. Bouchy, F. Diehl, J. Catal. 227 (2004) 436-447.

[3]. G. Muralidhar, F.E. Massoth, J. Shabtai, J. Catal. 85 (1984) 44-52.

[4]. M. Toba, Y. Miki, T. Matsui, M. Harada, Y. Yoshimura, Appl. Catal. B 70 (2007) 542-547.

[5]. D.J. Pérez-Martínez, S.A. Giraldo and A. Centeno, International Symposium on advances in hydroprocessing of oil fractions (ISAHOF), Ixtapa-Zihuatanejo, Mexico, 2009.

[6]. G. Shi, D. Fang, J. Shen, Microporous Mesoporous Mater. 120 (2009) 339–345.

[7]. Y. Fan, G. Shi, H. Liu, X. Bao. Appl. Catal. B 91 (2009) 73–82.

[8]. C. Flego, V. Arrigoni, M. Ferrari, R. Riva, L. Zanibelli, Catal. Today 65 (2001) 265-270.

[9]. Y. Fan, J. Lu, G. Shi, H. Liu, X. Bao, Catal. Today 125 (2007) 220–228.

[10]. R. Zhao, C. Yin, H. Zhao, C. Liu, Fuel Process. Tech. 81 (2003) 201-209.

[11]. N. Dos Santos, H. Dulot, N. Marchal, M. Vrinat, Appl. Catal. A 352 (2009) 114–123.

[12]. F.A Carey, Organic Chemistry, third ed., Mc Graw Hill, Madrid, 1999.

[13]. Powder Diffraction File, Joint Committee on Powder Diffraction Standards, International Centre for Diffraction Data (JCPDS-ICDD), 1996.

[14]. V.G. Baldovino-Medrano, P. Eloy, E.M. Gaigneaux, S.A. Giraldo, A. Centeno, Catal. Today 150 (2010) 186–195.

[15]. P. Berteau, B. Delmon, Catal. Today 5 (1989) 121-137.

[16]. S.R. De Miguel, A. Caballero Martinez, A.A. Castro, O.A. Scelza, J. Chem. Tech. Biotechnol. 65 (1996) 131-136.

[17]. A.V. Deo, T.T. Chuang, I.G. Dalla Lana, J. Phys. Chem. 75 (1971) 234-239.

[18]. S.R. De Miguel, O.A. Scelza, A.A. Castro, J. Soria, Topics in Catalysis, 1 (1994) 87-94.

[19]. H. Knözinger, P. Ratnasamy, Catal. Rev. Sci. Eng. 17 (1978) 31-70.

[20]. V. La Parola, G. Deganello, A.M. Venezia, Appl. Catal. A 260 (2004) 237–247.

[21]. G. Busca, Chem. Reviews 107 (2007) 5366-5410.

[22]. Usman, T. Kubota, I. Hiromitsu, Y. Okamoto, J. Catal. 247 (2007) 78–85.

[23]. F. Dumeignil, K. Sato, M. Imamura, N. Matsubayashi, E. Payen, H. Shimada, Appl. Catal. A 315 (2006) 18–28.

[24]. J. Ramirez, P. Castillo, L. Cedeño, R. Cuevas, M. Castillo, J. M. Palacios, A. Lopez-Agudo, App. Catal. A 132 (1995) 317-334.

[25]. C. Flego, W.O. Parker Jr., Appl. Catal. A 185 (1999) 137-152.

[26]. F. Dumeignil, M. Guelton, M. Rigole, J.-P. Amoureux, C. Fernandez, J. Grimblot, J. Colloids Surf. A 158 (1999) 75–81.

[27]. F. Dumeignil, M. Rigole, M. Guelton, J. Grimblot, Chem. Mater. 17 (2005) 2369-2377.

[28]. C. Li, Y.-W. Chen, Catal. Lett. 19 (1993) 99-108.

[29]. W.-J. Wang, Y.-W. Chen, Catal. Lett. 10 (1991) 297-304.

[30]. K.P. Peil, L.G. Galya, G. Marcelin, J. Catal. 115 (1989) 441-451.

[31]. K. Tanabe, Solid Acids and Bases, Academic Press, New York, 1970.

[32]. S. Sato, M. Kuroki, T. Sodesawa, F. Nozaki, G.E. Maciel, J. Mol. Catal. A 104 (1995) 171-177.

[33]. V. La Parola, G. Deganello, C.R. Tewell, A.M. Venezia, Appl. Catal. A 235 (2002) 171–180.

[34]. J.E. Herrera, D.E. Resasco, J. Catal. 221 (2004) 354–364.

[35]. R.L. Chin, D.M. Hercules, J. Phys. Chem. 86 (1982) 3079-3089.

[36]. Y. Okamoto, T. Imanaka, S. Teranishi, J. Catal. 65 (1980) 448-460.

[37]. Y. Saih, K. Segawa, Appl. Catal. A 353 (2009) 258–265.

[38]. T.I. Koranyi, I. Manninger, Z. Paal, O. Marcs, J.R. Günter, J. Catal. 116 (1989) 422-439.

[39]. B. Pawelec, T. Halachev, A. Olivas, T.A. Zepeda, Appl. Catal. A 348 (2008) 30-41.

[40]. H. Jeziorowski, H. Knözinger, P. Grange, P. Gajardo. J. Phys. Chem. 84 (1980) 1825-1829.

[41]. L.E. Makovsky, J.M. Stencel, F.R. Brown, R.E. Tischer, S.S. Pollack, J. Catal. 89 (1984) 334-347.

[42]. G. Mestl, T.K.K. Srinivasan, Catal. Rev.-Sci. Eng. 40 (1998) 451-570.

[43]. N.F.D. Verbruggen, G. Mestl, L.M.J. von Hippel, B. Lengeler, H. Knözinger, Langmuir 10 (1994) 3063-3072.

[44]. U. Usman, M. Takaki, T. Kubota, Y. Okamoto, Appl. Catal. A 286 (2005) 148–154.

[45]. P. Torres-Mancera, J. Ramirez, R. Cuevas, A. Gutierrez-Alejandre, F. Murrieta, R. Luna, Catal. Today 107–108 (2005) 551–558.

[46]. D.J. Pérez-Martínez, G.A. Acevedo, S.A. Giraldo, A. Centeno, Rev. Fac. Ing. Univ. Antioquia, Accepted for publication.

[47]. S. Hatanaka, M. Yamada, O. Sadakane, Ind. Eng. Chem. Res. 36 (1997) 5110-5117.

[48]. H. Topsøe, B.S. Clausen, F.E. Massoth, in: J.R. Anderson, M. Boudart (Eds.), Hydrotreating Catalysis, Science and Technology, Springer-Verlag, Berlin, 1996.

[49]. V. Belliere, C. Geantet, M. Vrinat, Y. Ben-Taarit, Y. Yoshimura, Energy Fuels 18 (2004) 1806-1813.

[50]. M. Arias, D. Laurenti, V. Bellière, C. Geantet, M. Vrinat, Y. Yoshimura, Appl. Catal. A 348 (2008) 142-147.

[51]. W. Gruse, D. Stevens, The chemical technology of Petroleum, 2nd ed., Mc Graw Hill, New York, 1942.

[52]. N.F.D. Verbruggen, H. Knozinger, Langmuir 10 (1994) 3148-3155.

[53]. A. Corma, Chem. Rev. 95 (1995) 559-614.

[54]. H. Hattori, Chem. Rev. 95 (1995) 537-550.

[55]. J. Li, R.J. Davis, Appl. Catal. A 239 (2003) 59–70.

[56]. S. Hatanaka, M. Yamada, O. Sadakane, Ind. Eng. Chem. Res. 36 (1997) 1519-1523.

2. INTERPRETATION OF THE CATALYTIC FUNCTIONALITIES OF CoMo/ASA FCC-NAPHTHA-HDT CATALYSTS BASED ON ITS ACID PROPERTIES

2.1. INTRODUCTION

As it was already stated in the introduction of the preceding paper, in the case of selective classical HDS, various attempts to develop selective catalysts for this purpose are found in literature [1-5,8-13]. Among them, support modification appears to be a good approach to obtain catalysts more selective to the HDS [1, 8-13]. In the preceding chapter it was found that improvements in the selectivity to HDS could be found by both modifications of alumina: reducing (doping it with Na or K) or increasing (doping it with B) its acidity. However, at the same time reduction in HDS activity was observed with dopant introduction. This was related to changes in the distribution of Co and Mo species in the oxide state of the doped catalysts as compared with the undoped one found by XRD, Raman and XPS. It was shown also that these changes in the distribution of Co and Mo species were related with the modification of the alumina surface OH groups because of dopant introduction.

Thus, in order to keep searching for catalysts more selective to HDS but avoiding losses of the HDS activity, an alternative to using alumina modified supports would be using a support whose acid-base properties could be modified directly during its synthesis. Taking into account that most of the works in literature have been focused in support more basic than alumina and that in these works it was always found that the HDS activity was reduced unavoidably [1, 3, 8, 10]; in the present chapter we intended to study CoMo catalyst supported on materials more acidic than alumina. In this sense, La Parola et al. [13] showed by using CoMo catalysts supported on amorphous aluminosilicates, that improvements in the HDS activity could be found by varying the silica/alumina ratio. On the other hand, although

some references about improvements in the HDS/HydO selectivity using more acidic catalysts can be found [10,11]; unfortunately, a detailed explanation of this behavior based on its acid properties and its influence in the catalytic performance, was not given. Consequently, there is still a lack of information about not only the catalytic performance of CoMo catalysts supported on acid-type materials, but also the influence of changes in the different acid properties in the HDT of FCC naphtha.

In this chapter, the performance of amorphous-aluminosilicate-supported CoMo catalysts with different Si/(Si+Al) ratios in the HDT of synthetic FCC naphtha was studied in order to determine the influence of support composition on the catalyst acid properties and the corresponding influence of these acid properties on the catalytic functions: HDS, HydO, and acidity.

2.2. EXPERIMENTAL

2.2.1. Preparation of catalysts

Amorphous aluminosilicate supports with different Si/(Si+Al) ratios (0.15, 0.25, 0.33, 0.5 and 0.75) were prepared by the sol-gel route according to the procedure described by La Parola et al. [14]. All operations were performed under N_2 atmosphere. The required amounts of aluminum tri-sec-butoxide (Aldrich, 97%) and tetraethyl orthosilicate (Aldrich, 98%) were mixed together. The solution was stirred for 3 h at room temperature (r.t.) under N_2 flow in order to obtain a homogeneous mixture. Then, the temperature was increased to 353 K, and water (pH = 9 for ammonia) in stoichiometric amount was added to the rapidly stirred mixture of both alkoxides in order to promote hydrolysis [15]. The gel formed was left 5 h under reflux and constant stirring, and, subsequently, it was aged in air for at least 5 days at ambient conditions. The gel was washed several times with anhydrous sec-butanol to remove the possible traces of non-hydrolyzed alkoxide.

The xerogels were dried under airflow at 343 K for 2 h and, finally, air calcined at 773 K for 12 h.

CoMo catalysts supported on ASA containing 10% MoO_3 and 2% CoO were prepared by successive incipient wetness impregnation. The supports and the catalysts were named ASAxx and CMSxx respectively, where xx represents the % Si/(Si+Al). An initial impregnation step was performed with an aqueous solution of $(NH_4)_6Mo_7O_{24}\cdot 4H_2O$ (Merck), and subsequently the solids were impregnated with an aqueous solution of $Co(NO_3)_2\cdot 6H_2O$. After each impregnation step, solids were dried under airflow at 343 K for 2 h and, finally, air calcined at 773 K for 12 h. A conventional CoMo catalyst supported on a commercial γ-Al_2O_3 (Procatalyse), named here CMA, was also prepared by the same method for comparison purposes. In this case, after each impregnation step, the solids were dried under airflow at 393 K for 12 h and, finally, air calcined at 773 K for 4 h.

2.2.2. Characterization of catalysts

2.2.2.1. Catalysts composition

The catalyst and support nominal compositions were verified by X-ray fluorescence (XRF) using a Shimadzu EDX 800 HS apparatus.

2.2.2.2. Textural properties

The specific surface area (A_{BET}) of both catalysts and supports was estimated by the same method described in 1.2.2.1.

2.2.2.3. Confocal laser Raman microscopy (Raman)

Raman spectra of the catalysts were taken following the procedure already described in 1.2.2.5.

2.2.2.4. Acid properties

Acid properties of both catalysts and supports in the oxide state were determined by NH_3 temperature programmed desorption (TPD) and Fourier transformed infrared (FT-IR) spectra of adsorbed pyridine according to the procedures already described in 1.2.2.6.

2.2.3. Catalytic evaluation

Catalytic tests were made according the procedure already described in 1.2.3.

2.2.3.1. Expression of results

In this chapter the results were expressed in the same way as in the preceding one (1.2.4).

2.3. Results and Discussion

2.3.1. Influence of the Si/(Si+Al) ratio on the catalysts surface properties

Table 2.1 shows the A_{BET} of catalysts and supports measured by N_2 adsorption-desorption isotherms. From the analysis of the adsorption-desorption curves hysteresis, it can be inferred that all materials are mainly mesoporous with only a small proportion of micropores as expected due to the basic hydrolysis used in the sol-gel synthesis of these materials [14,15]. With the exception of ASA75, all ASA supports presented an A_{BET} higher than the one of γ-Al_2O_3. Blocking of both the micropores and the smallest mesopores by the active metal deposition could explain the important reduction in the A_{BET} of the CMSxx catalysts, when comparing them with their respective supports [16]. The deterioration of the ASAxx textural properties after active metal incorporation, especially in the A_{BET}, has also been reported by other authors [13,14,16].

Table 2.1. Textural properties of ASA supports and CoMo catalysts supported on these.

Si/(Si+Al) ratio	Support	A_{BET} ($m^2.g^{-1}$)	Catalysts	A_{BET} ($m^2.g^{-1}$)
0	γ-Al_2O_3	210	CMA	194
15	ASA15	397	CMS15	269
25	ASA25	550	CMS25	259
33	ASA33	378	CMS33	146
50	ASA50	508	CMS50	264
75	ASA75	117	CMS75	69

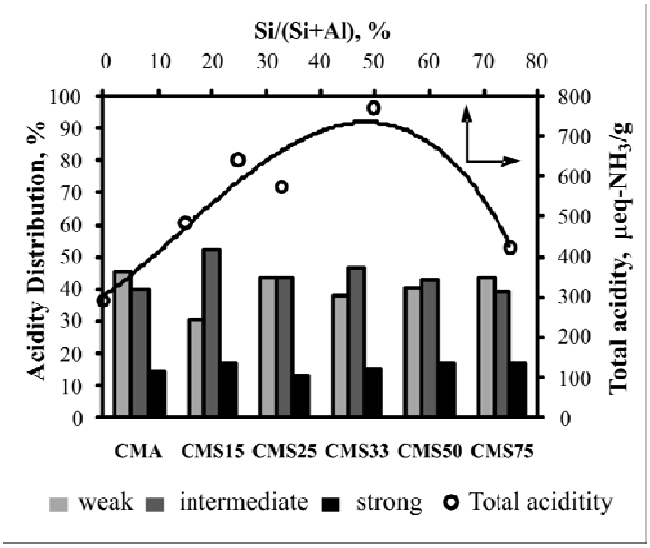

Fig. 2.1. Total acidity and acidity distribution measured by NH_3 TPD of the CoMo catalysts supported on ASA. weak (T<423 K), intermediate (423 K <T<573), strong (T>573).

Fig. 2.1 presents the total acidity and the acidity strength distribution measured by NH_3 TPD as a function of the Si/(Si+Al) ratio. The zero value in the X axis represents the conventional catalyst CMA. The strength of the acid sites was arbitrarily classified as weak (<423 K), intermediate (423-573 K), and strong (>573) according to the temperature of NH_3 desorption [17]. The values reported represent the percentage of NH_3 desorbed between the temperatures listed above relative to the total NH_3 desorbed. There are almost no substantial changes in the

acidity strength distribution with increasing Si/(Si+Al) ratio. The only exception was the CMS15 catalyst, where an augmentation in the intermediate acid sites at expense of the weak ones is observed. Total acidity increases with the Si/(Si+Al) ratio and exhibits a maximum around 50 % Si/(Si+Al). Similar results were reported by other authors using a similar series of ASA prepared by a different method [18,19].

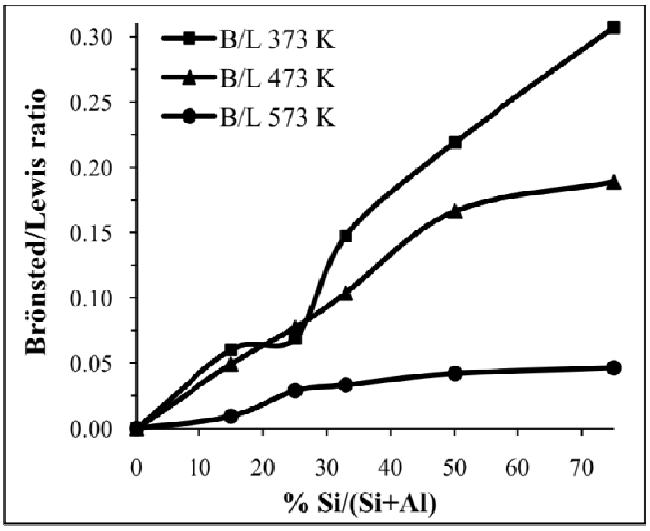

Fig. 2.2. Brönsted/Lewis ratio of the ASA supported CoMo catalysts determined by FT-IR spectra of adsorbed pyridine after evacuation at 373, 473 and 573 K.

Peaks at 1453 and 1545 cm^{-1} in the IR spectra of adsorbed pyridine (not shown), attributed in the literature [14,20] to pyridine bonded to Lewis and Brönsted sites respectively, were mathematically decomposed using Gauss-type curves. The values resulting from their integration were used to calculate the Brönsted/Lewis ratio, which was plotted as a function of the % Si/(Si+Al) in Fig. 2.2. For the CMA catalyst the Brönsted/Lewis ratio is zero because no Brönsted sites were detected using pyridine as model molecule, but it increases continuously with increasing Si/(Si+Al) ratio. It is also observed that the Brönsted/Lewis ratio diminished after the evacuation at high temperatures, which indicates that there is, comparatively, a higher population of intermediate and strong Lewis acid sites than Brönsted sites.

The increase in the total acidity observed in the CMSxx catalysts in comparison with the one of CMA has been attributed to the formation of a Si-Al mixed phase in the ASA supports [13,14,21]. The substitution of Al in the Si framework gives rise to new superficial defects which create new both Lewis and specially Brönsted acid sites [13]. The Brönsted acid sites arise from silanol groups, which can be generated when a trivalent cation, such as Al^{3+}, is present in tetrahedral coordination with oxygen. When the oxygen anions are shared between the cations, a net negative charge is created on aluminum, which is compensated by protons giving rise to terminal silanol groups and to the more acidic bridging hydroxyl groups [13]. The Lewis acidity arises from partly uncoordinated metal cations and anions present at the surface of metal oxides, which along with water (always present in the environment) produces surface hydroxy-groups [13]. They are also formed through the isomorphous substitution of Si^{4+} lattice sites by Al^{3+} ions [13].

The change in the acid properties of the ASA-supported catalyst with the Si/(Si+Al) ratio are due to the fact that the Si-Al mixed phase is not formed homogeneously for all the Si/(Si+Al) ratio [21]. In fact, the maximum of the mixed oxide formation have been found between 50 and 75% Si/(Si+Al) [19,21,22], which coincides with the maximum in the total acidity found in Fig. 2.1 and in the Brönsted/Lewis ratio found in Fig.2.2. According to these authors [19,21,22], below 50% SiO_2 content, the mixed phase is progressively diluted by alumina, which appears as a distinct phase below 40-30% SiO_2 being responsible for the increase in the surface density of Lewis sites as observed in Fig. 2.2 [21]. As the major part of the catalysts prepared in this work were in that range, the IR spectra of the OH region of dehydrated supports were analyzed in order to identify the existence of different phases in the support surface (Fig. 2.3) . It was found that for ASA supports in the range 50-75 % Si/(Si+Al) ratio, only the peak of silanol groups (at ca. 3790 cm^{-1}) was found [20]. However, in the ASA supports in the range 15-33 % Si/(Si+Al) ratio along with the silanol groups a little peak ca. 3790 cm^{-1} and a shoulder at ca. 3730

cm^{-1} are also observed. These new bands match well with alumina type IB and IIA OH groups of Knözinger classification [23]. It is observed that these new peaks vanish with increasing Si/(Si+Al) ratio, even for the CMS33 catalyst, these are hardly observed. This kind of OH groups was also observed by Bandosz et al. [24] in their protonic acidity distribution (PAD) measurements performed for their silica-alumina supports. Other authors [25] have also observed the existence of Al in octahedral coordination, which is attributable to an alumina distinct phase in the Al^{27} MAS NMR spectra of their ASA.

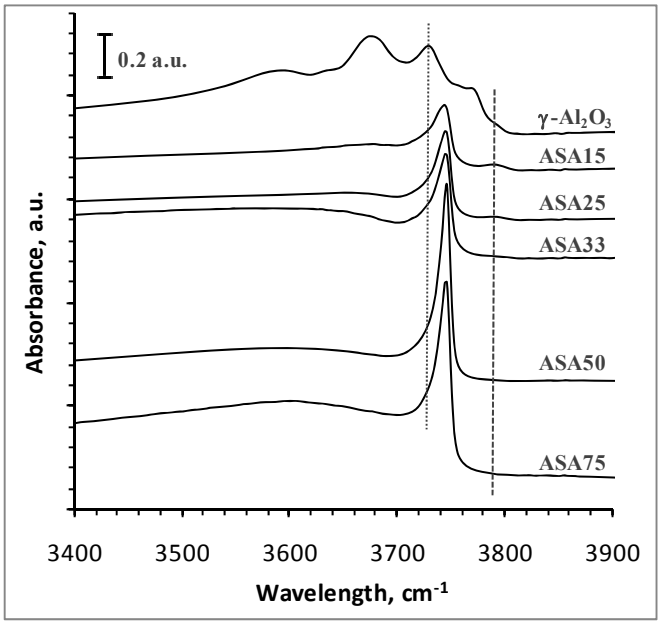

Fig. 2.3. OH region FT-IR spectra of ASA(x) supports compared with pure alumina.

This heterogeneity of phases present in ASA supports gives rise to some heterogeneity in the nanoscale composition as shown by Sârbu and Delmon [26]. Thus, when the ASA are used as supports for CoMo HDT catalysts, the OH groups that would be available to attach these metals depend on the Si/(Si+Al) ratio. In consequence, changes in the Mo coordination, speciation and dispersion with variations of the Si/(Si+Al) ratio would be expected. In order to study these changes, the Raman spectra of the catalysts were taken (Fig. 2.4). First of all, it

can be noticed that both Co and Mo are well dispersed on the different supports, because of the lack of peaks characteristic of Co compounds (681, 477 and 199 cm^{-1}) and free MoO_3 aggregates (990-1000 cm^{-1}) [27-29]. Additionally, the presence of $Al_2(MoO_4)_3$ (1000-1010 cm^{-1}) can be ruled out [29]. The CMA catalyst Raman spectrum shows a broad band at ca. 920-950 cm^{-1} with shoulders at both sides ca. 900 and 960 cm^{-1}. There are also other broad bands at ca. 320-360 and 225 cm^{-1}. The region 750–1000 cm^{-1} is where the bands for stretching of Mo–O bonds are typically observed [27,29]. Inside the broad band at ca. 920-950 a variety of Mo species could be placed; the more likely according to literature [27-31] are $Mo_7O_{24}^{6-}$ octahedral species (946-951, 360 and 220 cm^{-1}, continuous lines) and MoO_4^{2-} with distorted tetrahedral symmetry (916 and 320 cm^{-1}, dotted lines). Some contributions from Mo-O-Co stretching vibrations in $CoMoO_4$ species (939, 873, 820, 370 and 340 cm^{-1}, dashed lines) cannot be ruled out [32]. The shoulder at ca. 900 cm^{-1} can be attributed to monomeric undistorted MoO_4^{2-} species (at ca. 892 and 807 cm^{-1}), and the other shoulder at ca. 960 cm^{-1} can be attributed to larger polymeric species like $Mo_8O_{26}^{4-}$ (958-960 cm^{-1}).

Regarding ASA supported CoMo catalysts in the CMS15 catalyst Raman spectrum, the peaks centered at ca. 915-920 cm^{-1} and at ca. 320 cm^{-1} evidence the majority presence of Mo species with distorted tetrahedral symmetry. Even though a higher frequency shoulder can also be observed around 940-950 cm^{-1}, the presence of $Mo_7O_{24}^{6-}$ octahedral species should be low because no peak close to 225 cm^{-1} is observed. This augmentation in the tetrahedral Mo species with increasing Si content up to 20 wt.% on ASA was also reported by Vakros et al. [33]. In the CMS25 catalyst spectrum, the shoulder close to 940-950 cm^{-1} is higher in comparison with the one of the CMS15 catalyst, and the peak close to 225 cm^{-1} is now clearly observed. This fact indicates that although the Mo species with distorted tetrahedral symmetry are still majority on the CMS25 catalyst, the population of $Mo_7O_{24}^{6-}$ octahedral species is higher than the one on the CMS15. With the subsequent increments in the Si/(Si+Al) ratio, the population of $Mo_7O_{24}^{6-}$

octahedral species continues increasing at expenses of the population of distorted tetrahedral species.

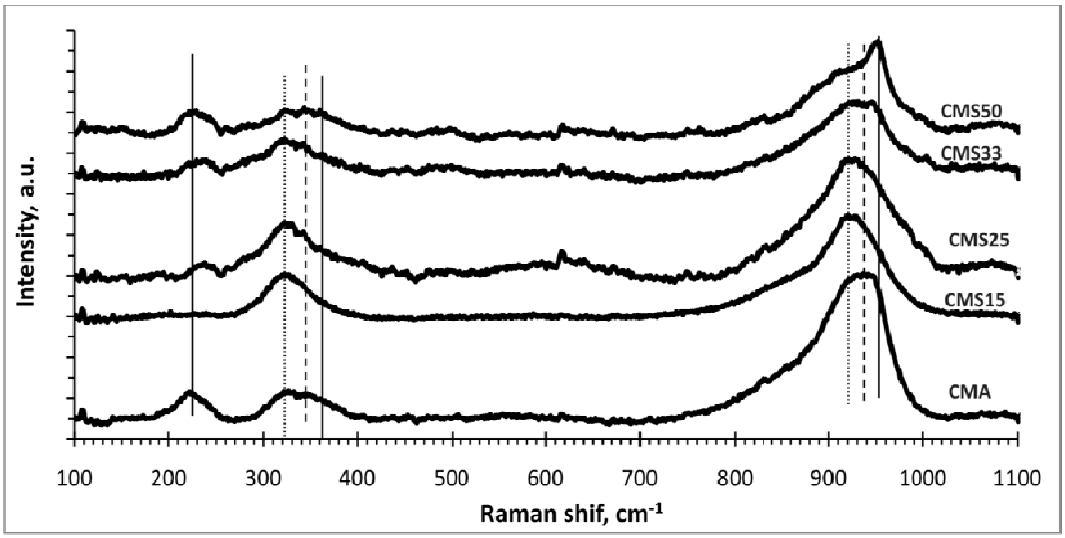

Fig. 2.4. Raman spectra of the ASA supported CoMo catalysts compared with that supported on alumina.

It is known that the pH of the solution of ammonium heptamolybdate, determines the structure of the solution species according to the equilibrium between poly- and monomeric molybdates established in eq. 1.2 and 1.3 [29]. Thus, at pH values higher than 6.5, the MoO_4^{2-} anion is stable, and a decrease in pH to 4.5 leads to complete formation of $Mo_7O_{24}^{6-}$. A further decrease in pH to 1.5 leads to polymerization of $Mo_8O_{26}^{4-}$. Therefore, during the impregnation process, the Mo species, which will be deposited on the support surface, seem to be governed by the surface pH, more precisely by its point of zero charge (PZC) [29,31]. The surface pH can be drastically altered by chemisorption; consequently, the surface pH is determined by the overall system Mo-oxide/support [29,31]. For instance, alumina has a PZC of 8-9, whereas MoO_3 has one of 1.5. Thus, low Mo loadings (< 1 Mo atom/nm^2) on alumina (around 200 m^2/g), which are equivalent to high

surface pH values, favoured the adsorption of MoO_4^{2-} species [29,31]. At increasing the Mo loading, the PZC of the surface drops; therefore, increasing quantities of $Mo_7O_{24}^{6-}$ will be adsorbed. On the other hand, silica has a PZC of 4-5 [13]; thus, on silica pH values high enough for monomolybdate formation are usually not reached. Consequently, under hydrated conditions, only polymeric species will be adsorbed [29]. Also it has been found that Mo is more weakly attached on silica than on alumina leading to the easy formation of MoO_3 [13,27,29].

Therefore, it would be expected that Mo species supported on ASA supports exhibit an intermediate behavior between alumina and silica, i.e, with increasing the Si content it should increase the density of polymeric species. However and apparently in contradiction with what has been already said, in the Fig. 2.4 is observed that in the CMS15 catalysts practically only distorted tetrahedral Mo species are present. Thus, we have to consider another variable influencing this fact. The 10 wt.% MoO_3 loading used in this work is equivalent to a loading of 2 Mo atom/nm^2 for the alumina used, but the A_{BET} of the ASA(15) is almost twice that of alumina; thus, for the ASA(15) the equivalence is 1 Mo atom/nm^2. Considering that the ASA supports would be composed of a mixed oxide phase diluted in a separated alumina phase, the ASA(15) would have the highest concentration of the segregated alumina phase, and consequently, its PZC will be close to the one of alumina. Thus, the unexpected majority presence of distorted tetrahedral Mo species on ASA(15) would be explained by its high A_{BET}. The other ASA supports also have high surface areas, but with increasing the Si/(Si+Al) ratio, the PZC decrease [13] explaining the increase in the polymeric Mo species population at expense of the monomeric ones.

2.3.2. Influence of the Si/(Si+Al) ratio on the catalytic performance in the HDT of synthetic FCC Naphtha.

A lot of organic substances were found in the condensable products at the reactor outlet. A complete identification of all reaction products was done. In the section 1.3.3.1, we have already described reaction schemes for 2-MT and branched olefins (TM1P and TM2P) based on the product identification along with the comparison with other reaction schemes proposed in the literature [1,5-8,11,12,35].

The yield of the reaction products listed in section 1.3.3.1 (stacked columns) and the conversion of the reactants (dotted lines) were plotted as a function of the Si/(Si+Al) ratio in Fig. 2.5 and 2.6 for essays type A and B respectively. In Fig. 2.5.a the 2-MT conversion and its product yields are shown; the same is shown for the TM1P and TM2P in Fig. 2.5.b. The product distribution was found to depend strongly on the Si/(Si+Al) ratio of the support used to prepare the catalysts. The 2-MT conversion of the ASA-supported catalysts was higher or at least at the same level than the one observed for the conventional catalysts. In the case of CMA, the main 2-MT products were C5s resulting from the HDS reaction and as secondary product a small yield to 2-MTHT was also observed. In general, an increase in the alkylation yield together with a simultaneous decrease in the HDS one was observed when increasing the Si/(Si+Al) ratio. However, it is noticeable that this augmentation of the alkylation yield at expense of the HDS one was not gradual; an abrupt change in the products distribution is observed in the region between 15 and 25 % Si/(Si+Al). Thus, it can be said that this is a kind of transition zone between catalysts that are more selective to HDS and those that are more selective to alkylation.

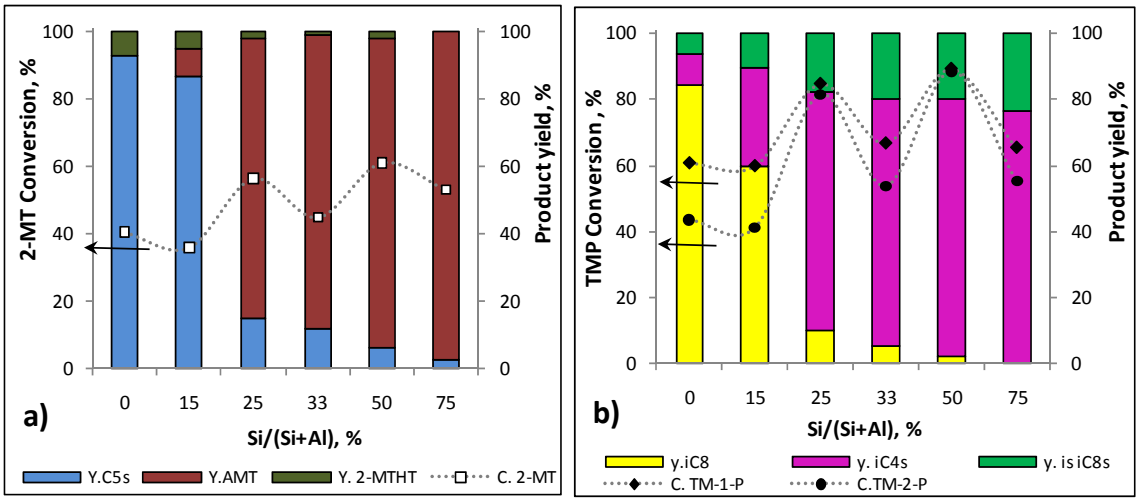

Fig. 2.5. Influence of the Si/(Si+Al) ratio on the CMSxx catalysts reactant conversions (lines) and product yields (stacked columns) in essays type A (branched olefins).

Fig. 2.5.b shows that the tendency of TM1P and TM2P conversions and their product distribution are similar to those obtained with 2-MT. It is observed that as the Si/(Si+Al) ratio increases, acid-type reactions—skeletal isomerization and cracking of olefins—become prevalent at the expense of the HydO activity, and again an abrupt change is observed between the catalysts with 15 and 25 % Si/(Si+Al). For the Si-rich catalysts, equilibrium between cracking and skeletal isomerization of olefin reactions was reached; however, comparing Si-rich catalysts with the Al-rich ones, the increase in the cracking activity was higher than the one of the skeletal isomerization activity.

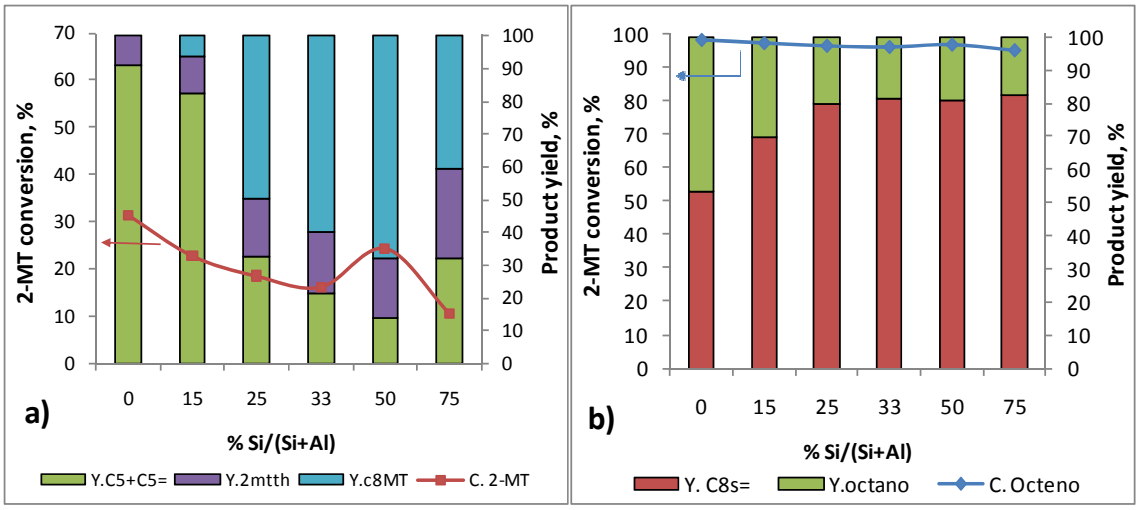

Fig. 2.6. Influence of the Si/(Si+Al) ratio on the CMSxx catalysts reactant conversions (lines) and product yields (stacked columns) in essays type B (linear olefins).

In the Fig. 2.6.a is observed that in essays type B the 2-MT conversion diminishes with increasing Si/(Si+Al) ratio with the only exception of the CMS50 catalyst, where a local maximum with a value similar to that of the CMS15 is observed. In addition is observed that the conversion of 2-MT in essays type B were lower than that observed in essays type A for all of the catalysts. Concerning the 2-MT product distribution, it is observed a behavior quite similar to the one observed in essays type A. The yield to alkylation products increase with the Si/(Si+Al) ratio with an abrupt change between 15 and 25 % Si/(Si+Al). Then, for catalysts with % Si/(Si+Al) ≥ 25 gradual increments are observed with a maximum around 50 % Si/(Si+Al). However, in comparison with essays type A the catalysts with a % Si/(Si+Al) ≥ 25 have a higher yield to HDS products. In the Fig. 2.6.b, it is observed that the abrupt changes in product distribution are not localized in the range between 15 and 25 % Si/(Si+Al) ratio. In these case a first high increment in the yield of isomerization products is observed for the CMS15 catalyst. Then a second increment is observed for the catalyst with 25 % Si/(Si+Al) ratio, where an equilibrium between the HydO and the double-bond isomerization is reached and there are not more increments with further increments of the Si/(Si+Al) ratio.

The selectivity HDS/HydO usually presented in literature [8] is not adequate to completely analyze the catalytic performance taken into account the great complexity of the reaction system when ASA supported catalysts are used. In this work, we decided to apply a definition of HDS selectivity taking into account acid-type reactions. Therefore, selectivity to HDS (S^{HDS}) was defined as the ratio between the 2-MT HDS activity and the addition of olefin cracking and HydO activities (Equation 2.1). Cracking reaction was also included in the denominator because the products of this reaction are gaseous, causing a decrease in gasoline production, which must also be avoided [1,4,5]. On the contrary, the products from the skeletal isomerization are not included because they have a similar octane number to the one of 2,4,4-TMPs [36]; thus, their production is favorable because it does not affect the octane number and it is in competition with HydO and cracking.

$$S^{HDS} = \frac{\dfrac{\text{mol HDS products}}{\text{initial mol } 2-\text{MT}}}{\dfrac{\text{mol HYDO products} + \text{mol cracking products}}{\text{initial mol TM1P} + \text{TM2P}}} \qquad (2.1)$$

The case of 2-MT is a little bit more complicated; the production of AMT is not good from the viewpoint of a classical HDS process because these kinds of products are also sulfur-containing compounds and, they are even more difficult to desulfurize. However, the boiling point of AMT is higher enough to allow its separation by distillation. In fact, a commercial alternative desulfurization based in this type of reactions was developed by the British Petroleum and named olefinic alkylation of thiophenic sulfur (OATS) [6,7]. Therefore, the production of AMT is a reaction, which can be potentially part of a desulfurization process. Having into account that alkylation competes with HDS in the transformation of 2-MT, a selectivity to alkylation (S^{Alkyl}) was defined in the same terms of the S^{HDS} (Equation 2.2) to quantify somehow the inclination of the catalysts to produce alkylation products.

$$S^{Alkyl} = \frac{\dfrac{\text{mol Alkylation products}}{\text{initial mol 2-MT}}}{\dfrac{\text{mol HYDO products + mol cracking products}}{\text{initial mol TM1P + TM2P}}} \qquad (2.2)$$

In the case of essays type B the ratio isom/HydOL, already defined in the section 1.3.3.1 was also calculated.

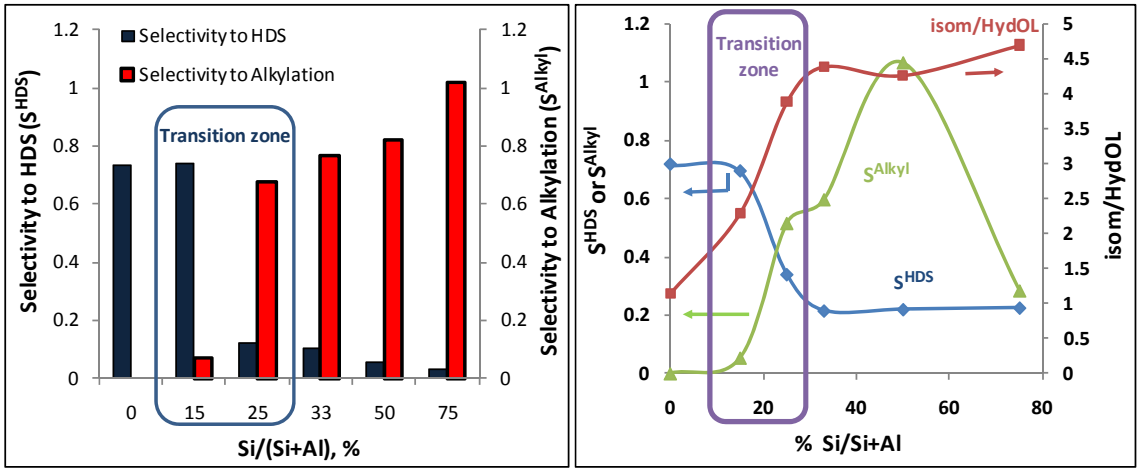

Fig. 2.7. Influence of the Si/Si+Al ratio on CMSxx catalysts selectivities to HDS and alkylation in essays type A (a) and B (b).

The above defined selectivities were plotted as a function of the Si/(Si+Al) ratio in Fig. 2.7. As it can be predicted from the activity results, the general trend is a diminution of S^{HDS} and an increase of S^{Alkyl} when increasing the Si/(Si+Al) ratio in both kind of essays. The CMA exhibited a high S^{HDS} and a zero value of S^{Alkyl}; meanwhile, the CMS15 catalyst exhibited a value of S^{HDS} similar to the one of CMA accompanied by a low one of S^{Alkyl}, and again an abrupt change in the selectivity with a decrease in the S^{HDS} and an increase in S^{Alkyl} was observed for the CMS25. Beyond that point, in essays type A, continuous but gradual diminutions are observed in the S^{HDS}, at the same time that continuous and gradual increments of

the S^{Alkyl} are observed with increasing the Si/(Si+Al) ratio. On the other hand, in essays type B, S^{HDS} diminishes until the CMS33 catalyst and then stay stable, whereas the S^{Alkyl} reaches a maximum at the CMS50 catalyst and then it diminishes. The ratio isom/HydOL increase in two steps, its value for the CMS15 catalyst is twice the one of CMA and a similar increase is observed comparing the CMS25 with the CMS15 catalysts.

Therefore, according to the catalytic behavior observed in Fig. 2.5–2.7, the catalysts could be divided into two groups in the studied Si/(Si+Al) range. The first group of catalysts is composed by the reference CMA catalyst and the CMS15 one, and the second group is composed by those supported on ASA with a Si/(Si+Al) ratio higher than 0.25. It is quite interesting that inside these groups, the changes in product distribution and selectivities are gradual, but despite the small difference in the Si/(Si+Al) ratio between the catalysts in the boundary of both groups; CMS15 and CMS25, the changes in product distribution and selectivities are huge. Thus, this constitutes a transition zone between the catalysts that preferably promote HDS and HydO reactions and those that promote acid-type ones. This transition zone could be explained considering that ASA-supported CoMo catalysts combine HDS, HydO, and the acid-type functions in the same catalyst; thus, reacting molecules (2-MT and olefins) have the possibility to adsorb and transform in many different sites, and the preference by one or other reaction will be related with the relative population and the activity of the different sites.

According to the discussion in section 2.3.1, with increasing Si/(Si+Al) ratio both the Mo species distribution in the oxide state as well as the acid properties of the catalysts are strongly modified. However, regarding the Mo species distribution in the oxide state, its changes as a function of the Si/(Si+Al) ratio do not match with those of the catalytic performance. For instance, the catalytic performance of CMA and CMS15 catalysts was quite similar, with the highest S^{HDS} and HDS activity but the distribution of the Mo species in the oxide state was quite different. The CMA

catalysts exhibit a mixture of octahedral polymeric and tetrahedral monomeric Mo species with prevalence of the octahedral ones, whereas the CMS15 exhibit a majority of distorted tetrahedral monomeric species. It is considered that the distorted tetrahedral monomeric Mo, although easier to reduce than the undistorted ones, they are harder to reduce/sulphidate than the octahedral polymeric ones, and consequently, less active [33,35]. However, it should also be considered that the presence of the distorted tetrahedral Mo species could improve the Mo dispersion [28,35], thus, compensating somehow its lack of reduction/sulphidation easiness. This fact could explain why the HDS activity of the CMS15 is quite similar to the CMA despite of its different distribution of Mo oxide species. On the other hand considering the catalysts in the limit of the transition zone (CMS15 and CMS25), the difference between their Mo oxide species distribution is not significant enough to justify the huge reduction in the HDS activity and the S^{HDS} which is observed in Fig. 2.5–2.7 when comparing them.

On the other hand, changes in the acid properties with the Si/(Si+Al) ratio seem to be more related with the catalytic performance. Acid-type reactions such as isomerization and cracking of olefins, and alkylation of 2-MT with olefins are accepted to proceed via carbenium ion intermediates, which normally needs the presence of a Brönsted acid site to take place [11,20,37,38]. Thus, when both acid type (especially Brönsted) and coordinative unsaturated sites (CUS) of Mo promoted by Co are present on the catalysts surface, this type of reaction is more energetically favorable than HDS or even HydO reactions [1,38]. The comparatively very low energy needed to perform the acid type reactions [38] in comparison with HDS and HydO causes that when the acid-sites density and strength increase, reactant molecules adsorb preferentially in this kind of sites, thus, competing with the adsorption in CUS sites. As a consequence, the HDS and HydO reactions are inhibited, as described above. Also it is important to take into account that according to the literature, weaker Brönsted acid sites are able to perform isomerization reactions, whereas stronger Brönsted acid sites are needed

for cracking and alkylation [38]. This fact could justify the existence of a point beyond which the combination of the increment of Brönsted acid sites density with the increment of its strength, gives origin to a preference of reactants to react via cracking and alkylation instead of HDS and HydO. In our case, this point would be located somewhere in the aforementioned transition zone. In the Fig. 2.3, it can be observed that at 373K the Brönsted/Lewis ratio is quite similar for the CMS15 and the CMS25 catalysts, but at 473 and 573K it is higher for CMS25 than for CMS15, especially at 573K where the Brönsted/Lewis ratio is very low for the CMS15 and the other ASA-supported ones have very similar values. Thus, the aforementioned transition zone could be due to the existence of strong Brönsted sites in the catalysts supported on ASA with Si/(Si+Al) ratio ≥ 0.25, which does not exist at all or in the sufficient quantity in catalysts with Si/(Si+Al) ratio ≤ 0.15.

So far, we have discussed the existence and the possible causes of a transition zone between HDS type catalyst and acid-type ones. As we already said above all acid-type reactions are not detrimental to the objective of improve the selectivity to HDS; however, what we have not mentioned is that some of these reactions (double-bond and skeletal isomerization reactions) could even help to improve it. It has been shown in the literature that the isomerization of the double bond can play an important role in avoiding the HYD of the branched olefins [8,12]. Terminal olefins are much easier to hydrogenate than internal ones [1,3,4,12]. This is explained by the steric effect caused by the substitution of hydrogen atoms linked to carbon atoms making part of the double bond [39]. Therefore, it will be desirable to avoid the double-bond isomerization from internal to terminal olefins or even displace the equilibrium of the reaction to produce internal olefins from terminal ones. In the case of essays type B, this reaction is even more important because internal linear olefins have a much better octane number than terminal ones [34]. In this sense, it could be said that the CMS15 catalysts have a superior catalytic performance than the CMA in the HDT of FCC naphtha because they have quite

similar HDS activities and selectivities to HDS, but the CMS15 has twice the isom/HydOL ratio than the CMA.

Skeletal isomerization was also a beneficial reaction, not only because its products have similar octane number than 2,4,4TMPs, but also because of its competition with HydO and cracking reactions. In the Fig. 2.5, it is observed that both skeletal isomerization and cracking activities increase with increasing Si content, but cracking increment is more accentuated. This can be explained because isomerization reactions are easier to perform by the weak acid sites and the increase in Brönsted/Lewis ratio, acid site density and strength promotes the activity in cracking reactions [38]. However, for the three catalysts with higher Si contents, equilibrium between both reactions was found. The equilibrium between both reactions is due to the skeletal isomerization reaction, which mainly produces other TMP (2,3,4-TMP and 3,4,4-TMP) different from 2,4,4-TMP and a few dimethylhexenes, so inhibiting in some way the cracking. The cracking of 2,4,4-TMP proceeds via a type A β-scission, which involves the formation of a tertiary carbenium ion to produce also another carbenium ion (isobutene). This is the most energetically favorable type of β-scission [20,37] and is the most probable mechanism to explain our results, because our principal cracking products were only isobutene and isobutane. On the contrary, the cracking of the other TMP and dimethylhexenes proceeds via type B1 or B2 β-scission, which starts with a secondary ion to finish with a tertiary one, and starts with a tertiary ion to finish with secondary one respectively [37]. Both type B β-scissions are much less energetically favored than type A β-scissions [37]. Thus, the skeletal isomerization plays a double role, on one hand, controlling the HydO, and on the other hand, controlling the cracking.

As a general remark, it can be said that when ASA is used as support for naphtha HDT catalysts, it is possible to manipulate the catalytic functions HDS, HYD, and acid type by changing the support Si/(Si+Al) ratio and, therefore, the acid

properties. However, the manipulation of only the Si/(Si+Al) ratio was not enough to further refine the control of the acidity of these materials in order to find a point where only double-bond and skeletal isomerization reactions would be promoted, avoiding the undesirable olefin cracking reaction, and consequently, inhibiting only the HydO without the inhibition of the HDS. However, for the CMS15 it was found that although its selectivity to HDS and HDS activity were similar to that of the CMA, the CMS15 catalyst produces twice the quantity of internal linear olefins than CMA.

2.4. CONCLUSIONS

With increasing Si/(Si+Al) ratio, the activity of acid-type reactions was enhanced at expense of the activity of HDS and HydO. The changes in selectivity and product distribution were not gradual. A kind of transition zone was observed between 15 and 25 % Si/(Si+Al), where changes in selectivity and product distribution were surprisingly huge. This fact matches with an increment in the Brönsted acid sites density and strength, which due to its competition with CUS for the reactants adsorption gives origin to a preference of reactants to react via cracking and alkylation instead of HDS and HydO after its value reaches certain a point in the transition zone.

It was established that in addition to the control effect that double-bond isomerization from external to internal olefins exerts over HydO, skeletal isomerization could also contribute in the control of this reaction, as well as in the control of cracking. Consequently, promotion of skeletal isomerization could aid to the preservation of octane number during FCC naphtha HDT.

It was demonstrated that by modifying the support composition, it is possible to manipulate the three basic catalytic functions of the catalysts: HDS, HydO and acidity.

2.5. REFERENCES

[1] S. Brunet, D. Mey, G. Pérot, C. Bouchy, F. Diehl, Appl. Catal. A 278 (2005) 143-172.

[2] C. Song, Catal. Today, 86 (2003) 211-263.

[3] R. Zhao, C. Yin, H. Zhao, C. Liu, Fuel Process. Tech. 81 (2003) 201-209.

[4] S. Hatanaka, M. Yamada, O. Sadakane, Ind. Eng. Chem. Res. 36 (1997) 1519-1523.

[5] S. Hatanaka, M. Yamada, O. Sadakane, Ind. Eng. Chem. Res. 36 (1997) 5110-5117.

[6] V. Belliere, C. Geantet, M. Vrinat, Y. Ben-Taarit, Y. Yoshimura, Energy & Fuels 18 (2004) 1806-1813.

[7] M. Arias, D. Laurenti, Virginie Bellière, C. Geantet, M. Vrinat, Y. Yoshimura, Appl. Catal. A 348 (2008) 142-147.

[8] D. Mey, S. Brunet, C. Canaff, F. Maugé, C. Bouchy, F. Diehl, J. Catal. 227 (2004) 436-447.

[9] S. Hatanaka, T. Miyama, H. Seki, S. Hikita, EP 0736589 A1 (1996).

[10] C. Flego, V. Arrigoni, M. Ferrari, R. Riva, L. Zanibelli, Catal. Today 65 (2001) 265-270.

[11] G. Muralidhar, F.E. Massoth, J. Shabtai, J. Catal. 85 (1984) 44-52.

[12] M. Toba, Y. Miki, T. Matsui, M. Harada, Y. Yoshimura, Appl. Catal. B 70 (2007) 542-547.

[13] V. La Parola, G. Deganello, A.M. Venecia, Appl. Catal. A 260 (2004) 237-247.

[14] V. La Parola, G. Deganello, S. Scirè, A.M. Venecia, J. Solid State Chem. 174 (2003) 482-488.

[15] J.B. Miller, I.E. Ko, Catal. Today 35 (1997) 269-292.

[16] V.L. Barrio, P.L. Arias, J.F. Cambra, M.B. Güemez, B. Pawelec, J.L.G. Fierro, Fuel, 82 (2003) 501-509.

[17] P. Berteau, B. Delmon, Catal. Today 5 (1989) 121-137.

[18] J.-P Damon, B. Delmon, J.M. Bonnier, J. Chem. Soc., Faraday Trans. 1 73 (1977) 372-380.

[19] P.O. Scokart, F.D. Declerck, R.E. Sempels, P.G. Rouxhet, J. Chem. Soc., Faraday Trans. 1 73 (1977) 359-371.

[20] G. Busca, Chem. Reviews 107 (2007) 5366-5410.

[21] C. Defossé, P. Canesson, P.G. Rouxhet, B. Delmon, J. Catal. 51 (1978) 269-277.

[22] R.E. Sempels, P. G. Rouxhet, J. Colloid Interface Sci. 55 (1975) 263-273.

[23] H. Knözinger, P. Ratnasamy, Catal. Rev. Sci. Eng. 17 (1978) 31-70.

[24] T.J. Bandoz, Ch. Lin, J.A. Ritter, J. Colloid Interface Sci. 198 (1998) 347-353.

[25] B. Xu, C. Sievers, J.A. Lercher, J.A. Rob van Veen, P. Giltay, R. Prins, J.A. van Bokhoven, J. Phys. Chem. C 111 (2007) 12075-12079.

[26] C. Sârbu, B. Delmon, Appl. Catal. A 185 (1999) 85-97.

[27] V. La Parola, G. Deganello, C.R. Tewell, A.M. Venezia, Appl. Catal. A 235 (2002) 171–180.

[28] J.E. Herrera, D.E. Resasco, J. Catal. 221 (2004) 354–364.

[29] G. Mestl, T.K.K. Srinivasan, Catal. Rev.-Sci. Eng. 40 (1998) 451-570.

[30] B. Pawelec, T. Halachev, A. Olivas, T.A. Zepeda, Appl. Catal. A 348 (2008) 30-41.

[31] C.C. Williams, J.G. Ekerdt, J.-M. Jehng, F.D. Hardcastle, I.E. Wachs, J. Phys. Chem. 95 (1991) 8791-8797.

[32] H. Jeziorowski, H. Knözinger, P. Grange, P. Gajardo. J. Phys. Chem. 84 (1980) 1825-1829.

[33] J. Vakros, A. Lycourghiotis, G.A. Voyiatzis, A. Siokoub, C. Kordulis, Appl. Catal. B 96 (2010) 496–507.

[34] W. Gruse, D. Stevens, The chemical technology of Petroleum, 2nd ed., Mc Graw Hill, New York, 1942.

[35] H. Topsoe, B.S. Clausen, F.E. Massoth, in J.R. Anderson, M. Boudart (Eds.), Hydrotreating Catalysis, Science and Technology, Springer-Verlag, Berlin, 1996.

[36] W. Gruse, D. Stevens, The chemical technology of Petroleum, 2nd ed, MC Graw Hill, New York, 1942.

[37] J. S. Buchanan, J. G. Santiesteban, W. O. Haag, J. Catal. 158 (1996) 279-287.

[38] A. Corma, Chem. Rev. 95 (1995) 559-614.

[39] F.A Carey, Química Orgánica, Mc Graw Hill, 3ª ed, Madrid, 1999.

3. IMPROVING THE SELECTIVITY TO HDS IN THE HDT OF FCC NAPHTHA USING SODIUM-DOPED AMORPHOUS ALUMINOSILICATES AS SUPPORTS OF COMO CATALYSTS

3.1. INTRODUCTION

In the preceding chapter CoMo catalysts supported on amorphous aluminosilicates with different Si/(Si+Al) ratios were essayed in the HDT of synthetic FCC naphtha. It was encountered that the Brönsted acidity of this catalysts increased with the Si/(Si+Al) ratio, thus, conducting to produce acid-type reactions like cracking and isomerization of olefins, and the alkylation of 2-MT with olefins. These acid-type reactions competed with the hydrodesulfurization (HDS) and the hydrogenation of olefins (HydO). Even, they inhibit the HDS and HydO at all in the case of the catalysts with the highest Si content in essays type A. From the analysis of the product distribution of these reactions, it was concluded that a way to inhibit olefin saturation was by achieving an acid-properties balance. Therefore, promoting only double-bond and skeletal isomerization reactions, but avoiding cracking. As a consequence, the HydO could be inhibited by a double effect. On one hand, harder to hydrogenate olefins are produced in the case of the double-bond isomerization [1-4], on the other hand, there is a competition for the adsorption of olefins between the acid sites and the HydO ones (section 2.3.2). However, in this chapter was concluded that modifications of only the Si/(Si+Al) ratio were not enough to control finely the acid properties.

In the literature, it can be encountered some works [5, 6] where their authors succeeded in controlling finely the acid-base properties of their catalysts by combining modifications which conduct to improve the acidity with another which conduct to reduce it. La Parola et al. [6] showed that improvements in the

thiophene HDS can be achieve by using sodium modified amorphous aluminosilicates (ASA) as support for CoMo catalysts. Fan et al. [5] have shown that by doping alumina simultaneously with P and K highly selective to the HDS catalysts can be obtained. This was consequence of a balance of the acid properties as well as a good compromise between the dispersion of the CoMoS phase and the stacking level of the MoS_2 slabs.

In this chapter, it was intended to finely control the acid properties of the ASA supports by doping them with sodium. The acid properties were followed by various methods and the dispersion and coordination of Co and Mo were also followed using Raman. These surface properties were used to try to explain the catalytic behavior of our catalysts in the HDT of synthetic FCC naphtha.

3.2. EXPERIMENTAL

3.2.1. Preparation of Catalysts

ASA supports with different Si/(Si+Al) ratios (0.15, 0.25, 0.33, 0.5 and 0.75) were prepared by the sol-gel route according to the procedure described by La Parola et al. [7] and already described in section 2.2.1.

ASA supports were modified with sodium (3 wt.%) by incipient wetness impregnation with an aqueous solution of $NaNO_3$ (Merck). The impregnated solids were dried under airflow at 343 K for 2 h and air calcined at 773 for 12 h. CoMo catalysts supported on NaASAxx containing 10% MoO_3 and 2% CoO were prepared by successive incipient wetness impregnation. The supports and catalysts were named here NaASAxx and CMNaSxx respectively, where “xx” represent the Si/(Si+Al) ratio. An initial impregnation step was performed with an aqueous solution of $(NH_4)_6Mo_7O_{24}{\cdot}4H_2O$ (Merck); subsequently, the solids were impregnated with an aqueous solution of $Co(NO_3)_2{\cdot}6H_2O$. After each impregnation step the same thermal treatment used after Na impregnation was done. A

conventional CoMo catalyst supported on a commercial Procatalyse γ-Al_2O_3 (CMA) and another catalyst supported on γ-Al_2O_3 modified with 3 wt.% Na CMANa were also prepared by the same method for comparison purposes. In this case, after each impregnation step, the solids were dried under airflow at 393 K for 12 h and air calcined at 773 K for 4 h.

3.2.2. Characterization of catalysts

3.2.2.1. Catalysts composition

The catalysts and support nominal compositions were verified by X-ray fluorescence (XRF) using a Shimadzu EDX 800 HS apparatus.

3.2.2.2. Textural properties

The specific surface area (A_{BET}) of both catalysts and supports was estimated by the same method described in 1.2.2.1.

3.2.2.3. X-ray diffraction (XRD)

XRD was performed according the procedure described already in 1.2.2.3.

3.2.2.4. Acid-base properties

The acidic properties of catalysts in the oxide state were determined by NH_3 temperature programmed desorption (TPD) and Fourier transformed infrared (FT-IR) spectroscopy using pyridine as a probe molecule. On the other hand, the base properties of the alkaline metal modified catalysts were determined by FT-IR spectroscopy using CO_2 as probe molecule. These procedures were already described in section 1.2.2.6.

3.2.2.5. Confocal laser Raman microscopy (Raman)

Raman spectra of the catalysts were taken following the procedure already described in 1.2.2.5.

3.2.3. Catalytic evaluation

Catalytic tests were made according to the procedure already described in 1.2.3.

3.2.4. Expression of results

In this chapter the results of the catalytic tests were expressed in the same way used in preceding ones (1.2.4).

3.3. Results

3.3.1. Influence of sodium and Si/(Si+Al) ratio on the structure of the catalysts

Table 3.1. Textural properties of the prepared catalyst

Catalyst	A_{BET} (m^2g^{-1})	PV (cm^3g^{-1})	PD (Å)
CMA	194	0.49	100
CMANa	183	0.48	106
CMNaS15	88	0.32	145
CMNaS25	253	0.483	76
CMNaS33	110	0.193	70
CMNaS50	165	0.304	74

A_{BET}: specific surface area; PV: pore volume; PD: average pore diameter

Table 3.1 presents the textural properties of CMNaSxx catalysts compared with the one of CMA and CMANa. From the analysis of the adsorption-desorption curves

hysteresis, it can be inferred that all materials are mainly mesoporous with only a small proportion of micropores as expected due to the basic hydrolysis used in the sol-gel synthesis of these materials [7, 8]. There are not defined trends of the A_{BET}, PV or the PD with the Si/(Si+Al) ratio. However, it is noteworthy that the CMNaS15 catalyst, which is the one with the lowest A_{BET}, is by far the catalyst with the highest PD. In the section 2.3.1 (Table 2.1) was shown that there was a great reduction of the A_{BET} when comparing the unmodified ASAxx supports with the respective CoMo catalysts supported on them (CMSxx). This reduction was explained by the blocking of both the micropores and the smallest mesopores as a consequence of the Mo and Co deposition. Comparing the results of table 3.1 with the ones of the table 2.1, it is noted that the reduction in the A_{BET} was accentuated by the sodium introduction. For instance, the A_{BET} was reduced from 397 cm^2g^{-1} for the ASA15 support to 269 cm^2g^{-1} for the CMS15 catalyst and 88 cm^2g^{-1} for the CMNaS15.

In the Fig. 3.1 are shown the XRD spectra of the CMA, CMNaS15, CMNaS25 catalysts compared with the respective catalysts supported on the unmodified supports: CMS15 and CMS25. No peaks corresponding to Mo or Co compounds are observed which indicate a good dispersion of these on the different supports. In the CMA catalysts are only observed broad bands typical of γ-Al_2O_3 with poor crystallinity [9]. A similar XRD spectrum was obtained for the CMANa catalyst (not shown). Whereas, in the catalysts supported on the unmodified ASA supports no peaks are observed as a consequence of the amorphous nature of ASA. However, when comparing the XRD spectra of CMNaS25 with CMS25, it is observed that the bands corresponding to γ-Al_2O_3 begin to appear. The same was observed in the CMNaS33 XRD spectrum compared with that of CMS33 (not shown). This fact is even more evident when CMNaS15 and CMS15 are compared; the γ-Al_2O_3 bands are now observed clearly along with peaks corresponding to $Na_2Al_2O_3$ [9]. On the contrary, no peaks are observed neither in the XRD spectrum of CMNaS50 nor in the one of CMS50. Consequently, it could be inferred that sodium introduction increased the crystallinity of the segregated alumina phase present in the supports

with less than 50 % Si/(Si+Al). In the section 2.3.1 (Fig. 2.3) we have already reported the presence of alumina type IB and IIA OH groups of Knözinger classification [10] in the ASAxx unmodified supports with a Si/(Si+Al) ratio less than 50 %. This fact confirms the presence of a segregated alumina phase which dilutes the Si-Al mixed oxide phase in the ASAxx supports belonging to that range of Si/(Si+Al) as suggested by other authors before [11-13]. The increment in the segregated alumina phase crystallinity could explain the great reduction in the A_{BET} when comparing catalysts supported on the unmodified ASA support with those supported on the sodium modified one.

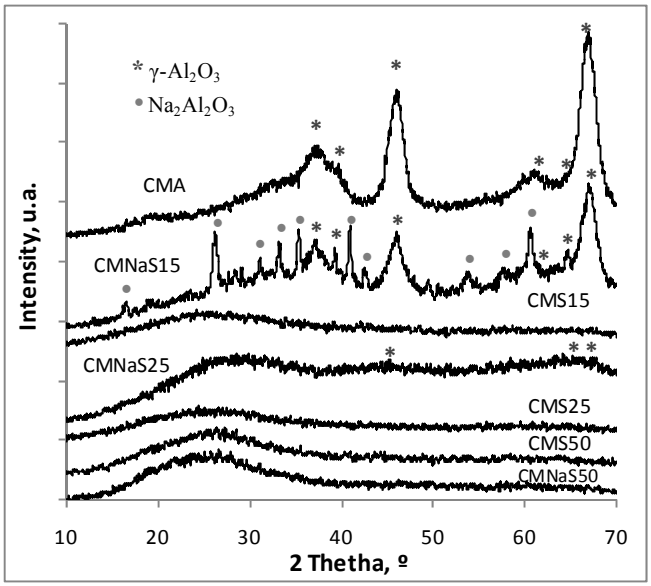

Fig. 3.1. XRD of some selected catalysts

In the Fig. 3.2 are shown the Raman spectra of the CMNaSxx catalysts compared with the ones of CMA and CMANa. First of all, it can be notice that both Co and Mo are well dispersed on the different supports, because of the lack of peaks characteristic of Co compounds (681, 477 and 199 cm^{-1}) and free MoO_3 aggregates (990-1000 cm^{-1}) [14-16]. Also, the presence of $Al_2(MoO_4)_3$ (1000-1010 cm^{-1}) can be ruled out [16]. Beginning the analysis by the CMA catalyst spectrum,

it is observed a broad band at ca. 920-950 cm^{-1} with shoulders at both sides ca. 900 and 960 cm^{-1}. There are also other broad bands at ca. 320-360 and 225 cm^{-1}. The region 750–1000 cm^{-1} is where the bands for stretching of Mo–O bonds are typically observed [14, 16]. Inside the broad band at 920-950 cm^{-1} a variety of Mo species could be placed; the more likely, according to literature [14-18], are $Mo_7O_{24}^{6-}$ octahedral species (946-951, 360 and 220 cm^{-1}, continuous lines) and MoO_4^{2-} with distorted tetrahedral symmetry (916 and 320 cm^{-1}, dotted lines). Some contribution from Mo-O-Co stretching vibrations in $CoMoO_4$ species (939, 873, 820, 370 and 340 cm^{-1}, dashed lines) cannot be ruled out [19]. The shoulder at ca. 900 cm^{-1} can be attributed to monomeric undistorted MoO_4^{2-} species (at ca. 892 and 807 cm^{-1}) and the other one at ca. 960 cm^{-1} to larger polymeric species like $Mo_8O_{26}^{4-}$ (958-960 cm^{-1}).

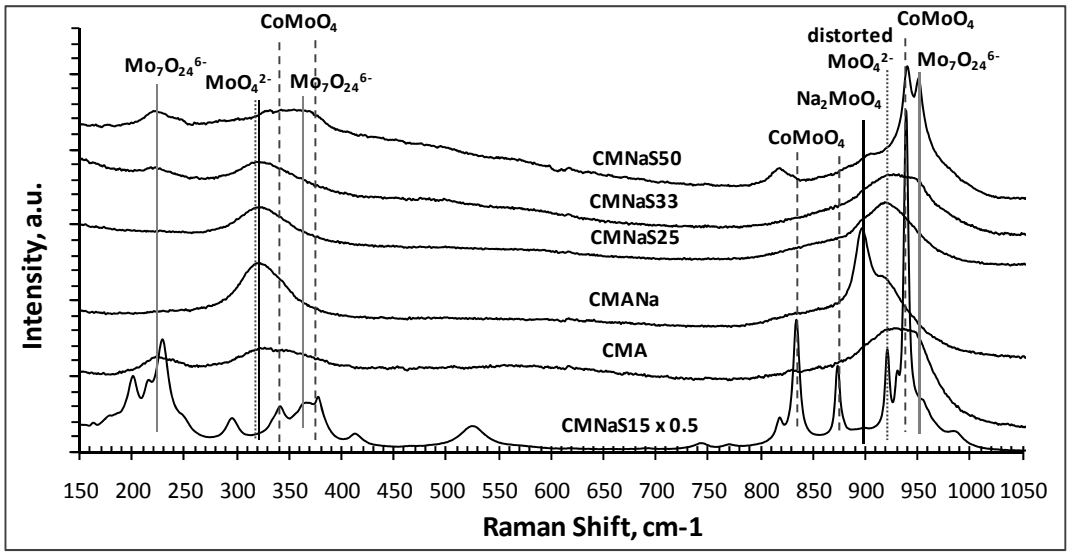

Fig. 3.2. Raman spectra of the prepared catalysts.

Comparing the spectrum of the CMANa catalysts with the CMA one, it is observed that bands belonging to octahedral $Mo_7O_{24}^{6-}$ and $CoMoO_4$ practically disappear. Whereas, some contribution of MoO_4^{2-} distorted tetrahedral species is still observed. In addition, it is observed a sharp peak close to 897 cm^{-1} which is

attributed to undistorted tetrahedral species like those present in the Na_2MoO_4 compound [15, 16]. Even though the presence of this compound was not detected in the diffractogram of the CMANa catalyst, it is presumed that it exists but the size of its crystals is not high enough to be detected by this technique, but it is high enough to be detected by Raman. In fact, its presence by XRD in a CoMo catalyst supported on alumina with 5 wt.% Na [15, 20] was clearly demonstrated in the section 1.3.2 (Fig. 1.2) as well as in other works in the literature [6, 20, 21]. The formation of the Na_2MoO_4 implicates a very strong Mo-support bond even stronger than that present in the catalysts supported on unmodified alumina [6, 20, 21]. This fact is detrimental to the HDS and HydO activity of the catalysts because the strong bond Mo-support gives origin to Mo species very hard to reduce/sulphide [6, 20-23].

Regarding the CMNaSxx catalysts Raman spectra, it is observed that the one of the CMNaS15 catalyst is clearly different from the others. It is the only one which exhibit markedly defined peaks, clear sign of crystallinity, whereas in the other catalysts there are predominantly amorphous species. These well defined peaks match well with β-$CoMoO_4$ species [19, 20]. The detection of crystalline Mo species in the CMNaS15 catalyst is in agreement with the detection of crystalline support species by XRD. This fact also supports the idea, already expressed above, that the ASA15 was the support most sensitive to sodium regarding the increase in crystallinity not only of the phases which compose the support itself but also of the supported ones. However β-$CoMoO_4$ specie is not the only Mo specie present in the catalyst. It is logical to think this because of the Co/(Co+Mo) ratio used in this work. Even if all the Co exists in the form of $CoMoO_4$ only 1/3 of the Mo will be consumed. In fact, the CMNaS15 Raman spectrum shown in Fig. 3.2 was multiplied by 0,5 for a better observation of the other spectra, but observing it in detail, shoulders at ca. 950 and 920 cm^{-1} are also observed. Thus, there are also $Mo_7O_{24}^{6-}$ and distorted tetrahedral MoO_4^{2-} species on the catalyst. In this case the higher intensity of bands corresponding to β-$CoMoO_4$ species is only sign of a

higher crystallinity and it cannot be affirmed that it is in a higher proportion [16]. The relative intensity of the shoulder at ca. 920 cm^{-1} is higher than the one of the shoulder at ca. 950 cm^{-1}. Thus, the CMNaS15 catalyst could fit in the tendency shown by the other CMNaSxx catalysts, but, with an important presence of β-$CoMoO_4$ species additionally. In the other CMNaSxx catalysts Raman spectra at low Si/(Si+Al) ratios is observed a prevalence of distorted tetrahedral monomeric MoO_4^{2-} species with some presence of Na_2MoO_4. However, different from the catalyst supported on the sodium modified alumina where the Na_2MoO_4 was the major tetrahedral Mo specie, the distorted MoO_4^{2-} one was the majority on the CMNaSxx catalysts. With increasing Si/(Si+Al) ratio, it is observed an increment of the octahedral species at expense of the tetrahedral ones.

Comparing the CMNaSxx catalysts Raman spectra with the respective CMSxx one (Fig. 2.4), in both kinds of catalysts was observed the same tendency of increasing the population of octahedral species at expense of the tetrahedral ones with the Si/(Si+Al) ratio. However, sodium introduction causes an increment of the prevalence of tetrahedral species. Even, undistorted tetrahedral species not present in the CMSxx catalysts are present in the CMNaSxx ones. Therefore, sodium introduction increases the strength of the bond between the Mo phase and the support. The increment of octahedral Mo species with increasing the Si/(Si+Al) is related with the heterogeneity of phases encountered in the ASAxx supports. It has been already shown in the literature that the maximum of the mixed Si-Al oxide phase it is encountered at 50-75 % Si/(Si+Al) and that below that content the mixed Si-Al oxide phase is diluted by a segregated alumina phase[11-13]. Taking into account that this mixed Si-Al phase is related with the increase of the acidity and acidity strength of the ASA supports as it will be further described in section 3.3.2 [11-13], it will be expected that the point of zero charge of the support decrease with increasing Si/(Si+Al) ratio. It is also known that during the impregnation process, the Mo species which will be deposited on the support surface seems to be governed by the surface pH, more precisely by its point of

zero charge (PZC) [16, 18] according to eq. 1.2 and 1.3. Thus at pH values higher than 6.5 the MoO_4^{2-} anion is stable and a decrease in pH to 4.5 leads to complete formation of $Mo_7O_{24}^{6-}$ [16]. A further decrease in pH to 1.5 leads to polymerization of $Mo_8O_{26}^{4-}$ [16]. The augmentation of the prevalence of tetrahedral species with the sodium introduction could be explained in these sense as well since it would be expected an increase in the PZC because of it.

3.3.2. Influence of sodium and the Si/(Si+Al) ratio on the acid-base properties of the catalysts

In the Fig. 3.3 is presented the total acidity and the acidity strength distribution obtained by NH_3 TPD of the CMNaSxx catalysts compared with those of the CMA and CMANa catalysts. The strength of the acid sites was arbitrarily classified as weak (<423 K), intermediate (423-573 K), and strong (>573) according to the temperature of NH_3 desorption [24]. The total acidity of all the CoMo catalysts supported on the sodium modified supports is lower than the one of the CMA catalyst and it increase with the Si/(Si+Al) ratio. The CMANa catalyst exhibits the lowest total acidity, the highest proportion of weak and the lowest of strong acidity. Among the CMNaSxx catalysts the CMNaS15 present the highest proportion of weak and the lowest of the strong acidity.

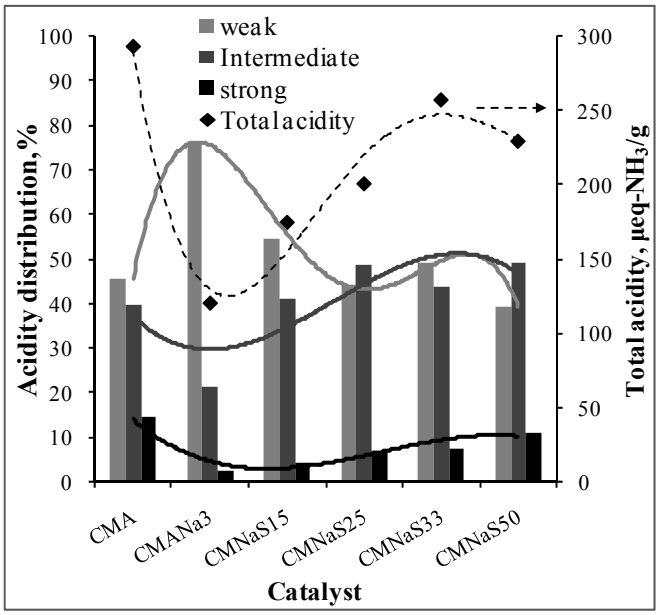

Fig. 3.3. Total acidity and acidity distribution of the prepared catalysts. Weak: T < 423 K, intermediate: 423 K < T < 573 K, strong T > 573

In the Fig. 3.4 is presented the IR spectra of adsorbed CO_2 on the prepared catalysts, which could be used to estimate the possible modifications of the catalysts basicity by sodium introduction [3, 25]. It is observed that compared with CMA the only catalysts which show an important increase in the adsorption of CO_2 is the CMANa. Also it is observed that the preferred adsorbed specie changes from hydrogen carbonates to bidentate carbonates. Whereas, the CMNaSxx catalysts present a CO_2 adsorption similar to that of CMA with similar adsorbed carbonate species. Other authors [26] have shown that Na is selectively adsorbed on the Al^{+3} tetrahedrally-coordinated-Lewis sites of alumina, which gives rise to the formation of an $[\equiv Al{-}OH]^{-}Na^{+}$ complex. This fact has been demonstrated by ^{27}Al-RMN studies where the disappearance of the band attributed to Al^{+3} was observed [26]. Thus, a double effect on the alumina surface is produced; stronger acid sites are poisoned and at the same time the complex formation increase the basicity of the site. On the other hand, on CMNaSxx catalysts, sodium only block the acid sites diminishing the total acidity in comparison with the respective without-sodium catalysts (Fig. 2.1), but no important creation of basic sites is observed.

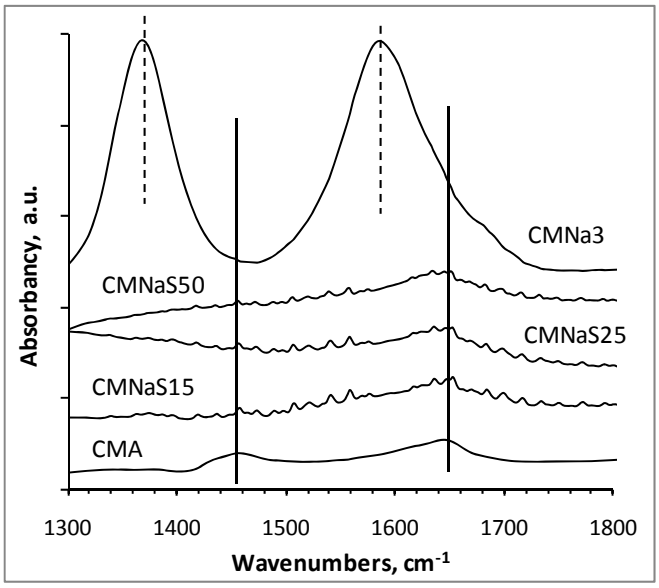

Fig. 3.4. IR spectra of adsorbed CO_2 on the prepared catalysts. Dashed lines: bidentate carbonates; continuous lines: hydrogen carbonates.

The kind of acid sites existing in the catalysts was quantified using IR spectra of adsorbed pyridine after desorption at r.t., 373, 473 and 573 K. Peaks at 1453 and 1545 cm^{-1} in the IR spectra of adsorbed pyridine (not shown), attributed in literature to pyridine bonded to Lewis and Brönsted sites respectively [7, 27], were mathematically decomposed using Gauss-type curves. The values resulting from their integration were used to calculate the Brönsted/Lewis ratio, which was plotted as a function of the % Si/(Si+Al) in Fig. 3.5. The zero value in the X axis represents the conventional catalyst CMA. For the CMA catalyst the Brönsted/Lewis ratio is zero because no Brönsted sites were detected using pyridine as model molecule; however, this fact do not discard the existence of very weak Brönsted sites unable to protonate pyridine. The Brönsted/Lewis ratio increases continuously with increasing the Si/(Si+Al) ratio at 373 K. Similar trends were observed at 473 and 573 K, however at 473 K Brönsted sites were detected only for catalysts with a % Si/(Si+Al) ≥ 25 and at 573 K only for catalysts with a % Si/(Si+Al) ≥ 50. Comparing the Brönsted/Lewis ratio of CMNaSxx catalysts with the one of CMSxx catalysts (Fig. 2.2), it could be inferred that sodium introduction brings about a reduction in

the strength of the Brönsted acid sites. This reduction was more evident in the catalysts with lower Si/(Si+Al) ratio. In the section 2.3.1 (Fig 2.3) was already demonstrated, by analyzing the OH groups present on the ASA supports surface using IR, that the increase of the Brönsted acidity with the Si/(Si+Al) ratio content was linked to an increase in the concentration of mixed Si-Al oxide phase, in agreement with other works in literature [11-13].

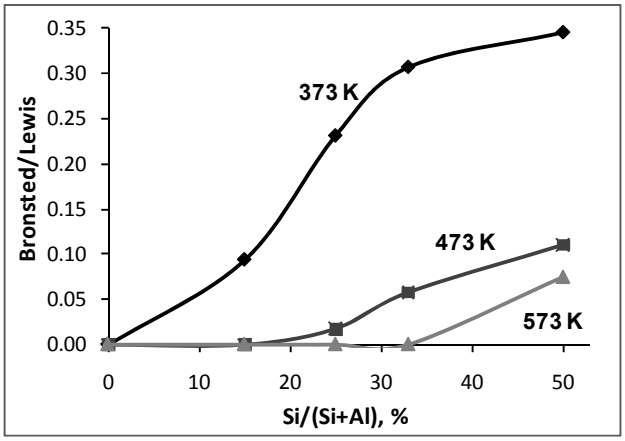

Fig. 3.5. Brönsted/Lewis ratio of sodium-modified-ASA supported CoMo catalysts at 373, 473 and 573 K.

3.3.3. Influence of sodium and the Si/(Si+Al) ratio on the catalytic performance

A lot of organic substances were found in the condensable products at the reactor outlet. A complete identification of all reaction products was done. In the section 1.3.3.1, we have already described reaction schemes for 2-MT and branched olefins (TM1P and TM2P) based on the product identification along with the comparison with other reaction schemes proposed in the literature [1, 3, 4, 21, 28-32].

The reactants conversions as well as their product yields in essays type A and B for the CMNaSxx catalysts compared with that of the CMA and the CMANa ones

are presented in Fig. 3.6 and 3.7 respectively. Reactants conversions are plotted as dashed lines and the yield of product as stacked columns.

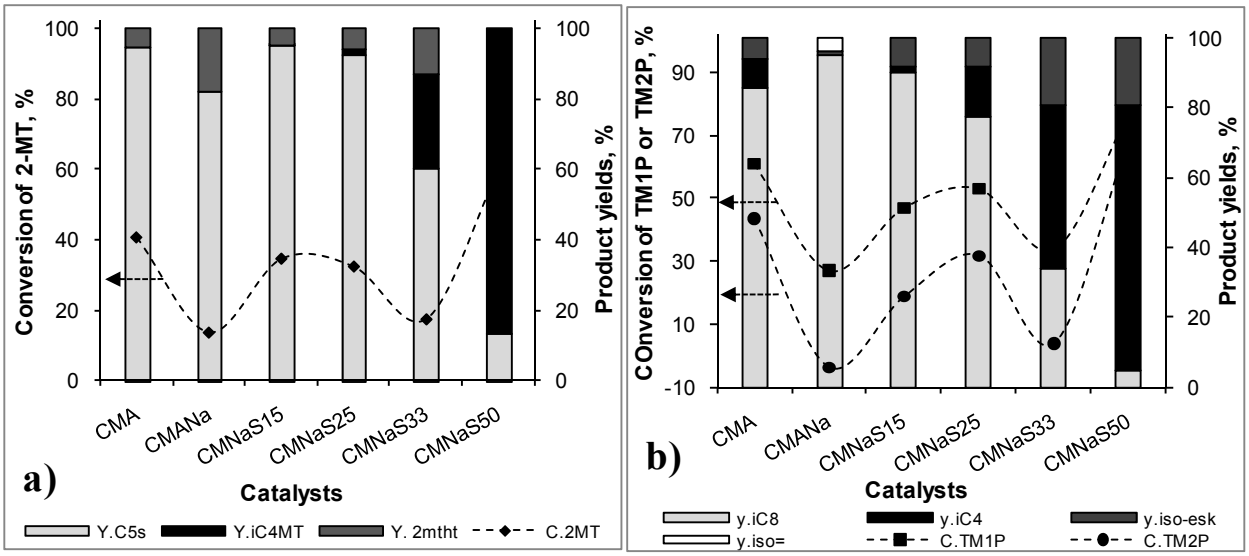

Fig. 3.6. Reactant conversions and their product yields in essays type A: feed compose by 2-MT and branched olefins (TM1P and TM2P).

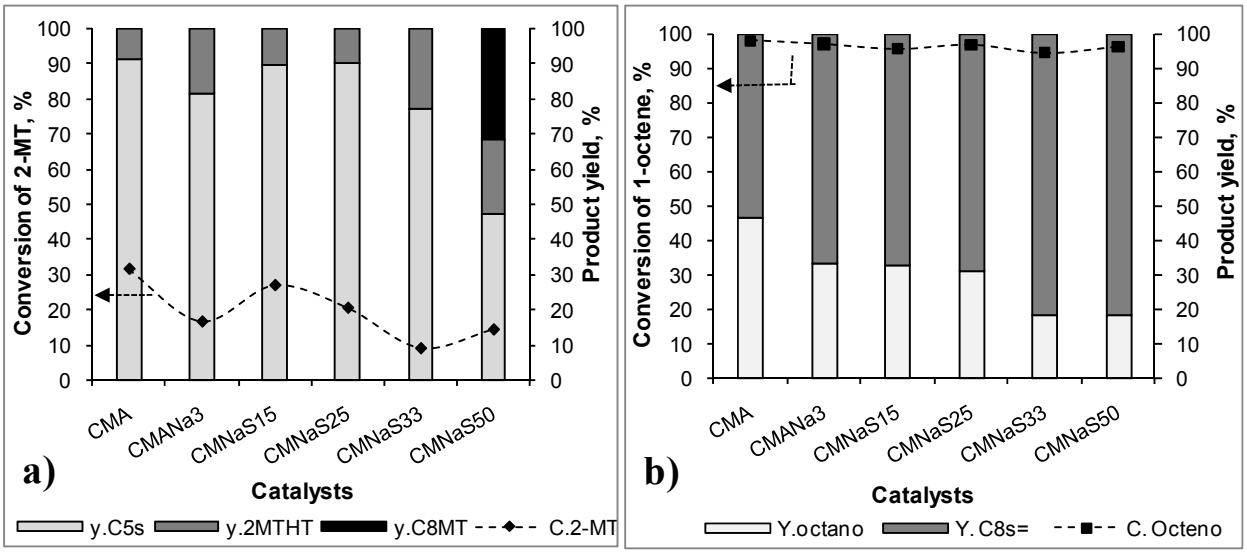

Fig. 3.7. Reactant conversions and their product yields in essays type B: feed compose by 2-MT and linear olefins (1-octene).

When the performances of the CMNaSxx catalysts in the HDT of FCC naphtha are going to be compared with the one of the conventional catalyst used in the industry (CMA), two separated effects should be considered: the sodium introduction and the variation of the Si/(Si+Al) ratio. The effect of the modification of the Si/(Si+Al) ratio will be described first by comparing the catalytic performance of the CMNaSxx catalysts with the one of the CMANa. It is observed that with increasing the Si/(Si+Al) ratio the yield of the HDS products (C5s + 2-MTHT), which is 100% for the CMANa catalysts, diminishes meanwhile the yield of the AMT ones increases (Fig. 3.6.a). With increasing the Si/(Si+Al) ratio up to 25 % the variations of the yields are scarce, however with the subsequent increments to 33 and 50% much higher variations are observed. Even, in the CMNaS50 catalysts a yield of the AMT around 80% is observed. A similar trend is observed for the yield of the olefin products (Fig 3.6.b). In this case for the CMANa catalyst a yield higher than 95% is observed for the hydrogenation product accompanied by lower yields of the skeletal and double-bond isomerization reactions. With increasing Si/(Si+Al) ratio the yield of isooctane diminishes meanwhile the yields of skeletal isomerization and cracking products increase. The yield of cracking products increases faster than the one of the skeletal isomerization. Again the higher variations of the product yields are observed when the Si/(Si+Al) ratio is increased to 33 and 50%. Thus, in essays type A the HDS and the HydO reactions are replaced progressively for acid-type reactions like alkylation in the case of 2-MT products, and skeletal isomerization and cracking in the case of olefin products. This fact seems to agree with the increase in the Brönsted sites density and strength described in the section 3.3.2. These Brönsted sites would compete with the HDS and the HydO sites for the adsorption of the reactants. Consequently, when the density and strength of the Brönsted sites increases enough, the reactants are adsorbed predominantly on these sites instead of on the HDS and HydO ones.

On the other hand, the effect of sodium introduction could be observed by comparing the performance of the catalysts supported on sodium modified

materials (ASA or alumina) with the one of the catalysts supported on the respective bare material. In the case of the catalysts supported on alumina, it is observed that the low cracking yield of the CMA catalysts disappeared as a consequence of the huge reduction in the total acidity and strength when the CMA and the CMANa catalysts are compared (Section 3.3.2). A similar effect of sodium is observed when the performance of the CMNaSxx catalysts in the Fig. 3.6 is compared with that of the CMSxx catalysts presented in Fig. 2.5. In the case of the CMNaSxx catalysts the main increments in the yield of the acid-type reaction are observed only when the Si/(Si+Al) ratio is increased to 33 and 50% and only the catalysts with 50% Si/(Si+Al) ratio presented a majority of the yield of acid-type products of both 2-MT and olefins (Fig. 3.6). Whereas, in the case of CMSxx catalysts the main increments in the yield of the acid-type reactions, with a majority of these, are observed for the catalysts with a Si/(Si+Al) ratio ≥ 25%. As in the case of alumina supported catalyst, a great reduction in the acid sites density and strength, specially the Brönsted ones, was observed for the CMNaSxx (Section 3.3.2) compared with the CMSxx ones (section 2.3.1, Fig. 2.1 and 2.2).

In the case of essays type B, all catalysts except for the CMNaS50 present a 100% yield of HDS products (Fig. 3.7). This one presents also a 30% yield of AMT. In the case of the CMSxx catalysts only a 6% yield of AMT was observed for the CMS15 catalysts and yields higher to 50% were observed for catalyst with Si/(Si+Al) ratio ≥ 25% (Fig. 2.6). This fact confirms the same effect of sodium encountered in essays type A. Regarding the olefin products, other acid-type reactions different from the double-bond isomerization were not detected when using linear olefins, even with the CMSxx catalysts (Fig. 2.6). In these essays, even for the CMA catalyst, the yield of the double-bond isomerization (53%) is higher than that of the hydrogenation (47%). Compared with the CMA catalysts the yield of the double-bond isomerization is higher for all the other catalysts: approximately 70% for the CMANa, CMNaS15 and CMNaS25 catalysts and approximately 80% for the CMNaS33 and CMNaS50 catalysts. As in the case of the essays type A is

observed that the catalysts with 33 and 50% are the ones with the highest yields of the acid-type reactions; however, in essays type B the difference with the other catalysts is not so marked.

Thus, in the case of essays type B, the product distribution is less affected by the support modification. This fact could be explained because linear olefins interact less easily with the acid sites because their corresponding carbocations (secondary) are less stable than the ones formed for the branched olefins (tertiary) [2, 27, 33, 34]. As a consequence, those reactions which need stronger acid sites to be undergone like cracking, skeletal isomerization and alkylation [27, 33, 34] would be affected especially. Thus, the density and strength of the acid sites of the catalysts used in this work are not high enough to produce other reactions different from the double-bond isomerization of the linear olefins and only the catalysts which presented strong Brönsted sites produce the alkylation of 2-MT with linear octenes. However, when branched olefins are used, catalysts with very weak (CMA) and weak (CMNaS15) Brönsted sites could produce skeletal isomerization in addition to the double-bond isomerization. Those with intermediate Brönsted sites (CMNaS25 and CMNaS33) produce in addition cracking and alkylation reactions in moderate yields, and finally, the catalyst with strong Brönsted sites produce alkylation and cracking in very high yields. In the essays type B there are less differences in the products distribution among the different catalysts because the only reaction performed by olefins is the double-bond isomerization, which needs less strong acid sites to be performed than cracking and skeletal isomerization, and these sites exist even in pure alumina [27, 34].

It is also interesting to highlight that the CMANa catalysts present a yield of the double-bond isomerization reaction similar to that of the more acidic catalysts supported on ASA modified with sodium. In section 3.3.2 was shown that the acid sites density and strength of the CMANa catalyst is much lower than the ones of the other catalysts, but an important increment in basic sites was observed. This

important increment in the basic sites could explain the high yield of the double-bond isomerization exhibited by this catalyst. Solid basic catalysts have been recognized early as efficient catalysts for the double-bond migration of alkenes with one advantage over solid acid ones, which is its lack of C-C bond cleavage ability [25]. This fact explains also why the increment of the yield of the acid-type reactions for the CMANa catalyst was only observed in the reactions type B and not in the reactions type A.

The variations in product distribution along with other factors which will be analyzed forward produces variations in the total conversion of the reactants. In the Fig. 3.6.a is observed that in essays type A the total conversion of 2-MT for the CMANa catalyst is extremely low compared with the one of the CMA catalyst (around 70% reduction), whereas for the CMNaS15 and CMNaS25 the reduction is within error limits (around 10%). But, for the CMNaS33 a significant reduction (60 %) is observed again and for the catalyst CMNaS50 the contrary trend was observed (around 50% augmentation). In the Fig. 3.6.b. is observed that the conversions of TM1P and TM2P have a similar trend to the one described for 2-MT. However, more drastic variations are observed for the olefin conversions than for 2-MT, especially in the case of TM2P. For this olefin the more drastic variation is observed in the case of the CMANa catalyst, which presents a negative conversion of TM2P, i.e., instead of being consumed it is produced by the double-bond isomerization of the TM1P [3, 35]. This fact, make us think that the double-bond isomerization from external to internal positions is also present in the other catalysts. Thus, the double-bond isomerization along with the steric effects explains the differences in the conversion of TM2P and TM1P [4, 30].

In order to try to explain the complicated trend of the total conversion of both reactants along the prepared catalysts let us separate the catalysts into two groups according to their product distribution: those where the HDS and HydO prevailed (CMA, CMANa, CMNaS15 and CMNaS25) and those where the acid-type

reactions do (CMNaS33 and CMNaS50). Starting for the first group, the great reduction of the total conversion of 2-MT observed for the CMANa catalyst in comparison with CMA could be interpreted like a reduction of the HDS activity because only HDS products were detected for this catalyst. In the section 3.1 was observed that for the CMANa catalyst the main Mo oxide specie detected by Raman was the Na_2MoO_4. The presence of Na_2MoO_4 in the catalysts has been associated with a very low HDS activity because these species implicate a very strong linkage of the Mo with the support; consequently, they are very hard to reduce/sulphide [6, 20-23]. As the HydO reaction is also associated with the state of reduction/sulfuration of the Mo phase [28], the great reductions in olefin total conversions observed for the CMANa catalysts compared with the CMA one could also be explained by the majority presence of Na_2MoO_4 species.

As in the case of CMA and CMANa catalysts, the catalytic performance of the CMNaS15 one is governed by the reactions promoted by the Mo and Co phases: HDS and HydO. As stated before, the HDS activity of this catalyst was close to that of CMA, the one with the highest HDS activity. However, great differences were observed in its Mo species distribution in comparison with CMA. The predominant species encountered in the CMNaS15 catalyst Raman spectra were MoO_4^{2-} distorted and β-$CoMoO_4$ species. The β-$CoMoO_4$ species have been reported before by other authors in CoMo catalysts supported in sodium modified ASA [6, 20]. The presence of these species has been associated with HDS highly active catalysts, contrary to that observed when the alpha species are present [6, 20, 36]. This difference in the catalytic performance of the α- and β-$CoMoO_4$ species was assigned to the coordination of Mo in the oxidic precursors. β- species exhibit a tetrahedral coordination, meanwhile α- ones exhibit an octahedral one [36]. Unlike, other tetrahedral Mo species like the Na_2MoO_4, which implicate a strong linkage of the Mo species with the support, the formation of β-$CoMoO_4$ species implicates less interaction with the support and also the prevention of forming less active $CoAl_2O_4$ and Co_3O_4 species, and the Na_2MoO_4 itself [15].

The CMNaS25 is the other catalysts which present a similar value of the HDS activity to that of the CMA and CMNaS15 ones. In this catalyst, although some presence of Na_2MoO_4 and octahedral $Mo_7O_{24}^{6-}$ species exist, the predominant Mo species are the distorted tetrahedral MoO_4^{2-} ones. These distorted tetrahedral MoO_4^{2-} species were also reported to be predominant in CoMo catalyst supported on ASA without sodium with low Si/(Si+Al) ratios (section 2.3.1, Fig. 2.4), as well as in works of other laboratories [37] using similar catalysts. In these works similar activities to that of CMA were also obtained. It is consider that the distorted tetrahedral monomeric Mo, although they are easier to reduce that the undistorted ones (Na_2MoO_4), they are harder to reduce/sulfidate than octahedral polymeric ones, and consequently; less active [21, 37]. However, it should also be considered that the presence of the distorted tetrahedral Mo species could improve the Mo dispersion [15, 21], thus compensating somehow its lack of reduction/sulfidation easiness. This fact could explain why the HDS activity of the CMNaS25 is quite similar to the CMA despite of its different distribution of Mo oxide species.

On the other hand, in the CMNaS33 and CMNaS50 catalysts acid-type reactions prevailed, thus, the inhibition of the HDS and the HydO activities is not so related with the structure of the CoMo phase. In this case the inhibition is more related with a competition of the HDS and HydO sites with the acid ones for the adsorption of the reactants. For instance, the CMNaS33 Raman spectra is similar to that of the CMA catalysts, however the total conversion of both reactants for the CMNaS33 catalyst diminishes with respect to CMA one. In the CMNaS33 catalyst, its Brönsted acid sites density and strength (only weak and intermediate sites) is not so high like in the CMNaS50 one, thus, the product distribution was equilibrated among the group of HDS and HydO reactions and the acid-type ones. As a consequence, the acid sites compete with the HDS and HydO sites preventing the adsorption on them, but the density and strength of the acid sites is not sufficient to produce enough acid-type products to equal the CMA catalyst total conversions.

Conversely, the acid sites density and strength present in the CMNaS50 catalysts are high enough to assure high yields of the acid-type products, which replaced the HDS and the HydO ones. Thus, the increment in the total conversions of both reactants observed in the essays type A is due to the high increment in the acid-type reactions activity. On the other hand, the decrease in the 2-MT total conversions observed for the CMNaSxx catalysts in comparison with CMA in essays type B, is due to the lesser stability of the carbocations of linear olefins that we already stated above.

Let us highlight the fact that the 2-MT conversions in essays type B were lower than the ones observed in essays type A for all catalysts, except for the CMANa catalyst where the contrary was observed. It has been already shown by other authors that the presence of olefins in the feed could inhibit the HDS of sulfur compounds [28, 32, 38, 39]. In this sense, it could be said that in the catalysts different from CMANa the linear olefins inhibit more the HDS that branched ones; meanwhile, the contrary occurs for the CMANa catalysts. This fact could be explained as follows, taking into account the different acid-base properties of these groups of catalysts. The inhibitory effect that olefins have on the HDS of 2-MT arises from the fact of a competitive adsorption of both reactants on the coordinative unsaturated sites (CUS) promoted by Co; the HDS ones [28, 32, 38, 39]. On one hand, it is known that, because of steric effects, the more the double-bond carbons are alkyl-substituted the harder to hydrogenate is the olefin [1-4, 32, 38].On the other hand, branched olefins interact easier than linear ones with the Brönsted acid sites because their carbocations are more stable [2, 27, 34], on the contrary, linear olefins interact easier than branched ones with the basic sites because their carbanions are more stable [2, 25]. Thus, in the catalysts supported on predominantly acidic materials (all catalysts used in this chapter except for CMANa: see section 3.3.2) two factors favor the higher inhibition of the HDS by linear olefins. First, the branched olefins interact easily with the acid sites; as a consequence, linear olefins are freer to interact with the HDS site. Second, the

linear olefins interact easier with the HDS sites because of the steric effect affecting branched ones. Whereas, in the case of catalysts supported on predominantly basic materials like the CMANa (see section 3.2) the two factors are in contradiction. The linear olefins can interact much easier with the basic sites than the branched ones, so, branched olefins are freer to interact with the HDS sites and inhibit the HDS reaction more. This last fact overcompensates the steric effect which would avoid the adsorption of branched olefins on the HDS site. Taking into account that in the FCC naphtha and the majority olefins are the branched ones [1], thus it would be better to use acidic catalysts because using them the HDS activity is less inhibited by this kind of olefins.

Up to here we have talked about the effects of sodium and Si/(Si+Al) ratio on the catalyst product distribution and reactant total conversions of the prepared catalyst. In the FCC naphtha HDT process like in all industrial process the activity is important but what really matters in this process is not losing the octane number of the FCC naphtha. Thus, at the end what we want to obtain is a catalyst with an HDS activity similar or higher to that of the conventional CoMo catalysts supported on alumina but with an improved selectivity HDS/HydO. In essays type A two kinds of branched olefins were used: terminal (TM1P) and internal (TM2P). Thus, in order to take into account individually the reactivity of each olefin, two selectivities HDS/HydO were defined according to the olefin used to calculate it: (i) the selectivity defined as the ratio between the HDS activity and the conversion of terminal branched olefins, named here as $S^{HDS/HydO-Bt}$ (equation 1.4); (ii) and the one defined as the ratio between the HDS activity and the conversion of internal branched olefins, $S^{Hds/HydO-Bi}$ (equation 1.5). With these definitions, cracking products are also taken into account as detrimental ones in the process. In essays type B, only 1-octene was used as representative of linear olefins, thus the selectivity was defined as the ratio between the HDS products and the HydO products and named here as $S^{HDS/HydO-L}$ (equation 1.6). In the case of essays type B, in order to take into account the relative importance of the double-bond

isomerization with respect to the HYD, the ratio between the double-bond isomerization and the HYD of linear olefins (isom/HydOL) was also calculated.

These three selectivities are presented in Fig. 3.8 along with the isom/HydOL ratio for the CMNaSxx catalysts compared with that of the CMA and the CMANa. In the Fig. 3.8.a are presented the selectivities related to essays type A and in the Fig. 3.8.b are presented the ones related to essays type B. Comparing the selectivity $S^{Hds/HydO-Bi}$ of the different catalysts it is observed that the CMANa catalyst presented the highest value. As we said before the conversion of TM2P for this catalyst was negative, as a consequence, according to our definition of the $S^{Hds/HydO-Bi}$ in eq. 1.5, its value for this catalyst is indefinite (∞). However, the inexistent HYD of the internal branched olefins is overcompensated by a high HYD activity of the terminal ones; consequently, a diminution of 50% is observed for the $S^{Hds/HydO-Bt}$ compared with that of the CMA catalyst. A similar diminution is observed for the $S^{Hds/HydO-L}$ of this catalyst. On the other hand, a value of twice the selectivity $S^{Hds/HydO-Bi}$, a slight improvement in the $S^{Hds/HydO-Bt}$ and a similar value of $S^{Hds/HydO-L}$ were observed for the CMNaS15 catalyst in comparison with the CMA. A similar behavior to that of the CMNaS15 catalyst is observed for the CMNaS25, however lower values of the selectivities $S^{Hds/HydO-Bi}$ and $S^{Hds/HydO-Bt}$ were observed. For the CMNaS33 catalysts a high value of the $S^{Hds/HydO-Bi}$ was observed again, but very low values of the $S^{Hds/HydO-Bt}$ and $S^{Hds/HydO-L}$. Finally, for the CMNaS50 catalyst very low values were observed for all the selectivities. As regards the isom/HydOL, it is observed that the CMANa, CMNaS15 and CMNaS25 catalyst have a value of twice the one of CMA, whereas the CMNaS33 and CMNaS50 have a value of four times the one of CMA.

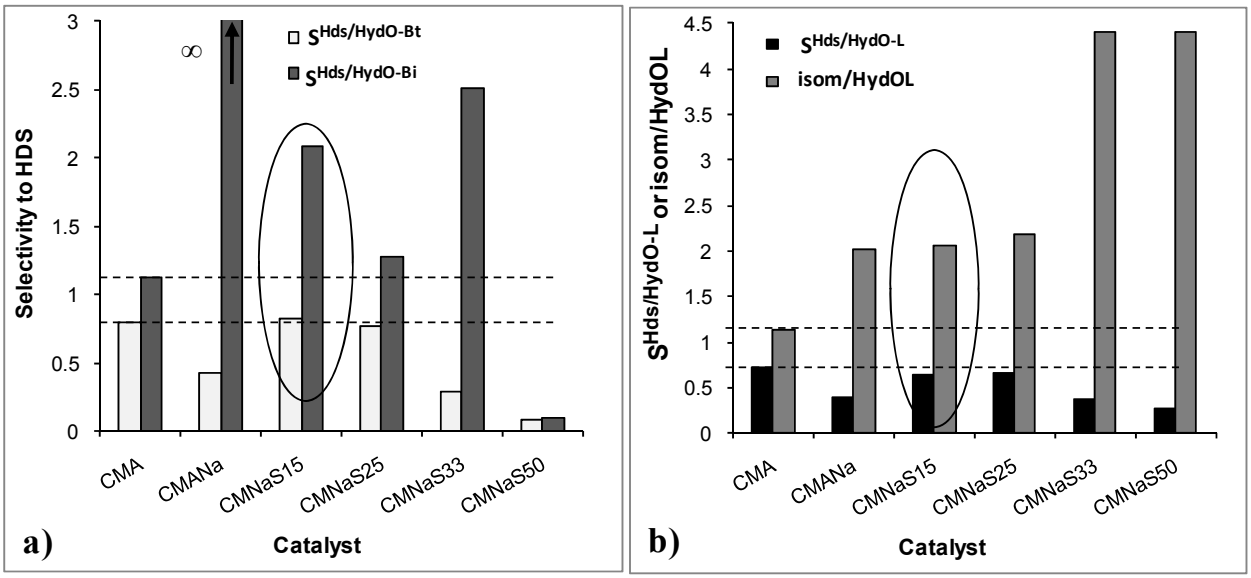

Fig. 3.8. Selectivity to the HDS according to the olefin used in essays type A and B.

Thus, the CMNaS15 catalyst was the one with the best integral performance because it was the only one which presents an important improvement of the $S^{Hds/HydO-Bi}$ and the isom/HydOL (twice that of the conventional CMA catalysts) without deterioration of the other selectivities or, even, the HDS activity. To explain this behavior two important factors have to be considered. On one hand, the Mo oxide species distribution, with the presence of β-$CoMoO_4$ species, conducts to a relatively high HDS activity rather similar to that of the CMA catalyst [6, 20, 36]. On the other hand, the singular acid-base properties of this catalyst, which only has weak Brönsted acid sites (pyridine desorbed at T < 373 K), makes that practically the only acid-type reaction promoted was the double-bond isomerization from terminal to internal positions [2, 27, 33, 34]. Consequently, there are not acid-type reactions competing with the HDS reaction, and the double-bond isomerization promotes the formation of internal olefins which are harder to hydrogenate [1-4, 32, 38].

The same factors could be used to explain the values of the selectivities observed in the other catalysts. For instance, for the CMANa catalysts, although its basic

sites also could promote selectively the double-bond isomerization over the other acid-type reactions [25] the Na_2MoO_4 present on its surface favored the formation of less active HDS and HydO species [6, 20-23]. The Na_2MoO_4 produce less active species because it is very difficult to reduce/sulphide so forming less quantity and less active CUS sites [6, 20-23]. In this sense, some authors have stated that the CUS sites responsible of the HDS reaction are more reduced that the ones responsible for the HYD reaction [40, 41]. Thus, it would be logical that hard to reduce/sulphide species like the Na_2MoO_4 produce a higher quantity of CUS sites capable of performing the HYD.

On the other hand, the CMNaS25 catalyst was a catalysts very similar to the CMNaS15 in product distribution and catalyst activity, but its selectivity values were lower than those of the CMNaS15. The explanation of this fact is that the CMNaS25 catalysts has also a low percentage of intermediate Brönsted sites which cause a significant production of cracking products increasing the olefins total conversion and thus the values of the denominators in Eq. 1.4 and 1.5. In the case of the CMNaS33 and CMNaS50 catalysts the existence of a higher density and strength of Brönsted sites could also explain their selectivity values.

As a general remark, it could be said that by combining the modification of the ASA supports Si/(Si+Al) ratio with the introduction of sodium on them it was possible to obtain a support with the ideal characteristics to prepare CoMo catalysts with a high selectivity to the HDS reaction as well as a good HDS activity. This support permits from one hand obtain Mo and Co oxidic precursors with a good compromise between its capability of dispersion of the active phase and that of reduction/sulfidation. Also, this support has specific acid-base properties; consequently, it could promote selectively the double-bond isomerization: a reaction which helps to avoid the HydO.

3.4. CONCLUSIONS

The sodium introduction on CoMo catalysts supported on amorphous aluminosilicates conduct us to obtain a catalyst (15 % Si/(Si+Al) ratio, 3 wt.% Na) with a Mo oxide species distribution with an important participation of β-$CoMoO_4$ crystalline species, and a selective formation of weak Brönsted acid sites (pyridine desorbed at T < 373 K). As a consequence of this especial balance of the acid properties and of the oxidic Mo-surface-species distribution, this catalyst presented an activity similar to that of the $CoMo/Al_2O_3$, but it presents also improvements in the selectivity to HDS.

In addition it was also encountered that when CoMo catalysts supported on materials of predominantly acidic nature are used linear olefins inhibit the HDS activity more than branched ones, whereas the contrary effect was encountered when supports of a predominantly basic nature are used.

3.5. REFERENCES

[1] S. Brunet, D. Mey, G. Pérot, C. Bouchy, F. Diehl, Appl. Catal., A. 278 (2005) 143-172.

[2] F.A. Carey, Organic Chemistry, third ed., Mc Graw Hill, Madrid, 1999.

[3] D. Mey, S. Brunet, C. Canaff, F. Maugé, C. Bouchy, F. Diehl, J. Catal. 227 (2004) 436-447.

[4] M. Toba, Y. Miki, T. Matsui, M. Harada, Y. Yoshimura, Applied Catalysis B: Environmental. 70 (2007) 542-547.

[5] Y. Fan, J. Lu, G. Shi, H. Liu, X. Bao, Catal. Today. 125 (2007) 220-228.

[6] V. La Parola, G. Deganello, A.M. Venezia, Applied Catalysis A: General. 260 (2004) 237-247.

[7] V. La Parola, G. Deganello, S. Scirè, A.M. Venecia, J. Solid State Chem. 174 (2003) 482-488.

[8] J.B. Miller, E.I. Ko, Catal. Today. 35 (1997) 269-292.

[9] Powder Diffraction File, Joint Committee on Powder Diffraction Standards, International Centre for Diffraction Data (JCPDS-ICDD), 1996.

[10] H. Knözinger, P. Ratnasamy, Catalysis Reviews: Science and Engineering. 17 (1978) 31 - 70.

[11] P.O. Scokart, F.D. Declerck, R.E. Sempels, P.G. Rouxhet, J. Chem. Soc., Faraday Trans. 1. 73 (1977) 359-371.

[12] R.E. Sempels, P.G. Rouxhet, J. Colloid Interface Sci. 55 (1976) 263-273.

[13] C. Defossé, P. Canesson, P.G. Rouxhet, B. Delmon, J. Catal. 51 (1978) 269-277.

[14] V. La Parola, G. Deganello, C.R. Tewell, A.M. Venezia, Applied Catalysis A: General. 235 (2002) 171-180.

[15] J.E. Herrera, D.E. Resasco, J. Catal. 221 (2004) 354-364.

[16] G. Mestl, T.K.K. Srinivasan, Catalysis Reviews: Science and Engineering. 40 (1998) 451 - 570.

[17] B. Pawelec, T. Halachev, A. Olivas, T.A. Zepeda, Applied Catalysis A: General. 348 (2008) 30-41.

[18] C.C. Williams, J.G. Ekerdt, J.M. Jehng, F.D. Hardcastle, I.E. Wachs, The Journal of Physical Chemistry. 95 (1991) 8791-8797.

[19] H. Jeziorowski, H. Knoezinger, P. Grange, P. Gajardo, The Journal of Physical Chemistry. 84 (1980) 1825-1829.

[20] A.M. Venezia, F. Raimondi, V. La Parola, G. Deganello, J. Catal. 194 (2000) 393-400.

[21] H. Topsøe, B.S. Clausen, F.E. Massoth, Hydrotreating Catalysis, Catalysis—Science and Technology, Springer-Verlag, Berlin, 1996.

[22] C.L. O'Young, The Journal of Physical Chemistry. 93 (1989) 2016-2018.

[23] N.F.D. Verbruggen, H. Knoezinger, Langmuir. 10 (1994) 3148-3155.

[24] P. Berteau, B. Delmon, Catal. Today. 5 (1989) 121-137.

[25] H. Hattori, Chem. Rev. 95 (1995) 537-558.

[26] S.R. de Miguel, O.A. Scelza, A.A. Castro, J. Soria, Top. Catal. 1 (1994) 87-94.

[27] G. Busca, Chem. Rev. 107 (2007) 5366-5410.

[28] N. Dos Santos, H. Dulot, N. Marchal, M. Vrinat, Applied Catalysis A: General. 352 (2009) 114-123.

[29] G. Muralidhar, F.E. Massoth, J. Shabtai, J. Catal. 85 (1984) 44-52.

[30] G. Shi, D. Fang, J. Shen, Microporous Mesoporous Mater. 120 (2009) 339-345.

[31] V. Bellière, C. Geantet, M. Vrinat, Y. Ben-Taârit, Y. Yoshimura, Energy & Fuels. 18 (2004) 1806-1813.

[32] S. Hatanaka, M. Yamada, O. Sadakane, Industrial & Engineering Chemistry Research. 36 (1997) 5110-5117.

[33] J.S. Buchanan, J.G. Santiesteban, W.O. Haag, J. Catal. 158 (1996) 279-287.

[34] A. Corma, Chem. Rev. 95 (1995) 559-614.

[35] R.S. Karinen, A.O.I. Krause, Applied Catalysis A: General. 188 (1999) 247-256.

[36] J.L. Brito, A.L. Barbosa, J. Catal. 171 (1997) 467-475.

[37] J. Vakros, A. Lycourghiotis, G.A. Voyiatzis, A. Siokou, C. Kordulis, Applied Catalysis B: Environmental. 96 (2010) 496-507.

[38] S. Hatanaka, M. Yamada, O. Sadakane, Industrial & Engineering Chemistry Research. 36 (1997) 1519-1523.

[39] J.-S. Choi, F. Maugé, C. Pichon, J. Olivier-Fourcade, J.-C. Jumas, C. Petit-Clair, D. Uzio, Applied Catalysis A: General. 267 (2004) 203-216.

[40] P. Grange, X. Vanhaeren, Catal. Today. 36 (1997) 375-391.

[41] Y.W. Li, B. Delmon, J. Mol. Catal. A: Chem. 127 (1997) 163-190.

4. GENERAL REMARKS ABOUT THE EFFECTS OF SUPPORT MODIFICATIONS ON THE CATALYTIC PERFORMANCE OF CoMo CATALYSTS IN THE HYDROTREATMENT OF FCC NAPHTHA

4.1. INTRODUCTION

In the preceding chapters various sets of support families with a wide range of surface properties were used to prepare CoMo catalysts in order to be used in the HDT of synthetic FCC naphtha. Although, each family of supports have different surface properties, which influence in a different way the catalytic performance of the catalysts, some common factors were observed in the catalysts with the better catalytic performances. It was found that support modification influences the catalytic performance by two essential factors. On one hand, the acid-base properties of the supports and the different OH surface groups existing on its surface have a strong influence in the distribution of Mo and Co oxide species. These Mo and Co oxide species are the precursor of the active sulfide phase; thus by affecting its distribution the HDS and HydO intrinsic activity of the catalysts is affected. On the other hand, the support itself promotes side reactions, predominantly of acid-type nature, like double-bond or skeletal isomerization, cracking and alkylation. It was found that these reactions compete with the HDS and the HydO. Additionally, it was found that depending of the acid-type reactions promoted and the extension of them, these could be helpful or detrimental to preserve the FCC naphtha octane number.

In this chapter, the intent is to highlight those common factors which we believe are important to understand the influence of support modification in order to obtain a catalyst which helps to preserve the octane number of FCC naphtha during the HDT process.

4.2. DISCUSSION

In the catalysts studied along the preceding chapters it was found that the support does not act only as a phase to disperse the sulfide CoMo specie(s). Supports have their own active sites, which according to their nature could be basic or acidic. It was found that the acid-base properties of the supports and consequently of the catalysts could be tailored by three ways. The simplest of those ways is modifying the acid-base properties of a well known support like alumina by impregnating it with a dopant like B, Na or K (section 1.3.1). A second way is to use a support consisting of a mixed oxide like the ASA, whose acid properties are known to vary with the Si/(Si+Al) ratio (section 2.3.1). The third way is combining the first two, i.e, vary the composition of the mixed oxide and doping it and the same time (section 3.3.2).

It was found that the introduction of alkaline metals on the alumina surface conduct to a large diminution of the total acidity as well as the acidity strength, whereas the basicity was improved (section 1.3.1). This performance was attributed to the selective adsorption of K or Na on the Al^{+3} tetrahedrally-coordinated-Lewis sites of alumina, which gives rise to the formation of a $[\equiv Al{-}OH]^{-}K^{+}$ complex [1-3]. Thus, a double effect on the alumina surface is produced; stronger acid sites are poisoned and at the same time the complex formation increase the basicity of the site. This effect was found to depend on the alkaline metal used and on its concentration. As a consequence of the reduction of the acid properties, the acid-type reactions like cracking, skeletal isomerization and alkylation were inhibited in comparison with the catalysts supported on undopped alumina. Also, it was observed that in catalysts where a considerable amount of basic sites were generated there was a considerable increase of the double-bond isomerization reaction. Thus, it was concluded that these basic sites were the direct responsible for the promotion of the double-bond isomerization in the CoMo catalysts supported on alkaline metal doped alumina.

On the other hand, when boron was used as dopant, with increasing boria content increments on the total acidity and the density and strength of the Brönsted sites of alumina were obtained. When bare and sodium modified ASA supports were used as supports of the CoMo catalysts similar trends were observed with increasing the Si/(Si+Al) ratio. These increments in the total acidity and the Brönsted sites density and strength were found to be related with the increase in the yield of the acid-type reactions like double-bond isomerization, skeletal isomerization and cracking of olefins, and alkylation of 2-MT with olefins. Even, in the catalysts with the higher values of the acid properties, it was found that the acid-type reactions, especially alkylation and cracking, compete with the HDS and the HydO respectively; thus, inhibiting them. Even the CoMo/γ-Al_2O_3 catalyst, whose Brönsted sites are so weak that they are not able to protonate pyridine [4], can produce the double-bond isomerization of both linear and branched olefins. In addition, it produces low yields of cracking and skeletal isomerization of branched olefins. In the catalysts where weak Brönsted sites were detected using pyridine as probe molecule ($T \leq 373$ K), the same acid-type reactions observed for the CMA catalyst were observed, but with higher yields of the double-bond isomerization of both linear and branched olefins. Those catalysts with intermediate Brönsted sites produce in addition cracking and alkylation reactions involving branched olefins in moderate yields. Finally, the catalyst with intermediate Brönsted sites accompanied by a very high total acidity and, even more, those with strong Brönsted sites produce alkylation and cracking reactions involving branched olefins in very high yields. In addition, these are the only catalysts able of produce the alkylation of 2-MT with linear olefins.

It was found that the selective obtention of only weak Brönsted sites make that the catalysts promote the double-bond isomerization selectively over the other acid-type reactions, and this fact coincides with the improvements in the selectivity (HDS)/(HYD of branched internal olefins) obtained for them. The same behavior was observed in the alkaline doped catalysts where the double-bond isomerization

was produced by the basic sites instead of Brönsted acid ones. It has been shown in the literature that the isomerization of the double bond can play an important role in avoiding the HydO [4-9]. Terminal olefins are much easier to hydrogenate than internal ones as a consequence of the steric effect caused by the substitution of hydrogen atoms linked to carbon atoms making part of the double bond [4-9]. Thus, this could explain the fact that improvements in the selectivity (HDS)/(HYD of branched internal olefins) could be obtained by both of the opposite ways: improving the acidity or the basicity of the support in comparison with alumina. In the case of essays with linear olefins, the double-bond isomerization reaction is even more important because internal linear olefins have a much better octane number than terminal ones [10].

Skeletal isomerization was also a useful reaction to maintain the octane number and the gasoline yield. On one hand, the products of this reaction have a similar octane number to that of 2,4,4-trimethyl-1-pentene and 2,4,4-trimethyl-2-pentene; thus, its production is not detrimental to the quality of the FCC gasoline. On the other hand, this reaction is in competition with the HydO in catalysts with weak Brönsted sites, and in catalysts with stronger Brönsted sites, where the cracking reaction predominates, the skeletal isomerization exerts a control over this by producing harder to crack products (section 2.3.2) [11, 12].

Another important to highlight fact, related with the acid-base properties of the catalysts, is the inhibition of the HDS reaction by the olefins. In this sense, it was observed that in the catalysts where a considerable amount of basic sites were generated, the presence of branched olefins inhibits more the HDS than the linear ones. In all the other catalysts, which are of a predominantly acidic nature, the opposite effect was observed; the presence of linear olefins inhibits more the HDS than the branched ones. In the section 3.3.2 it was shown that this behavior is related with the higher affinity of branched olefins for the acid sites [7, 11, 12] and the higher affinity of the linear olefins for the basic ones [7, 13].Taking into account

that in the FCC naphtha the majority olefins are the branched ones [6], thus it would be better to use acidic catalysts because when using them the HDS activity is less inhibit by this kind of olefins.

It was found by Raman and XPS that in the conventional CoMo catalyst supported on alumina the major Mo species were polymeric $Mo_7O_{24}^{6-}$ octahedral species and monomeric MoO_4^{2-} with distorted tetrahedral symmetry, although some contributions from $CoMoO_4$ species cannot be ruled out (section 1.3.2). The XPS suggest also a mixture of Co_3O_4, $CoMoO_4$ and $CoAl_2O_4$ species (section 1.3.2). It was found that the use of a different support like ASA or the modification of alumina conduct to obtain a different Mo and Co oxide species distribution. It was also found that the Mo and Co oxide species distribution was directly related with the HDS and HydO activity of the catalyst. In general when the modification of the support increased the support basicity the strength of the Mo-support bond was increased, whereas the opposite trend was observed when the acidity was increased. For instance, alkaline metals were selectively adsorbed on the Al^{+3} tetrahedrally-coordinated-Lewis sites of alumina, which gives rise to the formation of a $[\equiv Al{-}OH]^{-}K^{+}$ or $[\equiv Al{-}OH]^{-}Na^{+}$ complex [1-3]. Thus, when Mo was impregnated on these catalysts, it was deposited on this complex forming either K_2MoO_4 or Na_2MoO_4 species [14-17]. The formation of this alkaline metal molybdates increases the strength of the linkage Mo-support and difficults the formation of sulfide active species because they are very difficult to reduce/sulfide [4, 16-18]. Thus, there was a diminution in the formation of CUS sites and its degree of reduction. This fact could explain the large and continuous diminutions of the HDS and the HYDO activity with increasing alkaline metals content.

When the alumina was modified with boron with increasing boria content the alumina surface hydroxyls were progressively replaced by boron ones until the formation of a cover layer [19]. Thus, depending of the boria loading the Mo was deposited on the alumina hydroxyls or on boron ones. This fact could explain the

formation of larger polymeric Mo species in detriment of monomeric ones because, on one hand, Mo is stronger bonded to Al than to B atoms [20-23], and on the other hand, the increase in boria content causes an increase in the PZC, which could cause a displacement of the equilibrium between monomeric and polymeric Mo species to the polymeric ones [21-23]. The formation of larger polymeric species with boron introduction suggests a detriment in the Mo dispersion. This fact along with the increase in Brönsted acid sites density and strength, which gives origin to a competition between acid sites and the CUS for the adsorption of the reactants, could account for the reduction in the HDS and HydO activities.

In the case of the ASA supports there are various factors to take into account. We have to consider that ASA supports have at least twice the A_{BET} of the alumina; consequently, at the same loading of Mo the concentration of Mo per unit of area is the half. Lower concentrations of Mo per unit of area, which are equivalent to higher surface pH favored the formation of monomeric MoO_4^{2-} species [15, 24]. This explains why, despite of the lower PZC of the ASA supports, the catalysts supported on ASA with Si/(Si+Al) ratios ≤ 25 % have predominantly undistorted monomeric MoO_4^{2-} tetrahedral species. However, it was observed that with increasing Si/(Si+Al) ratio this undistorted monomeric MoO_4^{2-} tetrahedral species were progressively replaced by polymeric octahedral ones. In the section 2.3.1 it was shown that in the ASA support with % Si/(Si+Al) ratio < 50 the mixed oxide Si-Al is diluted with a segregated alumina phase [25-27]. Thus, when the Mo was impregnated this could be attached either on the segregated alumina phase or on the mixed oxide Si-Al. With increasing Si/(Si+Al) ratio the concentration of the segregated alumina phase diminished. As a consequence there was a diminution of the Mo-support interaction, thus promoting the formation of polymeric octahedral species.

It is considered that the distorted tetrahedral monomeric Mo, although they are easier to reduce than the undistorted ones, they are harder to reduce/sulfidate than

the octahedral polymeric ones, and consequently, it conduct to less active sulfide species [18, 28]. However, it should also be considered that the presence of the undistorted tetrahedral Mo species conduct to improve the Mo sulfide species dispersion [14, 18], thus, compensating somehow its lack of reduction/sulfidation easiness. This fact could explain why the HDS activity of the CoMo catalysts supported on ASA with 15 % Si/(Si+Al) is quite similar to the one of CoMo/γ-Al_2O_3 despite of its different distribution of Mo oxide species. In the other CoMo catalysts supported on ASA with higher Si/(Si+Al) ratios although the changes in the Mo species dispersion could account for some of the diminution in the HDS and HYDO activity, this diminution is more related with the large increment in the Brönsted acid sites density and strength, which compete with the CUS sites for the reactants adsorption.

In the case of the CoMo catalysts supported on sodium modified ASA, it was observed the same trend of increasing the polymeric octahedral species with increasing Si/(Si+Al) ratio exhibited by the catalysts supported on unmodified ASA. However, it was found that sodium brings about two separated effects. It strengthens the Mo-support interaction and also increase the crystallinity of all the oxide phases, even that of the support. This last effect was especially evident in the catalyst with 15 % Si/(Si+Al) ratio, where β-$CoMoO_4$ species were observed. The presence of these species has been associated with HDS highly active catalysts, contrary to that observed when the alpha species are present [29-31]. It was shown that these are not the only Mo species present on the catalyst and that probably undistorted tetrahedral species are majority, but definitively the presence of this β-$CoMoO_4$ species is important to account for the relatively high HDS activity of this catalyst.

Although the support influences separately the acid-base properties of the catalysts and the Mo and Co species distribution, these two effects of the support modification influence together the catalytic performance. Thus, in order to obtain

highly active and selective to HDS catalysts we have to take care of both effects of the support. For instance, when alkaline metal modified aluminas were used, although the basic sites promote selectively the double-bond isomerization and a very high selectivity (HDS)/(HYD of branched internal olefins) was obtained, the preferential formation of Na_2MoO_4 species conduct to a very low HDS activity. The same effect was observed in the boron doped catalysts were the double-bond isomerization was promoted by the selective formation of weak Brönsted acid sites, but the lowering of the Mo dispersion was detrimental to the HDS activity.

On the ASA supported CoMo catalysts although an HDS activity comparable to that of the CoMo/γ-Al_2O_3 was obtained for the catalyst with 15 % Si/(Si+Al), their acidity was not optimal to promote selectively the double-bond isomerization. In the other CoMo catalysts supported on ASA the acid properties were so high that the adsorption of the reactants on the acid sites inhibited the HDS activity. On the other hand, when the sodium modified ASA were used as supports the simultaneous variation of the Si/(Si+Al) ratio and the sodium introduction conducts to obtain a catalyst (15 % Si/(Si+Al), 3 wt.% Na) not only with a special distribution of acid sites, but also with a special balance of the Mo species distribution. As a consequence of this special combination of a highly active to HDS sulfide CoMo phase with the weak Brönsted sites promoting selectively the double-bond isomerization, this catalyst exhibit an activity comparable to that of the CoMo/γ-Al_2O_3 and twice its selectivity (HDS)/(HYD of branched internal olefins) and its ratio (isomerization)/(HYD of linear olefins)

Finally, as a general remark, it should be said that in order to design highly active and selective to HDS catalysts to be used in the FCC naphtha HDT it is necessary to improve both of two essential factors at the same time. On one hand, it is necessary to finely control the support characteristics, namely acid-base properties, which favored the production of helpful side reactions, like the double-bond and skeletal isomerization in order to inhibit the HydO. On the other hand, it

is also needed to pay attention to the support as a dispersant phase in order to maintain a good compromise between the dispersion and the reducidability /sulfidability of the CoMo phase; thus obtaining highly HDS active catalysts.

4.3. REFERENCES

[1] S.R. de Miguel, O.A. Scelza, A.A. Castro, J. Soria, Top. Catal. 1 (1994) 87-94.

[2] S.R. de Miguel, A.C. Martinez, A.A. Castro, O.A. Scelza, Journal of Chemical Technology & Biotechnology. 65 (1996) 131-136.

[3] A.V. Deo, T.-T. Chuang, I.G. Dalla Lana, The Journal of Physical Chemistry. 75 (1971) 234-239.

[4] D. Mey, S. Brunet, C. Canaff, F. Maugé, C. Bouchy, F. Diehl, J. Catal. 227 (2004) 436-447.

[5] M. Toba, Y. Miki, T. Matsui, M. Harada, Y. Yoshimura, Applied Catalysis B: Environmental. 70 (2007) 542-547.

[6] S. Brunet, D. Mey, G. Pérot, C. Bouchy, F. Diehl, Appl. Catal., A. 278 (2005) 143-172.

[7] F.A. Carey, Organic Chemistry, third ed., Mc Graw Hill, Madrid, 1999.

[8] S. Hatanaka, M. Yamada, O. Sadakane, Industrial & Engineering Chemistry Research. 36 (1997) 5110-5117.

[9] S. Hatanaka, M. Yamada, O. Sadakane, Industrial & Engineering Chemistry Research. 36 (1997) 1519-1523.

[10] W. Gruse, D. Stevens, The chemical technology of Petroleum, 2nd ed., Mc Graw Hill, New York, , 1942.

[11] J.S. Buchanan, J.G. Santiesteban, W.O. Haag, J. Catal. 158 (1996) 279-287.

[12] G. Busca, Chem. Rev. 107 (2007) 5366-5410.

[13] H. Hattori, Chem. Rev. 95 (1995) 537-558.

[14] J.E. Herrera, D.E. Resasco, J. Catal. 221 (2004) 354-364.
[15] G. Mestl, T.K.K. Srinivasan, Catalysis Reviews: Science and Engineering. 40 (1998) 451 - 570.
[16] N.F.D. Verbruggen, H. Knoezinger, Langmuir. 10 (1994) 3148-3155.
[17] N.F.D. Verbruggen, G. Mestl, L.M.J. von Hippel, B. Lengeler, H. Knoezinger, Langmuir. 10 (1994) 3063-3072.
[18] H. Topsøe, B.S. Clausen, F.E. Massoth, Hydrotreating Catalysis, Catalysis—Science and Technology, Springer-Verlag, Berlin, 1996.
[19] C. Flego, W.O.N. ParkerJr, Applied Catalysis A: General. 185 (1999) 137-152.
[20] Y. Saih, K. Segawa, Applied Catalysis A: General. 353 (2009) 258-265.
[21] P. Torres-Mancera, J. Ramírez, R. Cuevas, A. Gutiérrez-Alejandre, F. Murrieta, R. Luna, Catal. Today. 107-108 (2005) 551-558.
[22] U. Usman, M. Takaki, T. Kubota, Y. Okamoto, Applied Catalysis A: General. 286 (2005) 148-154.
[23] F. Dumeignil, K. Sato, M. Imamura, N. Matsubayashi, E. Payen, H. Shimada, Applied Catalysis A: General. 315 (2006) 18-28.
[24] C.C. Williams, J.G. Ekerdt, J.M. Jehng, F.D. Hardcastle, I.E. Wachs, The Journal of Physical Chemistry. 95 (1991) 8791-8797.
[25] C. Defossé, P. Canesson, P.G. Rouxhet, B. Delmon, J. Catal. 51 (1978) 269-277.
[26] P.O. Scokart, F.D. Declerck, R.E. Sempels, P.G. Rouxhet, J. Chem. Soc., Faraday Trans. 1. 73 (1977) 359-371.
[27] R.E. Sempels, P.G. Rouxhet, J. Colloid Interface Sci. 55 (1976) 263-273.
[28] J. Vakros, A. Lycourghiotis, G.A. Voyiatzis, A. Siokou, C. Kordulis, Applied Catalysis B: Environmental. 96 (2010) 496-507.
[29] J.L. Brito, A.L. Barbosa, J. Catal. 171 (1997) 467-475.
[30] V. La Parola, G. Deganello, A.M. Venezia, Applied Catalysis A: General. 260 (2004) 237-247.

[31] A.M. Venezia, F. Raimondi, V. La Parola, G. Deganello, J. Catal. 194 (2000) 393-400.

5. CONCLUSIONS

- The acid-base properties of the catalysts can be tailored by modifying the support composition and nature. When the alumina was doped with alkaline metals the acid sites density and strength of alumina decreased with increasing loading, whereas large quantities of basic sites were created. When alumina was doped with boron the acid sites density and strength, specially the Brönsted ones, of alumina was increased. When ASA supports were used the acid sites density and strength specially the Brönsted ones increased with increasing Si/(Si+Al) ratio. When sodium was introduced on ASA supports the acid sites density and strength decreased, specially the Brönsted ones, in comparison with the catalysts supported on the unmodified ASA.
- When basic sites were created in the support, the double-bond isomerization of branched and linear olefins was promoted selectively. Meanwhile, when the density and strength of the acid sites, in special the Brönsted ones, was increased, acid-type reactions like the double-bond isomerization, skeletal isomerization and cracking of olefins, and the alkylation of 2-MT with olefins were promoted.
- The yield of the different acid-type reactions was found to depend mainly on the Brönsted sites strength distribution of the catalyst and the kind of olefin used. It was found that the double-bond isomerization was promoted selectively when the catalyst has only weak Brönsted sites (pyridine desorbs at $T < 373$ K).
- The double-bond and skeletal isomerization and the cracking of olefins were found to inhibit the hydrogenation of olefins by competition of acid sites with the CUS ones for the reactants adsorption. The alkylation of 2-MT with olefins was found to inhibit the hydrodesulfurization in the same way.
- The improvements of the selectivity to HDS, especially when only internal branched olefins are taken into account, was found to be related with the

selective promotion of double-bond isomerization reaction from terminal to internal positions.

- The HDS activity of the catalysts was found to depend on the Mo oxide species distribution. The introduction of alkaline metals promotes the formation of alkaline metal molybdates, which are very hard to reduce Mo species; thus lowering the HDS activity. The increasing of the acidity of supports promotes the formation of polymeric octahedral species instead of monomeric tetrahedral ones, thus lowering the dispersion and consequently the HDS activity. The concentration of the Mo per unit area was found also to affect the Mo oxide species distribution by affecting the PZC of the combined system Mo-support. Sodium introduction on ASA with Si/(Si+Al) ratio ≤ 25 was found to increased the crystallinity of the Mo species.
- It was found that the catalytic performance depends on both of two effects of the support modification: the changes in the acid-base properties and in the Mo oxide species distribution.
- In order to obtain a catalyst highly active to the HDS and selective to the HDS at the same time both effects have to be improved at the same time as well. On one hand, generating weak Brönsted sites that promote selectively the double-bond isomerization over the other acid-type reactions, and on the other hand, promoting an appropriate balance in the Mo oxide species distribution.

PUBLICATIONS

In Peer Reviewed Journals:

- Effects of the H_2S partial pressure on the performance of bimetallic noble-metal molybdenum catalysts in simultaneous hydrogenation and hydrodesulfurization reactions.
  David Pérez-Martínez, Sonia A. Giraldo, Aristóbulo Centeno
  Applied Catalysis A: General 315 (2006) 35–43.
- Comportamiento del catalizador CoMo/γ-Al_2O_3 modificado con boro y potasio en las reacciones simultáneas de hidrogenación de olefinas e hidrodesulfuración de 2-metiltiofeno
  David Pérez-Martínez, Albany M. Lozano, Carlos J. Arias, Vladimir C. Porras, Giovanny A. Olarte, Sonia A. Giraldo, Aristóbulo Centeno.
  Revista Colombiana de Química, 2008, 37(2): 219-231.
- Influencia del potasio en catalizadores CoMo/γ-Al_2O_3-K(x) sobre sus propiedades ácido-base y su efecto en reacciones simultáneas de HDS de 2-metiltiofeno y HID de olefinas.
  David Pérez-Martínez, Sonia A. Giraldo, Aristóbulo Centeno
  Inf. Tecnológica, 2009, vol. 20, no. 6, p. 11-20.
- Surface characterization of borated γ-alumina by using proton affinity distributions
  David Pérez-Martínez, Guillermo A. Acevedo, Sonia A. Giraldo, Aristóbulo Centeno
  Accepted for publication in Rev. Fac. Ing. Univ. Antioquia.
- Control of selectivity in FCC naphtha hydrotreating by modifying the acid-base balance of CoMo/γ-Al2O3 catalysts
  David Pérez-Martínez, Pierre Eloy, Eric M. Gaigneaux, Sonia A. Giraldo, Aristóbulo Centeno

Submitted to Applied Catalysis A: General. Manuscript number APCATA-D-10-00718.

- Interpretation of the catalytic functionalities of CoMo/ASA FCC-naphtha-HDT catalysts based on its acid properties
  David Pérez-Martínez, Eric M. Gaigneaux, Sonia A. Giraldo, Aristóbulo Centeno
  Submitted to Journal Molecular Catalysis A: Chemical. Manuscript number MOLCAA-D-10-00575 Chemical.
- Improving the selectivity to HDS in the HDT of FCC naphtha using sodium doped amorphous aluminosilicates as supports of CoMo catalysts
  David Pérez-Martínez, Eric M. Gaigneaux, Sonia A. Giraldo, Aristóbulo Centeno
  In preparation to be submitted to Applied Catalysis A: General.

In Scientific Events:

- **Oral:**

- Efecto del sodio en el desempeño de catalizadores CoMo soportados en aluminosilicatos amorfos en el hidrotratamiento de nafta de FCC.
  David Pérez Martínez, Sonia A. Giraldo, Aristóbulo Centeno.
  XXII Congreso Iberoamericano de Catálisis, Viña del Mar, Chile, 5-10 de septiembre de 2010.

- Effect of the Acidity of Supported CoMo on its Catalytic Functions in Naphtha Hydrotreating.
  David Pérez Martínez, Sonia A. Giraldo, Aristóbulo Centeno.
  International Symposium on Advances in Hydroprocessing of Oil Fractions (ISAHOF 2009). Ixtapa-Zihuatanejo, Guerrero, Mexico, June 14-18, 2009.

- Influencia de la acidez de catalizadores CoMo soportados en alúmina modificada con Boro en reacciones simultáneas de HDS de 2-metiltiofeno y HID de olefinas.
  XXI Simposio Iberoamericano de Catálisis (XXI SICAT). Málaga-Benalmádena-Costa, España, Junio de 2008.
  David Pérez Martínez, Sonia A. Giraldo, Aristóbulo Centeno.
- Efecto de la acidez del catalizador en las funciones ácida, HDS y HID de olefinas en ambientes de HDT.
  Memorias del V Simposio Colombiano de Catálisis (V SICAT). Bucaramanga, Colombia, Octubre de 2007.
  David Pérez Martínez, Sonia A. Giraldo, Aristóbulo Centeno.

- **Posters:**

- Aplicación de la Descomposición de 2-propanol como técnica de caracterización acido-base de catalizadores CoMo soportados en alúmina y aluminosilicatos amorfos.
  Andrea L. Moreno, Ángela M. Orozco. V, David J. Pérez Martínez, Sonia A. Giraldo, Aristóbulo Centeno.
  XXII Congreso Iberoamericano de Catálisis, Viña del Mar, Chile, 5-10 de septiembre de 2010.

- Estudio cinético del hidrotratamiento de nafta de FCC sobre un catalizador CoMo/g-Al2O3.
  Gustavo A. Granados, Carlos E. Bravo, David J. Pérez-Martínez, Sonia A. Giraldo y Aristóbulo Centeno
  XXII Congreso Iberoamericano de Catálisis, Viña del Mar, Chile, 5-10 de septiembre de 2010.
- Caracterización de γ-Al2O3 modificada con B por el método de distribución de afinidad protónica (PAD)

David Pérez-Martínez, Guillermo A. Acevedo, Sonia A. Giraldo, Aristóbulo Centeno

VI Simposio Colombiano de Catálisis, Medellin, Octubre 28-30 2009.

- Effect of Sodium on the Acidity and Catalytic Functions in Naphtha Hydrotreating of CoMo Supported on Amorphous Aluminosilicates.

  David J. Pérez-Martínez, Eric M. Gaigneaux, Sonia A. Giraldo, Aristóbulo Centeno.

  Europacat IX 2009. Salamanca, España, 30 agosto – 4 de septiembre de 2009.
- Influence of the Boron Modified Alumina Supported CoMo catalyst acidity on FCC naphtha Hydrotreating.

  Société Real de Chimie – 6ème Journées-Rencontres des Jeunes Chimistes, Wépion, Belgique 19-20 de mars 2009.

  David Pérez Martínez, Sonia A. Giraldo, Aristóbulo Centeno.
- Influencia del potasio en catalizadores CoMo/γ-Al_2O_3-K(x) sobre sus propiedades acido-base y su efecto en reacciones simultáneas de HDS de 2-metiltiofeno y HID de olefinas.

  David Pérez Martínez, Sonia A. Giraldo, Aristóbulo Centeno

  XXI Simposio Iberoamericano de Catálisis (XXI SICAT). Málaga-Benalmádena-Costa, España, Junio de 2008.
- Comportamiento del catalizador CoMo/γ-Al_2O_3 modificado con B y K en hidrogenación de olefinas simultánea con hidrodesulfuración de 2-metiltiofeno

  Carlos J. Arias, Albany M. Lozano, Vladimir C. Porras, Giovanny A. Olarte,

  David Pérez Martínez, Sonia A. Giraldo, Aristóbulo Centeno.

  Memorias del V Simposio Colombiano de Catálisis (V SICAT). Bucaramanga, Colombia, Octubre de 2007.